The sublethal effects of nanosilver on thyroid hormone-dependent frog metamorphosis

by

Amanda Carew
BSc, University of Ottawa, 2007

A Thesis Submitted in Partial Fulfillment
of the Requirements for the Degree of

MASTERS IN BIOCHEMISTRY

in the Department of Biochemistry and Microbiology

© Amanda Carew, 2013
University of Victoria

All rights reserved. This thesis may not be reproduced in whole or in part, by photocopy or other means, without the permission of the author.

Supervisory Committee

The sublethal effects of nanosilver on thyroid hormone-dependent frog metamorphosis

by

Amanda Carew
BSc, University of Ottawa, 2007

Supervisory Committee

Dr. Caren C. Helbing, Department of Biochemistry and Microbiology
Supervisor

Dr. Christopher J. Nelson, Department of Biochemistry and Microbiology
Departmental Member

Dr. C. Peter Constabel, Department of Biology
Outside Member

Abstract

Supervisory Committee
Dr. Caren C. Helbing, Department of Biochemistry and Microbiology
Supervisor
Dr. Christopher J. Nelson, Department of Biochemistry and Microbiology
Departmental Member
Dr. C. Peter Constabel, Department of Biology
Outside Member

Nanoparticles (NPs) are engineered in the nanoscale (<100nm) to have unique physico-chemical properties from their bulk counterparts. Nanosilver (nAg) is the most prevalent nanoparticle in consumer products due to its strong antimicrobial action and can be released to the environment during product manufacture, usage and disposal. The predicted environmental concentrations are within the North American guidelines for the protection of aquatic life and in drinking water. While nAg toxicity at high concentrations has been well described, the sublethal effects at environmentally-relevant concentrations are relatively unknown. Initial screening in our lab showed nAg was a potential endocrine disrupting chemical (EDC). Amphibian metamorphosis is mediated by thyroid hormone (TH), and nAg perturbed TH-dependent transcriptional responses in the tailfin of bullfrog (*Rana catesbeiana*) tadpoles. The primary objective of this thesis was to further investigate and characterize the effects of low, environmentally relevant concentrations of nAg on TH-dependent metamorphosis in *R. catesbeiana* and *Xenopus laevis*.

Two chronic, 28 day *in vivo* exposures at 0.06 and 6µg/L nAg were conducted with premetamorphic *R. catesbeiana* tadpoles using TH to induce precocious metamorphosis. Ionic silver (iAg) was also examined to control for the complete dissolution of Ag. Analysis of metamorphic stage progression demonstrated nAg-induced acceleration of hindlimb growth and development. After 6 days of nAg exposure, analysis with quantitative real-time polymerase chain reaction (QPCR) demonstrated nAg-induced disruption of TH-responsive transcripts in a tissue-

specific manner. Furthermore, the nAg effects could not be fully explained by iAg, indicating NP-specific disruption.

Two chronic, 28 day exposures to 0.018-1.8 µg/L nAg were conducted on *X. laevis* premetamorphic and prometamorphic tadpoles. nAg was found to significantly bioaccumulate in tadpole tissue after 28 days. Furthermore, nAg increased the hindlimb length during early premetamorphosis and in post-metamorphic juvenile tadpoles. Using an in-house MAGEX microarray and QPCR transcriptional analysis, 7 biomarkers of nAg exposure were validated. Five of these targets showed disruption to their TH-response. Furthermore, the increased mRNA abundance of two peroxidases indicated that nAg generated reactive oxygen species (ROS) even at low, environmental concentrations.

This thesis demonstrates that nAg has consistent EDC actions across two distinct amphibian species, and the data suggest that regulatory guidelines for silver may need revision.

A *X. laevis* derived fibroblast-like TH-responsive cell line, XTC-2, was used in conjunction with the 7 biomarkers of nAg exposure to gain mechanistic insight into the role of ROS in TH signaling disruption. Monocultures were created and validated to increase the specificity of TH-response. While the monocultures were successfully created, the biomarkers were not responsive to nAg in this cell line.

Additional investigations were made into the relationship between genetic sex and responsiveness to TH. Genetic sexing methods were used to investigate transcriptional differences between males and females during natural and TH-induced metamorphosis. The sexing protocol was optimized and validated successfully. The genetic sex was determined for premetamorphic and prometamorphic *X. laevis* tadpoles exposed to TH for 48 h. QPCR and microarray analysis was used to identify three markers that demonstrated transcriptional sex-bias during early gonadal differentiation stages.

Table of Contents

List of Tables

List of Figures

Abbreviations

Note on nomenclature: proper use of italics and capitalization for genes/transcripts/proteins is species-specific, following the example listed below. Derived from (<www.xenbase.org/gene/static/geneNomenclature>; <www.informatics.jax.org/mgihome/nomen/gene>; and <http://en.wikipedia.org/wiki/Gene_nomenclature>). Each unique gene/transcript/protein is therefore only listed in the abbreviation section as it first appears, with appropriate variations in text.
Protein families defined by function are capitalized, eg. MAPK.

Species	Gene/Transcript	Protein
human	*THRA*	THRA
mouse/rat	*Thra*	THRA
amphibian	*thra*	Thra

Acth	adrenocorticotropin
AF	activation factor
akr1c3	hydroxysteroid (17-beta) dehydrogenase 5 gene
AKT1	protein kinase B
AMA	amphibian metamorphosis assay
AMP	adenosine monophosphate
Ar	androgen receptor
ATP	adenosine triphosphate
Atp1b3	Na^+/K^+ ATPase
BSA	bovine serum albumin
cat	catalase gene
Cdk8	cyclin-dependent kinase 8
cDNA	reverse-transcribed RNA, complementary DNA
CNS	central nervous system
cps	carbamoyl phosphate synthetase gene
Creb	cyclic AMP response element binding protein
Crebbp	Creb binding protein
Crh	corticotropin releasing hormone
Ct	cycle when QPCR signal passes threshold
d	days
DBD	DNA-binding domain
dCt	difference between control and target Ct
ddH_2O	double distilled water
Dio1	deiodinase type 1
Dio2	deiodinase type 2
Dio3	deiodinase type 3
DIT	3,5-diiodotyrosine
DLS	dynamic light scattering
DNA	deoxyribonucleic acid

DO	dissolved oxygen
DOC	dissolved organic carbon
DR4	direct repeat of a consensus sequence 4 nucleotides apart
E_2	estradiol
EcR	ecdysone receptor
EDC	endocrine disrupting chemical
eef1a	elongation factor-1 alpha gene
Esr	estrogen receptor protein
Epx	eosinophil peroxidase
F	female
FFF-ICP-MS	field flow fractionation online with ICP-MS
Gpx	glutathione peroxidase
GRE	glucocorticoid response element
GSH	glutathione
h	hours
HAT	histone acetyltransferases
HDAC	histone deacetylases
Hdac3	histone deacetylase 3
Hi nAg	*X. laevis* exposure at 1.8µg/L nAg
HiAg	*R. catesbeiana* exposure at 6µg/L Ag
HMOX1	heme-oxygenase 1
HPA	hypothalamo-pituitary-adrenal/interrenal
HPT	hypothalamo-pituitary-thyroid axis
hsp30	heat shock protein 30
iAg	ionic silver, Ag^+
ICP-MS	inductively coupled plasma mass spectrometry
IgE	immunoglobulin E
Il	interleukin
JNK	c-Jun N-terminal kinase
Kat2b	lysine acetyltransferase/ p300/Crebbp-associated factor
Klf9	Kruppel-like factor 9/basic transcriptional element-binding protein
KW	Kruskal-Wallis statistical test
LBD	ligand binding domain
LDH	lactate dehydrogenase
LL	leg length
Lo nAg	*X. laevis* exposure at 0.018µg/L nAg
LoAg	*R. catesbeiana* exposure at 0.06µg/L Ag
Lpo	lactoperoxidase
M	male
MAGEX	multi-species analysis of gene expression
MAPK	mitogen-activated protein kinases
MDL	minimum detection limit
Med1	Thr associated protein 220/mediator complex subunit 1
Med nAg	*X. laevis* exposure at 0.18µg/L nAg
min	minute(s)

MIQE	minimum information for publication of quantitative real-time PCR experiments
MIT	3-monoiodotyrosine
Mpo	myeloperoxidase
mRNA	messenger RNA
MYCN	N-myc protein
MW	Mann-Whitney U statistical test
NAC	N-acetyl cysteine
nAg	nanosilver
Ncor1	nuclear receptor co-repressor 1/thyroid-hormone- and retinoic-acid-receptor-associated co-repressor 1
Ncor2	nuclear receptor co-repressor 2/silencing mediator for retinoid or thyroid-hormone receptors
NF	Nieuwkoop and Faber developmental stages for *X. laevis*
NFKB1	nuclear factor-kappa B
NIS	Na^+/I^- symporter
NP	nanoparticle
Nr3c1	glucocorticoid receptor/nuclear receptor subfamily 3, group C, member 1
OECD	Organization for Economic Cooperation and Development
PAA	polyacrylic acid
PCR	polymerase chain reaction
PEC	predicted environmental concentration
PESC	Pacific Environmental Science Centre
PI3K	phosphatidylinositol 3-kinase
Plc	phospholipase C
Pomc	proopiomelanocortin
ppm	parts per million
ppt	parts per thousand
premet	premetamorphic tadpole
Prkca	protein kinase C alpha
promet	prometamorphic tadpole
PTGS2	cyclooxygenase-2/prostaglandin-endoperoxide synthase 2
PTP	protein tyrosine phosphatases
QPCR	quantitative PCR
redox	reduction-oxidation
rlk1	*Rana* larval keratin type 1 gene
RNA	ribonucleic acid
ROS	reactive oxygen species
Rxr	retinoid X receptor
Sin3a	transcriptional repressor
Slc16a2	monocarboxylate transporter 8/solute carrier family 16, member 2
sox9	SRY (sex determining region Y) - box 9 gene
Src	steroid receptor co-activator
SVL	snout-vent length

T	testosterone
T_3	3,5,3'-triiodothyronine
T_4	thyroxine/3,5,3',5'-tetraiodothyronine
Tbl1	transducin beta-like protein
TEM	transmission electron microscopy
TGFB	transforming growth factor-beta
TH	thyroid hormone, T_4 or T_3
THBP	thyroid hormone serum binding proteins
Thr	thyroid hormone receptor, either isoform
Thra	thyroid hormone receptor alpha
Thrb	thyroid hormone receptor beta
TK	Taylor and Kollros developmental stages for *R. catesbeiana*
TL	tail length
TNF	tumour necrosis factor
Tpo	thyroid peroxidase
TRE	thyroid hormone response element
Trh	thyrotropin releasing hormone
Tsh	thyroid stimulating hormone/thyrotropin
Ttr	transthyretin
Vdr	vitamin D receptor
Vtg	vitellogenin
XTC-2	TH-sensitive *Xenopus laevis* tadpole "fibroblast-like" cell line

Acknowledgments

I would like to acknowledge the financial support from the Natural Sciences and Engineering Research Council (NSERC), the University of Victoria, the Biochemistry and Microbiology Department, and a National Research Council-NSERC-Environment Canada-Business Development Corporation Nanotechnology Initiative Strategic Network grant.

I would also like to thank our collaborators for the use of equipment or providing useful analyses. Specifically thanks go to Matt Moffitt for use of ZetaPALS Machine for DLS and zeta-potential analysis of nAg, Chris Metcalfe and Ehsanul Hoque from the Trent University for FFF-ICP-MS analysis of nAg, Kevin Wilkinson from the University of Montréal for providing nAg dissolution data, and Rachel Skirrow for the PESC exposures and for help in coordinating the analytical chemistry.

Many Helbing lab members contributed directly and indirectly to the completion of this thesis. Vicki Rehaume, Mitchel Stevenson, Lauren Bergman and Austin Hammond performed endless QPCR runs. Nik Veldhoen trained me on microarrays and answered my countless questions. Stacey Maher provided much feedback and guidance over the years. Ashley Hinther helped to train me and Pola Wojnarowicz helped to review this thesis and gave me constant companionship and support. Many thanks to all of the Helbing lab members present and past for constant support!

As well, thank you to my committee members and most especially Caren Helbing for helping me to develop my project and for much guidance, feedback and endless patience along the way.

Dedication

This thesis is dedicated to Ruben and my family for their constant loving support and encouragement.

1 Introduction

1.1 Nanosilver (nAg)

1.1.1 Nanoparticle (NP) and nAg Overview

Nanoparticles (NPs) are particles engineered in the nanoscale (<100nm) with unique physico-chemical properties from their larger, bulk sized counterparts. NPs are increasingly used in consumer products and industrial, biomedical, optical and electronic applications, and humans can potentially be exposed through product usage or at various stages of the product‘s lifecycle (Musee, 2011). Possible routes of entry into water systems include through run-off from landfills, or directly from manufacturing facility wastes, increasing environmental exposure and specifically endangering aquatic wildlife (Fabrega et al, 2011).

NPs generally consist of a solid core with a functionalized surface coating (Figure 1.1). The core can be made of various substances including metals (Ag, Au, Fe), semi-conductor materials (TiO_2, CdSe, Si, ZnO) or even synthetic substances (polystyrene). The surface coating, when present, is generally organic in nature, and common functionalizations include citrate, fatty acids, bovine serum albumin (BSA), or polymers like polyacrylic acid (PAA) or polyvinylpyrrolidone. The surface coating is generally chosen to modify the behaviour of NPs in solution by altering the hydrophilic/phobic nature or the rate of dissolution into ions. The small size of NPs means they are suspended as colloids and their large surface to volume ratio allows ions to be released more readily than from bulk-sized particles, although this is NP- and solution-specific.

Currently there are no guidelines in place in Canada or the USA regulating the nano-specific properties of these new compounds. The only applicable regulations are based on the amount of the bulk elemental or ionic forms in surface and drinking waters, based on their specific toxicity. This is problematic as the unique properties that make NPs so desirable in industry also imply a differential toxicity from their bulk counterparts. Specifically, their small size allows NPs to easily cross tissue and cell membranes directly or via endocytosis or phagocytosis, causing cellular damage and increasing the potential for

bioaccumulation. Their large surface area to mass ratio and specific surface coatings can cause increased reactivity leading to deleterious cytotoxic effects (Bakand et al, 2012; Kahru & Dubourguier, 2010). Altered toxicity has also been described between NPs due to size, shape, aggregation state or even between batches of the same NP. While research on potential toxicity and ecotoxicology of NPs is increasing (Kahru & Dubourguier, 2010), it is still insufficient to fully characterize NPs and their potential for harmful effects on humans and wildlife.

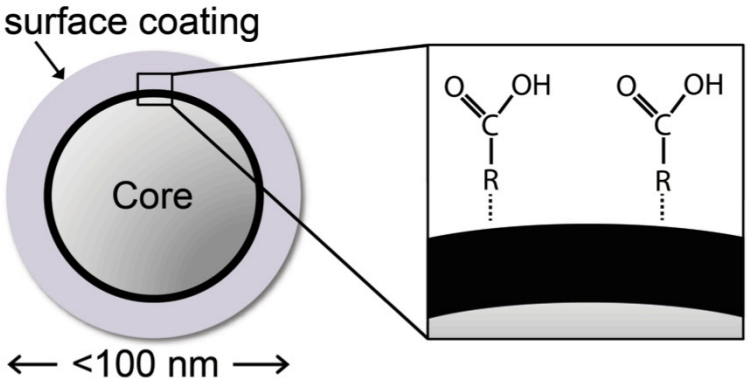

Figure 1.1 – General structure of nanoparticles (NPs). Defined by sizes <100nm, materials for NP core and surface coating vary based on desirable physico-chemical properties.

Nanosilver (nAg) is the most used NP in consumer products (Woodrow Wilson Database, 2012, <www.nanotechproject.org>), and is the second most researched after various carbon-based nanomaterials (Kahru & Dubourguier, 2010). nAg is widely used for its broad spectrum antimicrobial activity, although it has other distinctive properties including high thermal and electrical conductivity, catalytic activity and non-linear optical behaviour (Fabrega et al, 2011). nAg has been in production since the early 1990s and is most prevalent in consumer and medical products, found in a wide range of materials including textiles, plastics, pastes, soaps and metals (Fabrega et al, 2011). Studies have shown that nAg is released from nAg-infused washing machines (Farkas et al, 2011b) and socks (Benn & Westerhoff, 2008) in sufficient quantities to raise health concerns.

The powerful antimicrobial effect of nAg is generally attributed to the reactivity of its dissolved ion (iAg), although nano-specific effects from the whole NP are also possible. While nAg toxicity to prokaryotes has been well described, relatively few studies have directly investigated the mechanisms of action. There are a few mechanisms thought to be responsible for the antimicrobial action of nAg, including: interfering with the respiratory chain production of ATP, direct interaction with DNA preventing replication, generation of reactive oxygen species (ROS), and NP penetration through the cell wall and plasma membrane (Gou et al, 2010; Marambio-Jones & Hoek, 2010). It is currently unclear whether these mechanisms can impact similar structural components within eukaryotic cells, and mitochondria are a potential target for nAg deleterious effects due to their evolutionary link to bacteria (Kutschera, 2009). Eukaryotic species may even be more sensitive to nAg than certain bacterial strains with lower inhibitory/lethal concentrations in crustaceans, algae, fish and amphibians (Hinther et al, 2010b; Kahru & Dubourguier, 2010).

1.1.2 nAg Toxicity

While the overall mechanisms involved are still unclear, the toxicity of nAg on eukaryotes has been well established. Many studies have demonstrated significant toxicity of nAg in the mg/L (ppm) range using a variety of *in vitro* and *in vivo* models. At these higher concentrations, effects include cytotoxicity (via apoptosis and necrosis), lethality, oxidative stress, DNA and cell membrane damage, mitochondrial malfunction, inflammation and decreased cellular proliferation (Arora et al, 2008; Asare et al, 2012; AshaRani et al, 2009; Bouwmeester et al, 2011; Braydich-Stolle et al, 2010; Comfort et al, 2011; Eom & Choi, 2010; Griffitt et al, 2008; Hsin et al, 2008; Hussain et al, 2005; Johnston et al, 2010; Kawata et al, 2009; Kim et al, 2009a; Lankoff et al, 2012; Lim et al, 2012; Nishanth et al, 2011; Park et al, 2010; Scown et al, 2010; Yildirimer et al, 2011; Zanette et al, 2011; Zhang et al, 2012). These effects are all inherently linked as cytotoxicity and decreased proliferation can be caused by one or all of the above (Johnston et al, 2010).

ROS are extremely reactive oxygen-containing molecules such as hydrogen peroxide and oxygen radicals. Although endogenous ROS can have biochemical roles within cells, once the production of ROS exceeds the antioxidant capacity of the cell, oxidative stress occurs. Left unchecked, ROS can cause significant cellular damage including: DNA and RNA strand breakage, protein denaturation, and cell membrane damage both by interaction with membrane bound proteins and by lipid peroxidation cascades (Yildirimer et al, 2011). Glutathione (GSH) is a molecule capable of reducing free radicals by donating an electron from its thiol group. In conjunction with GSH reductase, GSH intracellular concentrations are often measured to indicate the degree of oxidative stress. Catalase (Cat), superoxide dismutase (Sod), and glutathione peroxidase (Gpx) are the primary enzymes responsible for reducing ROS. However, their enzymatic activity decreases as oxidative stress increases, and heme peroxidases such as eosinophil peroxidase (Epx), lactoperoxidase (Lpo) and myeloperoxidase (Mpo) become important ROS scavengers (Schaffer & Bronnikova, 2012).

Both iAg and nAg can cause ROS generation (Foldbjerg et al, 2010; Liu et al, 2010). Recent studies are beginning to elucidate the intracellular mechanisms and signaling pathways involved in nAg-induced toxic effects. Regulatory mechanisms activated by nAg that are involved in oxidative stress include c-Jun N-terminal kinase (JNK; Hsin et al, 2008), p38 mitogen-activated protein kinase (MAPK), and phosphatidylinositol 3-kinase (PI3K) signaling pathways (Eom & Choi, 2010; Kang et al, 2012; Lim et al, 2012). Furthermore, up-regulation of stress-response genes has been found after nAg application (AshaRani et al, 2009; Bouwmeester et al, 2011; Gou et al, 2010; Hinther et al, 2010b; Kawata et al, 2009; Rahman et al, 2009; Roh et al, 2009).

The involvement of ROS in nAg-induced toxicity can be demonstrated via recovery with antioxidants. Studies have used exogenous antioxidants to recover partially or fully from various nAg induced cytotoxicity and developmental abnormalities, specifically using N-acetyl cysteine (NAC; Foldbjerg et al, 2010; Hsin et al, 2008; Kawata et al, 2009; Kim et al, 2009a), vitamin C (Posgai et al, 2011) or trolox (Yang et al, 2012). Since NAC has the potential to act both as

antioxidant and ligand to iAg (Yang et al, 2012), it is currently unclear whether the recovered toxicity was due to ROS production or dissolution of iAg. Furthermore, Carlson et al (2008) saw a correlation between increased ROS and decreased GSH after nAg application, and suggested that nAg could even bind to GSH or GSH reductase to inhibit antioxidant responses. Therefore the production of ROS clearly accounts for at least part of nAg-induced toxicity.

nAg shows genotoxicity in eukaryotic cells through the micronucleus assay (AshaRani et al, 2009) and observations of chromosomal aberrations (Arora et al, 2008; Kumari et al, 2009; Wise et al, 2010). Although generated ROS are considered the major source of DNA damage, both nAg and iAg are capable of causing single and double strand DNA breaks, as iAg can covalently bind to nucleobases (Arakawa et al, 2001; Hossain & Huq, 2002). Furthermore, in response to DNA damage, nAg induced the up-regulation of the gene RAD51 and phosphorylation of histone variant H2A.X in mouse embryonic fibroblasts, both involved in DNA repair (Ahamed et al, 2008). Therefore DNA damage is a significant contributing factor to nAg-induced toxicity.

nAg causes damage to the cell membrane as shown by the LDH leakage assay (Hussain et al, 2005; Kim et al, 2009a; Liu et al, 2010). Damage can be caused both indirectly by generation of ROS and directly with interaction between nAg or iAg and membrane bound proteins. ROS generation and oxidative stress cause lipid peroxidation, with subsequent DNA damage and cell death, as demonstrated in *Drosophila melanogaster* (Ahamed et al, 2010b). nAg has been shown to interact extensively with proteins and other biological material. These associations can be mediated by either interactions between the surface coating and organic functional groups or by direct binding of Ag to thiol groups, denaturing proteins by disrupting disulfide bonds (Arora et al, 2012; Chen & Schluesener, 2008; Johnston et al, 2010). These interactions allow nAg to associate with membrane-bound proteins and cause perforations in the cellular membrane. nAg can also potentially inhibit the protective function of thiol-containing proteins, decreasing their catalytic or antioxidant capacity (Johnston et al, 2010). Additionally, the association of nAg with reporter proteins or dyes used

in enzymatic assays can affect the results causing false positives or negatives (Monteiro-Riviere et al, 2009). It is therefore extremely important to use appropriate controls to determine the influence of nAg on the assay output before examining its cellular response.

Mitochondria are a target of nAg-induced damage, specifically causing decreases in both mitochondrial membrane potential and energy production (Arora et al, 2012; Carlson et al, 2008; Hsin et al, 2008; Hussain et al, 2005), likely mediated by mitochondrial DNA and membrane damage. As mitochondria are the major source of cellular energy, Teow et al (2011) suggested that nAg-induced mitochondrial inhibition could prevent ATP-dependent DNA repair mechanisms, prolonging DNA damage. Therefore, nAg inhibition of mitochondrial function is similar to its antimicrobial action on prokaryotes.

Inflammation is a general immune response to environmental stressors, and is a common response to nAg (Hussain et al, 2005; Nishanth et al, 2011; Park et al, 2010). Park et al (2010) found an increased amount of pro-inflammatory cytokines in murine blood during a 28 day repeated oral dose exposure, including: interleukins (Il)1, Il4, Il6, Il10, Il12, and transforming growth factor-beta (TGFB). Immunoglobulin E (IgE) production and B cell distribution in lymphocytes were also increased, mediating the inflammatory response. Macrophages are involved in clearance of foreign material from the body and generate ROS as a primary defense mechanism. Nishanth et al (2011) demonstrated that murine macrophages exposed to nAg increased the mRNA and protein expression of inflammatory-responsive cyclooxygenase-2/prostaglandin-endoperoxide synthase 2 (PTGS2) and tumour necrosis factor-alpha (TNF), and increased the cellular release of Il6. These responses were mediated by ROS-induced expression of nuclear factor-kappa B (NFKB1). It is currently unknown whether the ROS-mediated inflammatory response is due to nAg or iAg, or whether it is a macrophage defense mechanism.

nAg has been found to interfere with cell cycle regulatory proteins and induce changes in proliferation. Long-lasting deleterious effects of nAg were observed by Zanette et al (2011) showing a decrease in human keratinocyte proliferation

that was sustained during a 6 day recovery period. In a mechanistic investigation, Braydich-Stolle et al (2010) demonstrated that the nAg-induced decrease in proliferation of mouse spermatogonial stem cells was due to the inhibited phosphorylation capacity of Fyn kinase, affecting downstream cell cycle regulatory targets protein kinase B (AKT1) and N-myc (MYCN). It was suggested by the authors that the inhibition was mediated by direct interaction of nAg with Fyn kinase, although this was not tested. Kawata et al (2009) investigated the involvement of cell-cycle regulatory proteins in nAg-induced proliferation changes in human hepatoma cells. They used microarray analysis to determine the disregulation of several checkpoint related genes. At lower (≤500μg/L Ag) and higher doses (>1mg/L Ag) nAg increased and decreased proliferation respectively. This emphasizes the observation that low concentration effects cannot always be predicted from extrapolation from effects at higher doses.

Within sublethal, but still moderate concentrations in the lower mg/L or higher μg/L ranges, nAg is a teratogen and causes developmental, neuronal and reproductive inhibitory effects. Asharani et al (2011) demonstrated that nAg caused developmental abnormalities in developing zebrafish including absence of eyes, growth retardation and undulated notochord. In mice nAg can impair brain function, causing neurodegeneration, disruption of the blood-brain barrier with subsequent brain edema, altered neurotransmitter signaling and behaviour, and changed expression of genes involved in neurodegenerative diseases (Lee et al, 2009; Yildirimer et al, 2011). This shows the potential for deleterious effects on events regulated by the central nervous system (CNS), such as behaviour and homeostasis.

It is unsurprising that nAg has effects on reproduction as silver has previously been shown to cause sterility in clams in the environment after a release of silver in the San Francisco Bay in the 1980s (Brown et al, 2003). After exposure to mg/L doses of nAg, the reproductive potential was directly decreased for various organisms including earthworms (Shoults-Wilson et al, 2011), aquatic midges (Nair et al, 2011) and *Caenorhabditis elegans* (Lim et al, 2012; Roh et al, 2009), with indirect effects observed through decreased proliferation of mammalian

spermatogonial stem cells (Braydich-Stolle et al, 2010) and cytotoxicity in testicular cells (Asare et al, 2012). With microarray analysis, Roh et al (2009) determined that the effects seen in *C. elegans* were mediated by oxidative stress. In a follow-up experiment, Lim et al (2012) determined that the oxidative stress-induced reproductive suppression was mediated by p38 MAPK activation. Taken together, these studies imply that nAg exposure could have serious impacts on wildlife populations and their ecosystems at non-lethal concentrations.

1.1.3 Factors Affecting nAg Toxicity

A complication when considering nAg toxicity is that additional factors must be considered that can vary even between batches of NPs. These include particle size, type of surface coating, and degree of aggregation in the experimental medium. Particle size is an important factor, with smaller particles generally showing greater toxicity in *in vitro* models (Braydich-Stolle et al, 2010; Carlson et al, 2008; Johnston et al, 2010; Liu et al, 2010). This is likely mediated by their increased capacity to enter cells, as well as having a larger surface to volume ratio that increases the potential for reactivity and iAg dissolution. However, the effects are not as clear when looking at multicellular organisms, as the mechanism of nAg uptake and distribution can vary depending on NP size (Park et al, 2010; Posgai et al, 2011; Scown et al, 2010; Yang et al, 2012).

The surface coating surrounding the Ag core can also play a role in the relative toxicity observed (Ahamed et al, 2008; Braydich-Stolle et al, 2010; Lu et al, 2010; Posgai et al, 2011; Yang et al, 2012), although currently there is no consensus on which surface coating may be least toxic. Differential results are likely mediated by NP behaviour in the exposure medium, the factor that is most variable between exposure systems (MacCuspie, 2010).

The degree of either aggregation/dispersion or dissolution into iAg plays a role in nAg toxicity. The general propensity of NPs to aggregate in solution decreases the relative toxicity of nAg *in vitro*, although this trend is more pronounced with higher mg/L concentrations and is likely mediated through

similar size-dependent effects as those noted above (Lankoff et al, 2012; Zook et al, 2011). Aggregation and iAg dissolution are dependent on the characteristics of the specific nAg tested as well as the preparation and mixing of the NPs prior to the exposure (Handy et al, 2012; Zook et al, 2011). Furthermore, these two factors can be influenced by conditions in the exposure medium such as pH, salinity, dissolved oxygen (DO) content and presence of organic material. This makes comparing results between different studies problematic, and it is recommended to thoroughly characterize the behaviour of nAg in each exposure system (Handy et al, 2012).

There is presently no consensus on whether observed toxicity is mediated by nano-specific properties of nAg or due to toxicity of the dissolved iAg component. It has even been suggested that nAg acts in a “Trojan-horse” type manner, whereby NPs are taken up and iAg is then released intracellularly, thus increasing the relative exposure to iAg (Limbach et al, 2007). There are a few studies which suggest that all of the observed effects can be explained by the dissolution of iAg (Bouwmeester et al, 2011; Xiu et al, 2011), although more often results have shown that there are NP-specific effects of nAg which exceed that accounted for by the dissolved fraction of Ag in the exposure system (AshaRani et al, 2009; Carlson et al, 2008; Eom & Choi, 2010; Griffitt et al, 2012; Griffitt et al, 2008; Hinther et al, 2010b; Kawata et al, 2009; Kim et al, 2009a; Navarro et al, 2008; Pokhrel & Dubey, 2012; Yang et al, 2012). In either case, iAg contributes to some degree in the observed responses.

It has been consistently demonstrated that when animals are exposed *in vivo*, Ag accumulates within the tissues, specifically the brain, lungs, kidneys, liver and gonads (Park et al, 2010). Various studies on mammalian models have demonstrated that liver is the main site of nAg accumulation *in vivo*, after the primary organ responsible for uptake, i.e. lungs for inhalation exposure (Johnston et al, 2010). This indicates that nAg becomes systematically available after entering the blood stream and can cross both the blood-brain barrier and the blood-testes barrier (Braydich-Stolle et al, 2010; Johnston et al, 2010). Furthermore, Kim et al (2009b) demonstrated sex-specific preferential

accumulation of nAg in female kidneys in rats, with twice as much Ag as in males. While the mechanisms behind this phenomenon are unknown, it is important to note that males and females could be differentially affected by nAg due to differences in bioavailability in various organs, or excretion via urine. In aquatic exposures, nAg accumulation has been demonstrated in the gills and/or liver of zebrafish (Choi et al, 2010; Griffitt et al, 2009), rainbow trout (Farkas et al, 2011a), brown trout (Scown et al, 2010), and Atlantic salmon (Farmen et al, 2012). The mechanisms for nAg uptake are not fully elucidated yet, although the uptake via the gills and ingestion are likely. Bouwmeester et al (2011) demonstrated that nAg and/or iAg can cross the intestinal lining using human intestinal cells. In brown trout, differential accumulation patterns of various nAg particle types and sizes in the liver and gills indicated uptake by both ingestion of aggregated particles and through the gill epithelium (Scown et al, 2010). Accumulation in the liver is expected as blood flowing from the intestinal tract is first filtered through the liver before subsequent circulation to the rest of the body. nAg uptake occurs via macrophages in the mononuclear phagocyte system within the liver (Johnston et al, 2010), and is mediated by macrophage scavenger receptors (Singh & Ramarao, 2012). It is currently unclear whether accumulated Ag is in the ionic or nanoparticulate form, as quantification methods cannot currently differentiate between the two.

1.1.4 nAg in the Environment

nAg has the potential for release into the environment as it is listed in more than 50% of products containing nanomaterials (Woodrow Wilson Database, 2012, <www.nanotechproject.org>). nAg can be released during several stages of the product life cycle including synthesis, manufacturing, usage and disposal (Marambio-Jones & Hoek, 2010). Benn and Westerhoff (2008) demonstrated that up to 1300 µg/L Ag is released from nAg-infused socks after a “washing” protocol. Also, nAg from commercially available nanowashing machines release average concentrations of 10.9 ±7.1 µg/L directly into municipal wastewater

systems (Farkas et al, 2011b). Therefore, nAg can be released into the aquatic environment allowing direct exposure to wildlife.

As mentioned above, particle behaviour such as aggregation and dissolution into iAg influences the toxicity of nAg in aqueous systems. In the environment, there are many different factors that can affect particle behaviour, including pH, salinity, DO content, potential ligands and macromolecules (Carlson et al, 2008; Fabrega et al, 2011; Marambio-Jones & Hoek, 2010). NP stability is affected by pH, with increased aggregation close to the isoelectric point of the surface coating, or at extremely acidic or alkaline pH (MacCuspie, 2010). Salinity is particularly important as Cl^- ions associate with free iAg and the resultant salts will precipitate out of solution, decreasing bioavailability. However, at high Cl^- concentrations, complexes of $AgCl_2^-$ and $AgCl_3^{2-}$ can form which are more soluble, keeping iAg in the water column (Gupta et al, 1998; Marambio-Jones & Hoek, 2010). The presence of DO in the water causes the oxidization of nAg, releasing iAg, and therefore nAg will not persist in oxygen-rich water for extended periods of time. Liu and Hurt (2010) determined that the complete dissolution of 5 nm nAg would take many days to months. iAg can also adsorb to the surface coating of the nAg it was released from, changing both the physico-chemical characteristics of the coating, as well as changing the type of nAg to which wildlife will be exposed. Finally, the surface coating of nAg readily associates with proteins and macromolecules such as dissolved organic carbon (DOC) through van der Waals forces and electrostatic interactions (Johnston et al, 2010). Increased DOC concentrations tend to decrease the toxicity of nAg on aquatic invertebrates, suggesting lowered bioavailability to organisms (Marambio-Jones & Hoek, 2010). All of the factors above affecting the behaviour of nAg in the environment can also vary between laboratory exposure systems, so understanding how the particle behaves within each experiment is critical (Handy et al, 2012). The ultimate fate and aging processes of nAg in the environment are still being investigated and need to be determined to allow relevant exposure designs with nAg types likely to be encountered by wildlife (Nowack et al, 2012).

Determining nAg concentrations in the environment is problematic, as current widely-available technology such as inductively-coupled plasma mass spectrometry (ICP-MS) cannot distinguish between Ag^0 and Ag^+. Particulate Ag is also present naturally in the environment, so measurement technology must be able to differentiate between both ionic and elemental Ag, as well as discriminate between various particle sizes. While it is possible to determine the presence and concentration of Ag in the environment, characterizing it as engineered nAg specifically is difficult. Furthermore, as noted above, during toxicity exposures there is a need for rapid characterization techniques that can fully elucidate nAg behaviour, and while significant improvements have recently been made in this regard, the cost and time-consuming nature of most techniques still make them inaccessible for toxicological assays (Handy et al, 2012).

Modelling has been used to predict the abundance of nAg in surface waters. Predicted environmental concentrations (PEC) ranged from 0.03 – 42.5 µg/L nAg in Europe, USA, and South Africa with variation between different predictive models and country usage patterns (Gottschalk et al, 2009; Mueller & Nowack, 2008; Musee, 2011). Exponential increases in discharge are expected in the future as more consumer products incorporate nAg, however the lack of comprehensive product lists and environmental monitoring means these predictions should be used with caution (Fabrega et al, 2011). Furthermore, the lower range of the concentrations predicted are lower than the minimum detection limit (MDL) of available technology, making validating these predictions even more problematic.

Currently nAg is regulated under the broad category of bulk silver in Canada and the USA. These guidelines were created based on toxicity data from bulk or dissolved Ag, and are likely not comprehensive of the excessive toxicity caused by the nanoparticulate form. For the protection of aquatic life, the limit for allowable Ag in water bodies is 0.1 and 3.2 µg/L in Canada and USA respectively (NRWQC 2006b; CCME 2007). In the USA, the limit of Ag allowable in drinking water is much higher at 0.1 mg/L (NDWR 2006a), while in Canada there is currently no upper limit (CCME 2008). Therefore, the recommended maximal

concentrations for the protection of both human and wildlife health fall well within the range of PEC noted above.

1.1.5 nAg Effects at Environmentally-Relevant Concentrations

In most of the toxicity studies described above, inhibitory effects such as cytotoxicity, genotoxicity, inflammatory responses, decreased proliferation, mitochondrial malfunction, and membrane damage were not tested below 100 µg/L. As noted above, these concentrations are much higher than those likely to be found in the environment, as well as the regulatory limit for the protection of aquatic life. Very few studies have investigated lower, environmentally-relevant concentrations. Regulatory limits are generally extrapolated from a dose-response curve generated from toxicity at higher concentrations. However, it is imperative to empirically examine the potential toxicity of nAg at low concentrations as toxins don't always behave in a linear dose-dependent manner.

While the data are not comprehensive, there are a few studies that have examined the effect of nAg at low µg/L or high ng/L concentrations. At these low concentrations, responses have been seen such as oxidative stress (Gagné et al, 2012; Pham et al, 2012), events associated with changed reproductive potential (Griffitt et al, 2012; Pham et al, 2012; Pokhrel & Dubey, 2012; Ringwood et al, 2010), and altered gill epithelium morphology (Griffitt et al, 2012) in various aquatic species.

There are a few studies that demonstrate low dose nAg effects that do not conform to a linear dose-dependent response. Hormesis is a phenomenon where a substance elicits inhibitory effects at higher concentrations but stimulatory responses at lower concentrations (Kendig et al, 2010). This process is likely mediated by perturbations to the maintenance of homeostasis, where doses lower than those likely to cause toxicity will still stimulate the responses, activating cell cycle programs and causing proliferation. Kawata et al (2009) described cellular proliferation in human HepG2 hepatoma cells at

concentrations of nAg much lower than those causing cytotoxicity. Hormetic responses have been described in other NP types as well (Iavicoli et al, 2010).

Another factor that could contribute to a non-monotonic dose response is the effect of concentration on NP behaviour. The aggregation state of nAg is dependent on the abundance of NP present, and generally decreases with lower concentrations (Zook et al, 2011). Therefore extrapolation from the effects at higher concentrations could potentially be erroneous, and effects at low, environmentally relevant concentrations need to be empirically examined.

Hormones are designed to be biologically active at low physiological concentrations and therefore can be perturbed by low concentrations of endocrine disrupting chemicals (EDCs). Disregulation of hormonal signaling by EDCs can interfere with a variety of important physiological responses. The mechanisms of disruption include: competing with or disrupting the binding of endogenous hormones to receptor sites, changing levels of circulating hormones (by altering synthesis, metabolism or interactions with plasma proteins), and altering nuclear receptor association with coactivators or corepressors (McLachlan, 2001). Furthermore, dose-response patterns are generally characterized by a non-monotonic curve due to various feedback and regulatory mechanisms important in hormonal signaling (Vandenberg et al, 2012).

There is limited evidence thus far that indicates nAg can act as an EDC. Although nAg concentrations were very high (200-1000 µg/L nAg), Nair and Choi (2012) demonstrated mRNA expression was perturbed for the ecdysone nuclear receptor (*EcR*) that regulates the response to the hormone ecdysone during invertebrate development. Only one initial study has looked at the potential EDC capacity of nAg on thyroid hormone (TH) signaling. Hinther et al (2010b) determined that nAg disrupted mRNA expression of TH-responsive genes in tailfin biopsies from North American bullfrog (*Rana catesbeiana*) tadpoles at concentrations between 0.06 and 6 µg/L nAg. At these low concentrations, no oxidative stress was detected through changes in heat shock protein 30 (*hsp30*) or catalase (*cat*) transcript abundance. Additionally, iAg showed dissimilar patterns of response to nAg, suggesting that these endocrine disrupting effects

were mediated by nanoparticle-specific actions. These initial results warranted further investigation, as TH signaling is critically important in all vertebrates, especially during postembryonic development, and therefore its disruption at low, environmentally-relevant concentrations could have deleterious effects on both aquatic wildlife and humans.

1.2 Amphibian Metamorphosis

1.2.1 Metamorphosis and TH

Amphibian development is an ideal model to test the capacity for endocrine disruption, as TH is both necessary and sufficient to drive frog metamorphosis. TH represents two tyrosine-derived molecules, thyroxine (T_4) and its metabolite and more bioactive form triiodothyronine (T_3). These hormones regulate transcription of target genes via nuclear receptors such as thyroid hormone receptors alpha (*thra*) and beta (*thrb*), by binding to TH response elements (TREs) on target genes. These two THs are bioactive in all vertebrates and even some marine larvae (Heyland, 2005), and their nuclear receptors are extremely well conserved, making comparisons of TH signaling across vertebrate species relevant.

TH is involved in many biochemical processes in adult vertebrates such as homeostasis, moulting in birds, lipid metabolism and mitochondrial respiration, as well as being critical for fetal brain and bone maturation during early development (Tata, 2006). T_3 drives metamorphosis by increasing in concentration until metamorphic climax with a subsequent decrease (Figure 1.2B). This pattern is mirrored during perinatal development in humans, with the spike in TH concentration occurring shortly after birth (Figure 1.2A). This pattern is critical in establishing normal brain function in humans, as TH deficiency can cause irreversible neurological defects and cretinism (Hetzel & Mano, 1989). Early mammalian development is difficult to experimentally manipulate and monitor due to the presence of the amniotic sac and so anuran metamorphosis has also

been used as a model for *in utero* TH-dependent development and potential EDC deleterious effects.

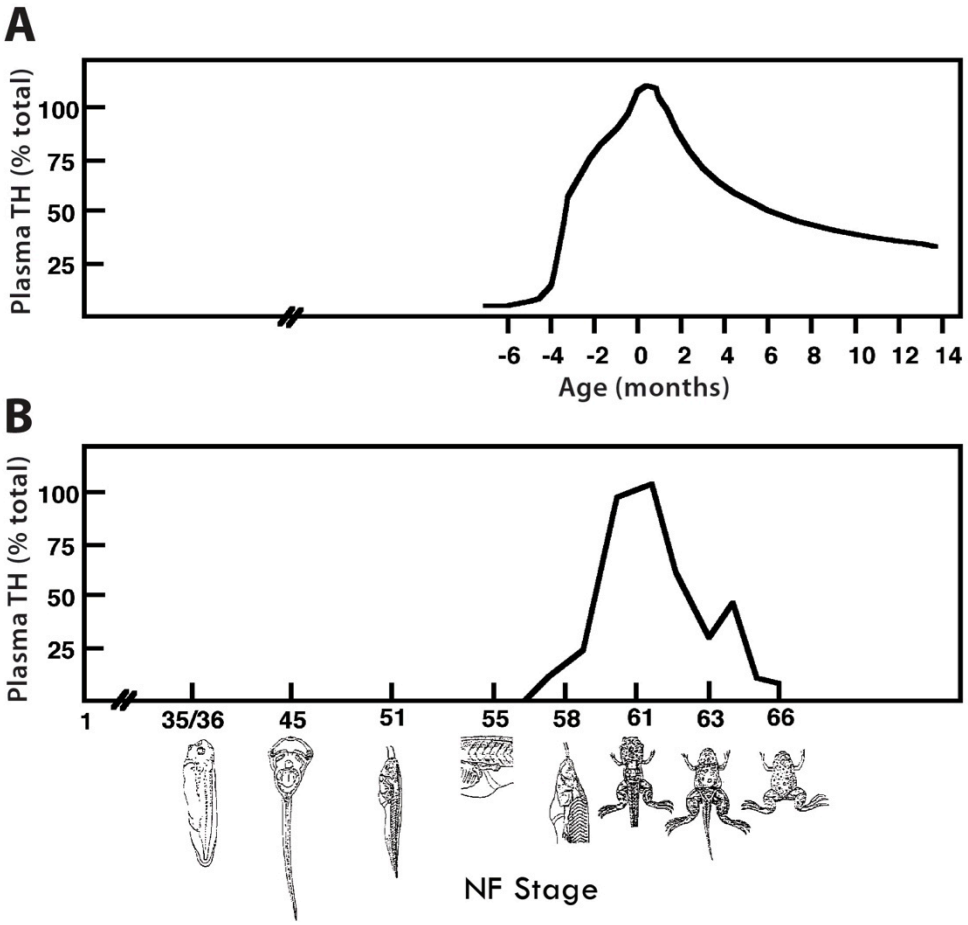

Figure 1.2 – Profile of plasma TH during the human perinatal period (A) or anuran metamorphosis (B). Visuals depicted of *X. laevis* Niewkoop and Faber (NF) developmental stages. (Adapted from Leloup & Buscaglia, 1977; Tata, 1993).

Before the initiation of metamorphosis, premetamorphic tadpoles (premets) are functionally athyroid with no circulating TH. In fact, if premets are denied TH either by thyroidectomy or inhibitory chemicals such as perchlorate, they will halt development at Nieuwkoop and Faber (NF) (Nieuwkoop & Faber, 1994) stage 54 and then continue grow in size as tadpoles, never completing metamorphosis. Furthermore, although premets have no endogenous TH, precocious

metamorphosis can be induced with exogenous TH, allowing experimental manipulation and monitoring of TH signaling interference. During natural metamorphosis, premets start to produce TH at approximately stage NF54, whence they become prometamorphic tadpoles (promets). Promets proceed to develop until metamorphic climax at stage NF60 marking the peak TH plasma concentrations, after which TH levels start to decrease until animals have become juvenile frogs (NF66).

TH modifies almost every tissue during metamorphosis, including *de novo* synthesis of limbs, apoptosis of the tail and gills, or extensive remodelling of tissues such as the intestine and eyes. There are two staging systems used to describe metamorphosis in this thesis, specifically Taylor and Kollros (TK; 1946) for *Rana catesbeiana*, and NF for *X. laevis*. Metamorphic stages are defined by the morphology of the hind and forelimb, head, eye, mouth and tail (Table 1.1). Hindlimb morphology describes early development with the formation of the limb bud and foot paddle, with subsequent digitation and growth. Prometamorphosis starts when the digits are fully formed, concurrent with the increase in TH plasma concentrations. In *X. laevis*, the forearms initially grow internally and emerge through the opercular skin at NF58. In Ranid species much more extensive internal growth of forearms is seen, which only emerge through the skin at climax. The structure of the tadpole head defines metamorphic climax, with subsequent stages using the relative positioning of the eyes and mouth. The eyes move from lateral to anterior positioning as the mouth widens. Apoptosis of the tail is one of the last changes during metamorphosis, as the lungs and limbs must develop fully for a terrestrial life. While not directly induced by TH, sexual differentiation of the gonads begins and progresses throughout metamorphosis, and is coupled to specific stages.

Although TH has pleiotropic effects on the various tissues during metamorphosis, it also acts in an organ-autonomous fashion. Exogenous TH administered to organ cultures cause those tissues to respond in their pre-programmed manner, for example, regression of cultured tailfin via apoptosis (Hinther et al, 2010a). These consistent responses as well as the complete

dependence of metamorphosis on TH make amphibians ideal models for the study of EDCs which impact TH signaling.

Table 1.1 - Niewkoop and Faber (NF) and Taylor and Kollros (TK) metamorphic stages and defining morphology. Feeding behaviour and sexual differentiation during metamorphosis are also noted. (Partially adapted from Hourdry et al, 1996; McDiarmid & Altig, 1999; OECD:AMA 2009).

Terminology	Premetamorphosis							Prometamorphosis			Metamorphic Climax				Froglet
NF Stage	48	49	50	51	52	53	54	55	56	57-58	59-60	61	62	63-65	66
TK Stage	I	II	III	IV	V	VI-VIII	IX-XI	XII	XIV-XVII	XVIII-XIX	XX	XXI	XXII	XXIII-XXIV	XXV
Hindlimb growth and digitation	X	X	X	X	X	X	X	X	X	X					
Forelimb growth and emergence[a]									X	X	X				
Head, mouth and eye morphology											X	X	X	X	
Tail Length														X	X
Sexual dimophism	Visually undifferentiated gonad							Visual identification becomes possible							
Feeding Behaviour	Filter feeding										Feeding temporarily halted during climax				Carnivorous feeding

a = for *X. laevis* only. *R. catesbeiana* forelimbs develop internally and emerge at metamorphic climax

Amphibians are considered to be environmental sentinels due to both their sensitivity to environmental stressors and their role in ecosystems. They undergo a larval aquatic phase, as well as an adult phase that is usually terrestrial, potentially exposing them to contaminants from both environments. As well, amphibians have moist, permeable skin through which gas exchange often occurs, and are anamniotes and therefore have unshelled eggs. These characteristics allow embryos, larvae and adults to be exposed directly to soil, water and sunlight, with integuments which can readily absorb toxic substances (Blaustein et al, 1994). Amphibians also are keystone species in ecosystems as they are both prey and predators, and this dynamic function contributes a great deal to ecosystem equilibrium. Therefore, substances that negatively impact amphibians are likely to have deleterious effects on other wildlife species, both directly and indirectly.

1.2.2 TH Metabolism and Regulation

As TH concentration is critical for co-ordinating metamorphosis, it is under tight control at the level of synthesis, transport in the blood and intracellular

metabolism, with feedback at various levels. TH synthesis is under neuroendocrine control by the hypothalamo-pituitary-thyroid axis (Figure 1.3). In amphibians, TH production is controlled by corticotropin releasing hormone (Crh), as opposed to thyrotropin releasing hormone (Trh) in mammals. Crh is produced in the hypothalamus and stimulates the thyrotropes in the anterior pituitary to release thyroid stimulating hormone/thyrotropin (Tsh), which in turn stimulates the thyroid gland to produce THs. TH itself causes inhibitory feedback on the hypothalamus and pituitary, decreasing its own production. As well as stimulating TH synthesis and release, Crh is involved in the hypothalamo-pituitary-adrenal/interrenal (HPA) axis, regulating stress responses, which is a conserved role in mammals. TH also indirectly stimulates the production of prolactin, a hormone produced in the lactotropes of the anterior pituitary. Prolactin has been shown to have inhibitory effects on metamorphosis, another level of regulation of metamorphic timing (Shi, 2000).

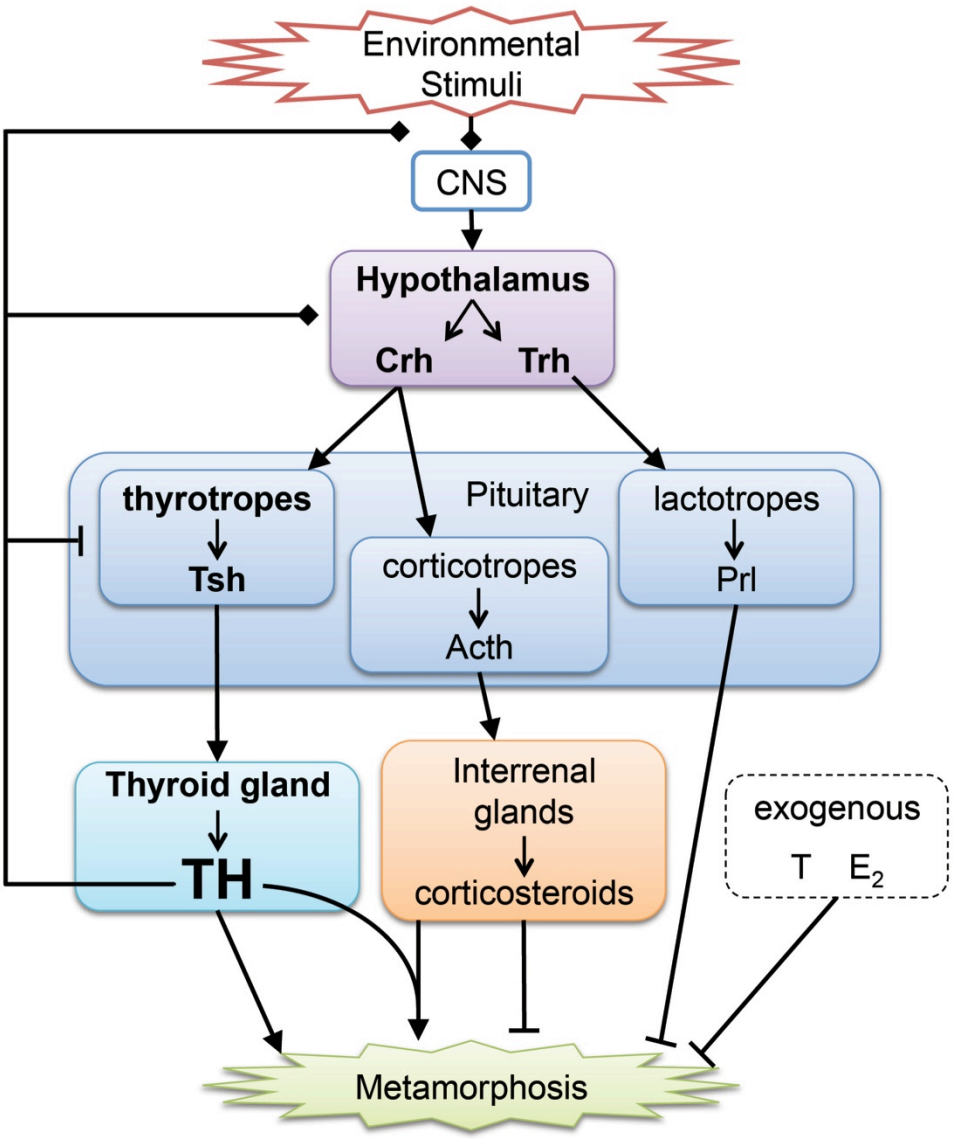

Figure 1.3 – Amphibian metamorphosis is regulated by neuroendocrine signaling of HPT axis, with regulatory feedback mechanisms and interaction with HPA axis. Solid arrows and blunt ends indicate stimulation and inhibition respectively; diamonds represent both actions. Open arrows indicate hormonal synthesis. CNS: central nervous system, Crh: corticotropin releasing hormone, Trh: thyrotropin releasing hormone, Tsh: thyroid stimulating hormone, Acth: adrenocorticotropin hormone, Prl: prolactin, TH: thyroid hormone, T: testosterone, E_2: estradiol.

THs are synthesized in the lumen and surrounding follicular cells of the thyroid gland. Tsh stimulates the synthesis of both the Na^+/I^- symporter (NIS), responsible for accumulation of intracellular iodide, and the TH precursor thyroglobulin, a large protein consisting of many sequential tyrosine residues.

Thyroglobulin is synthesized intracellularly and secreted into the lumen, where iodide is bound to the phenolic rings of the tyrosine residues at position 3 or positions 3 and 5 to make 3-monoiodotyrosine (MIT) and 3,5-diiodotyrosine (DIT) respectively. Thyroglobulin is hydrolyzed into smaller peptide fragments and shuttled back into the cytosol in endosomes that subsequently fuse with lysosomes to catalyze the synthesis of THs. DIT is coupled primarily with another DIT to make T_4, or alternatively with MIT to make T_3. Thyroid peroxidase (Tpo) is essential to thyroid synthesis, catalyzing the coupling of iodinated tyrosine residues, as well as the organification of inorganic I^- (Kovacic & Edwards, 2010). Although the exact mechanism of TH release is still unknown, Di Cosmo et al (2010) demonstrated the involvement of monocarboxylate transporter 8/solute carrier family 16, member 2 (Slc16a2) in TH secretion from the thyroid gland. T_4 is the primary form of TH released from the thyroid gland into the blood, accounting for the majority of synthesized TH (Fort et al, 2007; Utiger, 1995). At metamorphic climax, peak concentrations of plasma T_4 and T_3 are 9-13 nM and 8-9 nM, respectively in both *X. laevis* and *R. catebeiana* (Leloup & Buscaglia, 1977; White & Nicoll, 1981).

Once released into the blood, only a small fraction of total T_4 or T_3 is free for tissue uptake, the majority being bound to serum binding proteins (THBP) such as transthyretin (Ttr), lipoproteins and serum albumin (Figure 1.4; Shi, 2000). The relative priority each of these THBP plays in TH transport is species-dependent, the most important in amphibians being Ttr which binds more strongly to T_3 than T_4 (Fort et al, 2007). THBPs help regulate TH availability by prolonging TH lifespan and acting as a TH reservoir.

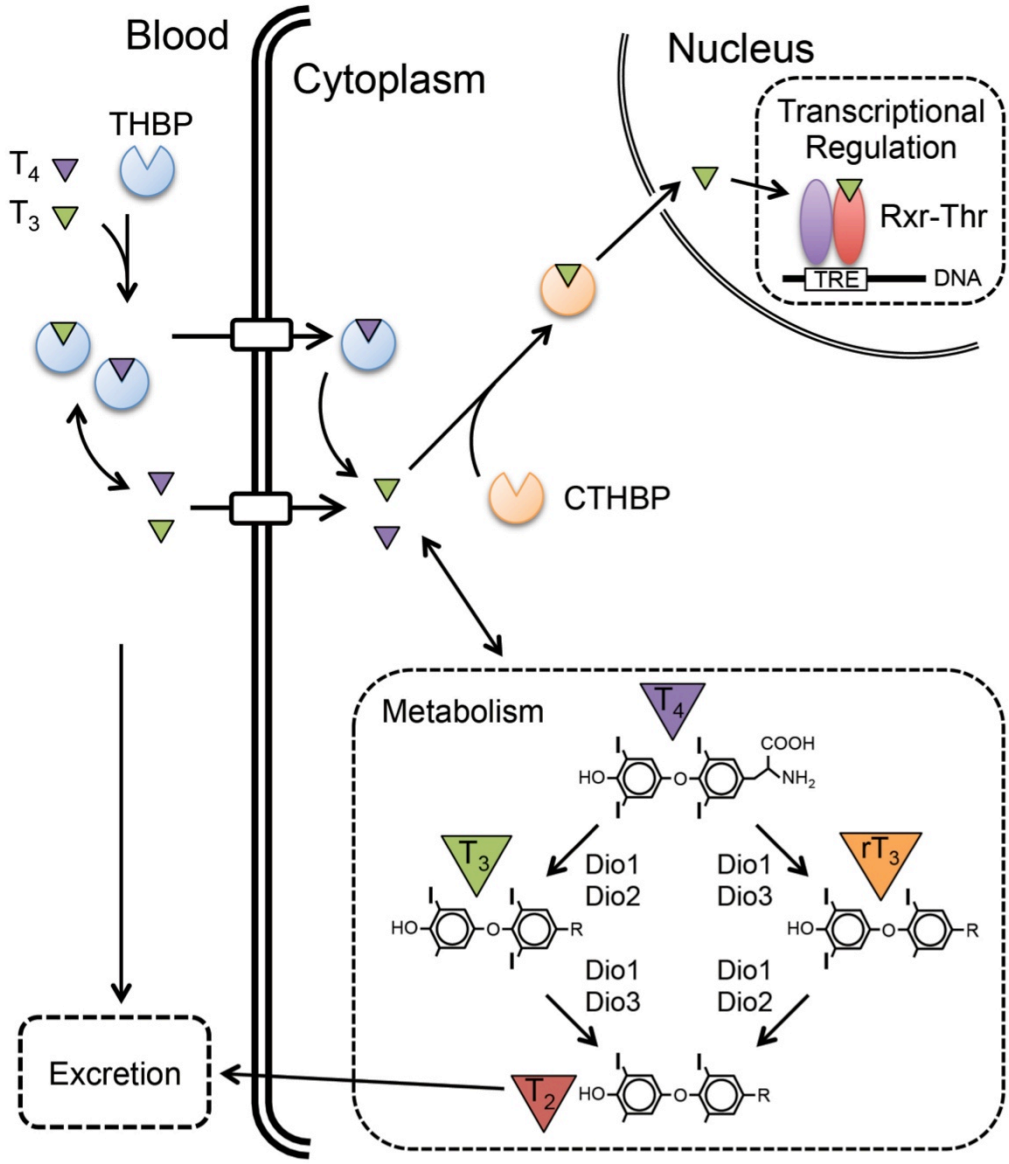

Figure 1.4 – Schematic of TH transport and intracellular metabolism. THBP: serum thyroid hormone binding proteins, CTHBP: cytoplasmic thyroid hormone binding proteins, Rxr-Thr: retinoid X receptor-thyroid hormone receptor dimer, Dio1/2/3: deiodinases type 1, 2 and 3, TRE: thyroid hormone response element.

THs are transported to tissues where uptake occurs via poorly characterized mechanisms. While it is possible for passive diffusion to occur across plasma membrane (Shi, 2000), evidence has been presented for active uptake by various transporters, such as amino acid transporters (Fort et al, 2007; Ritchie et al, 2003). Once in the cytoplasm free TH accounts for 0.5% of total THs with the majority bound to binding proteins, collectively referred to as cytoplasmic thyroid

hormone binding proteins (CTHBP). Unlike serum binding proteins, CTHBP are generally multifunctional, involved in other intracellular pathways than just regulation of free TH and include such proteins as pyruvate kinase, aldehyde dehydrogenase, disulfide isomerase, prolyl 4-hydroxylase and myosin light chain kinase (Fort et al, 2007; Yamauchi & Nakajima, 2002). CTHBP are another level of regulation for TH signaling, and act to transport TH inside the cell and to the nucleus, as well as to buffer free intracellular TH concentrations (Shi, 2000).

Another level of TH regulation is the intracellular metabolism of THs. Type 2 5'-deiodinase (Dio2) is generally considered to activate TH by removing an iodine molecule from the outer ring of T_4 to convert it into the more bioactive form, T_3 (Figure 1.4). T_3 is considered the active hormone as the binding affinity for nuclear receptors is 5-10 times greater than T_4 (Shi, 2000), although T_4 itself may be relevant to TH signaling in the brain during metamorphosis (Helbing et al, 2007a) and non-genomic signaling (see discussion below). Type 3 5-deiodinase inactivates THs by removing an inner ring iodine from either T_4 or T_3, converting them into reverse triiodothyronine (rT_3) and diiodothyronine (T_2) respectively. Further deiodination of inner and outer rings will finally produce thyronine (T_0) that is eliminated from the cells and excreted via the kidney (Davey et al, 1995; St Germain & Galton, 1997; St Germain et al, 1994). Type 1 deiodinase (Dio1) is capable of removing I^- from both the inner and outer rings of THs (Galton, 2005), although it is generally considered to play a minor role in amphibian metamorphosis (Fort et al, 2007). While the mRNA abundance of *dio1* was unchanged in the brain of *X. tropicalis*, *dio2* and *dio3* have tissue specific distributions, are responsive to exogenous TH and increase in concentration throughout metamorphosis, peaking at NF66 (Duarte-Guterman et al, 2010; Duarte-Guterman & Trudeau, 2011). The relative expression between these two isoforms contributes to concentration dependent tissue sensitivity to TH. For example, hind limb growth and development is initiated at very low TH concentrations while the tailfin does not regress until metamorphic climax at peak TH levels (Fort et al, 2007). Therefore, relative cytoplasmic deiodinase

concentrations are an important regulatory mechanism of TH availability and may facilitate tissue specific responses.

1.2.3 Transcriptional Regulation by TH

TH is capable of producing pleiotropic effects on target tissues in all vertebrates. TH causes responses in target tissues by altering the protein complement through transcriptional regulation of target genes. Cytosolic T_3 is transported to the nucleus where it binds to specific nuclear receptors called thyroid hormone receptors alpha and beta (Thra, Thrb). These receptors are bound to TREs in the promoter region of target genes in the absence of hormone, and bind as a monomer, homo- or heterodimer. The major functional form *in vivo* is considered to be a dimer between Thr and retinoid X receptor (Rxr), which has the highest binding affinity to TREs (Wong & Shi, 1995; Zhang & Lazar, 2000).

There are two separate genes encoding *thra* and *thrb* that are well conserved across vertebrates (see Thrb example, Figure 1.5), although within different species, various isoforms may exist for each. In *R. catesbeiana* only 1 isoform has been identified for each gene, while in the pseudotetraploid *X. laevis*, two genes exist for each receptor due to an incomplete chromosomal duplication event. Thra and Thrb are part of a large super-family of nuclear hormone receptors, with significant homology to nuclear receptors for vitamin D (Vdr), estrogen (Esr) and glucocorticoids (Nr3c1; Evans, 1988). The major domains of Thr include activation factors (AF), DNA binding domain (DBD), ligand binding domain (LBD), and hinge region (see Figure 1.5). AF1 and 2 are located on the N- and C-termini respectively and associate with co-activators during transcriptional up-regulation. The DBD is adjacent to AF1 and consists of two zinc-fingers that bind to the major groove of DNA at the TREs. The LBD is adjacent to the AF2 region and is where T_3 binds to the nuclear receptor, causing conformational changes in the AF2 region that assist in the transition between association with co-repressors and co-activators. The hinge region is located between the DBD and the LBD and has both nuclear localization and

transactivation functions. Dimerization occurs in both the DBD and LBD domains (Kress et al, 2009; Yen, 2001).

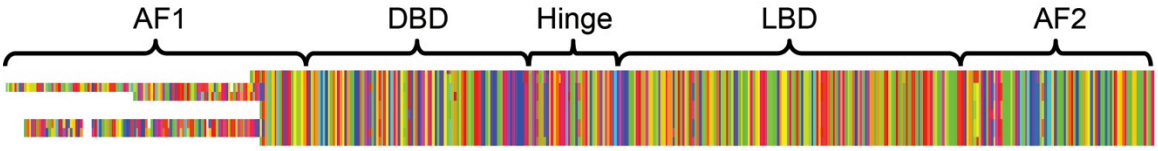

Figure 1.5 - Alignment of multiple Thrb protein sequences showing conserved domains. Various vertebrate Thrb orthologs from frogs to humans were aligned with the ClustalW algorithm using the BIRCH bioinformatics software (Fristensky, 2007). Amino acid residues are denoted by colour. AF:activating factor, DBD:DNA binding domain, LBD:ligand binding domain.

During metamorphosis, the expression profiles of *thra* and *thrb* differ. *thra* mRNA is first expressed during embryogenesis and is constitutively expressed throughout the premetamorphic period (Figure 1.6A). This accounts for the competence of premets to respond to exogenous T_3 in precocious metamorphosis, and prepares them to respond to endogenous T_3 during natural metamorphosis. *thra* expression is also is responsible for the repression of target genes before the onset of metamorphosis. *thrb* shows a different response pattern, and is not expressed until T_3 begins circulation during prometamorphosis. *thrb* is autoregulated with a TRE in its promoter region, which creates a positive feedback loop in the presence of T_3. *Thrb* also makes a good marker for exogenous T_3 administration, as nearly all tissues respond with dramatic increases in *thrb* abundance, whereas the *thra* response is tissue-dependent with modest increases (Shi, 2000). Thra plays a prominent role in proliferating tissues including the limbs, while Thrb is commonly associated with apoptotic events such as the tail regression (Denver et al, 2008).

T_3 has the potential to cause both up- and down-regulation of target genes *in vitro* and *in vivo*. Thra and Thrb heterodimerize with Rxr of which there are three isoforms, Rxra, Rxrb and Rxrg. The profile of *rxra* is similar to *thra* during metamorphosis (Figure 1.6A) allowing competency to T_3 induced transcriptional regulation. Target genes with a TRE in their promoter region are considered direct response genes as they are the first to be altered during T_3 challenge.

Many of these are transcription factors that allow T_3 to indirectly influence regulation of down-stream gene targets (Shi, 2000).

Unlike other nuclear receptors that bind to their ligand in the cytosol and then are transported to the nucleus, in the absence of TH, Thrs are already associated with the TRE of target genes. Depending on the TRE, conformational changes induced by binding of T_3 will either activate or repress transcription (Bassett et al, 2003; Buchholz et al, 2006). TREs are most commonly associated with a direct repeat of the consensus sequence AGGTCA, separated by 4 nucleotides (DR4), although binding can be promiscuous allowing nucleotide substitutions (Buchholz et al, 2006; Yen, 2001). The majority of direct response genes are up-regulated and contain a positive TRE (Buchholz et al, 2006; Helbing et al, 2007a; Helbing et al, 2007b). The few down-regulated genes which have been studied in depth contain negative TREs (nTRE), specifically Tsh and Trh (Eckey et al, 2003; Shibusawa et al, 2003; Wang et al, 2009).

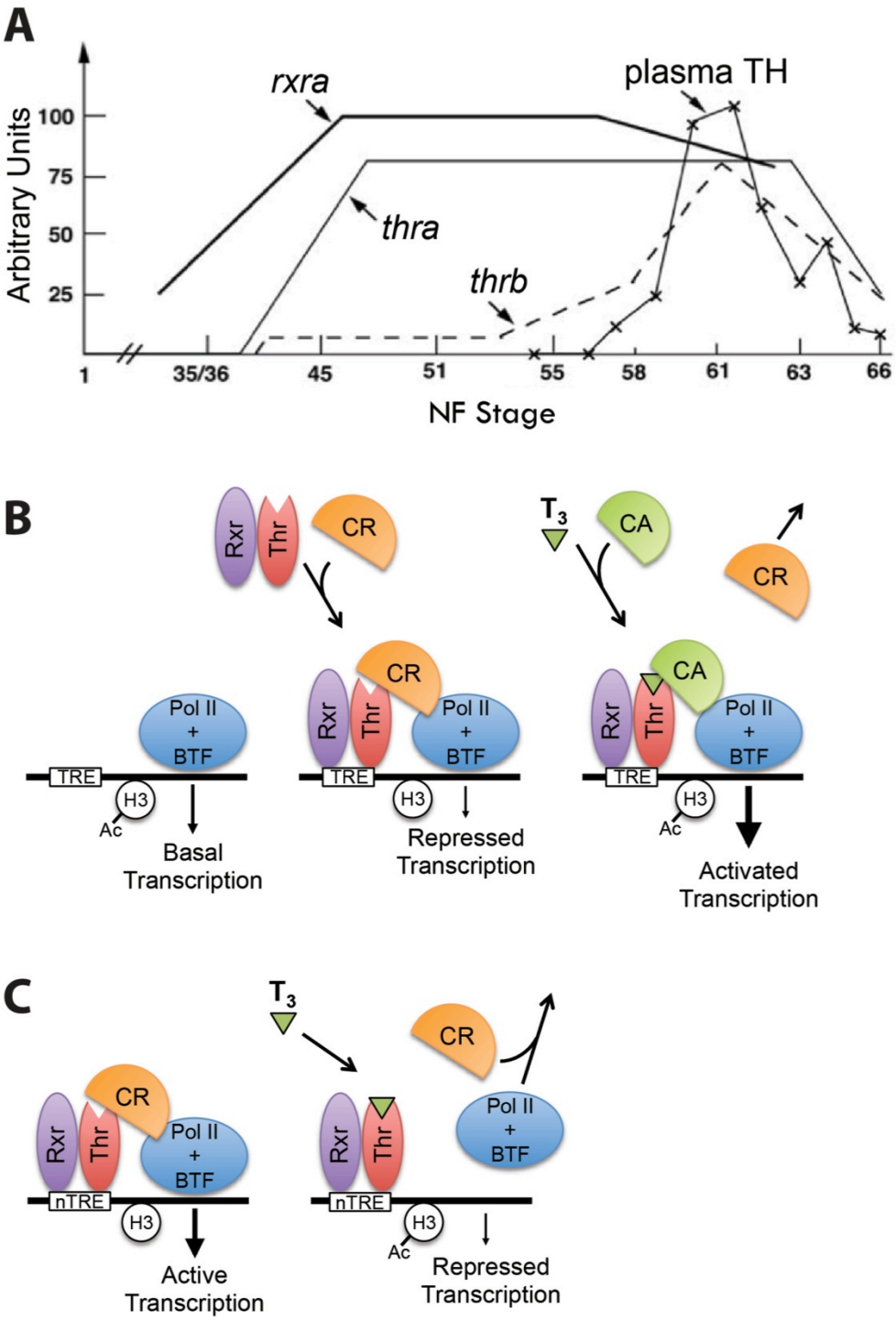

Figure 1.6 – mRNA profile of *thra*, *thrb*, *rxra* during metamorphosis (A) and T_3-dependent transcriptional up-regulation (B), and down-regulation (C). Pol II: RNA polymerase II, BTF: basal transcription factors, CR: co-repressor complex, CA: co-activator complex, (n)TRE: (negative) thyroid hormone response element, H3: histone H3, Ac: acetyl group. (Partially adapted from Das et al, 2010; Shi, 2000; Wang et al, 2009)

The majority of TH-responsive genes are up-regulated and have been studied extensively (Buchholz et al, 2006; Helbing et al, 2007a; Helbing et al, 2007b). In the absence of Thr-Rxr binding to TREs, basal transcription occurs (Figure 1.6B). Once the Thr-Rxr dimer is present in the nucleus, it binds to positive TREs to repress basal transcription (Bassett et al, 2003; Buchholz et al, 2006). In the absence of TH, various co-repressor complexes associate with Thr-Rxr to repress transcription by both condensing the chromatin structure through histone deacetylase (HDAC) activity, or by preventing the formation of the preinitiation complex needed for RNA polymerase II positioning at the transcriptional start site. Co-repressors interact with the LBD of Thr and include nuclear receptor co-repressors (Ncor1, Ncor2), the transcriptional repressor Sin3a, and Hdac3 (Eckey et al, 2003; Yen, 2001; Yen et al, 2006). Up-regulation occurs when T_3 is present in the nucleus and binds to the LBD of Thr, dissociating co-repressors and inducing conformational changes of the AF2 domain that subsequently associates with co-activator proteins (Perissi et al, 1999). Transcription is increased by histone acetylation that opens the chromatin structure and increased recruitment of proteins associated with the mediator complex and activation of the RNA polymerase II (Yen, 2001). Co-activators known to associate with Thr-Rxr that have histone acetyltransferase (HAT) activity include Creb binding protein (Crebbp), p300, steroid receptor co-activator (Src) and p300/Crebbp-associated factor/lysine acetyltransferase 2B (Kat2b). Other co-activators are involved with basal transcriptional machinery such as the Thr associated protein 220/mediator complex subunit 1 (Med1; Bassett et al, 2003; Yen, 2001).

T_3-induced down-regulation of genes is less common, and accordingly is less well characterized. While there is no overall model, TRE-Thr/Rxr interactions has been investigated in selected down-regulated target genes, such as T and Trh (Figure 1.6C; Wang et al, 2009)). Contrary to typical TH response, down-regulation is associated with both dissociation of the “co-repressor” complex and increased histone acetylation. nTREs have been found near the transcriptional start site or downstream of the TATA box (Shibusawa et al, 2003). Similar to up-

regulated genes, in the absence of T_3 the Thr-Rxr dimer is bound to DNA and associated with co-repressor proteins including Ncor1, Ncor2, Hdac3 and transducin beta-like protein (Tbl1; Eckey et al, 2003; Wang et al, 2009), however in this case the term co-repressor is a misnomer as the target genes are actively transcribed. Wang et al (2009) showed that overexpression of Ncor1 and Hdac3 in rat pituitary cells further stimulated transcription and was associated with decreased acetylation of histone H3. Additionally, inhibition of HAT activity increased transcription, whereas inhibition of HDAC activity decreased transcription, showing a negative correlation between acetylation and transcriptional activation. This is odd as HAT activity and H3 acetylation are typically associated with transcriptional activation (Yen, 2001; Zhang & Lazar, 2000). In the presence of T_3, the Ncor-Hdac3 complex dissociates from the Thr-Rxr complex, histone H3 acetylation increases along with HAT activity. While the observed down-regulation was at least partially mediated by increased histone acetylation, coregulator dissociation clearly plays a role, as HAT activity inhibitors did not prevent T_3-induced negative regulation (Wang et al, 2009). Furthermore, the decreased transcriptional activity is associated with decreased RNA polymerase II recruitment, although protein complexes post-ligand binding are currently unknown (Wang et al, 2009). Therefore, while they have opposite functions, both the Thr-Rxr-Ncor-Hdac3 complex and histone acetylation play a role in T_3-mediated up- and down-regulation.

The main mechanism of TH action is Thr-mediated transcriptional regulation and can take hours to days from initial TH uptake to the synthesis of proteins including all downstream targets. In addition to this mechanism, non-genomic actions of THs have been described which utilize existing proteins and signaling pathways, producing effects in seconds to minutes as no protein synthesis is necessary. Non-genomic actions are thought to help mediate proliferation and endothelial cell motility (Davis et al, 2008). In mammals, extracellular TH can bind to the integrin receptor alpha-V beta-3 to initiate signal transduction of the MAPK pathway via phospholipase C (Plc) and protein kinase C alpha (Prkca). Alpha-V beta-3 has higher affinity for T_4 than T_3 and activated MAPK can

phosphorylate both nuclear and cytoplasmic Thrb and Esr, indirectly affecting transcriptional regulation (Davis et al, 2005). It is also possible for intracellular T_3 to bind to cytoplasmic Thrb, activating the protein kinase B/Akt1 PI3K pathway (Cao et al, 2009) which causes increased abundance and activity of Atp1b3 in the plasma membrane, and altered transcriptional regulation of target genes (Cao et al, 2009; Lei et al, 2003).

Post-translational modification of Thrs have been shown to affect their transcriptional activity in mammals, although it is isoform specific. Thrb phosphorylation increases its binding affinity to TREs thereby increasing transcription (Chen et al, 2003). On the other hand, phosphorylation of Thra increases nuclear localization and prevents monomeric binding to the TRE (Nicoll et al, 2003; Tzagarakis-Foster & Privalsky, 1998). THs can also have effects on actin remodelling through binding of T_4 or rT_3 to a Thra-derived peptide, causing soluble actin to become filamentous and affecting cellular motility (Davis et al, 2008). In amphibians, the importance of phosphorylation in T_3-dependent metamorphic events and transcriptional changes has also been described. Inhibition of either Prkc or cyclin dependent kinase 8 (Cdk8) prevented T_3 induced tail apoptosis (Ji et al, 2007; Skirrow et al, 2008). Furthermore, genistein, a tyrosine kinase inhibitor, attenuated the *thrb* mRNA increase after T_3 addition in tailfin (Skirrow et al, 2008). Therefore, non-genomic actions of TH play an important role in modulating TH signals and coordinating metamorphic events.

Regulation of TH signaling is important as it allows tadpoles to respond to environmental stressors via metamorphic plasticity. As outlined above, there are six levels of regulation and signaling which are potential sites for EDC action: i) HPT axis and feedback mechanisms, ii) thyroid gland TH synthesis, iii) extra- and intracellular TH transport, iv) TH metabolism and elimination, v) Thr activity and synthesis and vi) non-genomic TH actions (Davis et al, 2008; Fort et al, 2007). All of these are important aspects of TH regulation and signaling, although determining at what level potential EDC act can be difficult. Disruption at different levels of regulation can have similar down-stream effects. For example,

increased direct response gene mRNA abundance can be due to: higher intracellular T_3 concentrations from increased synthesis or decreased catabolism in the thyroid or target tissue, variations in THBP binding kinetics, EDC agonistic binding to LBDs on Thrs, interference with coregulator proteins or even from Thrb phosphorylation in the nucleus, among other possibilities. Further complications in evaluating EDC potential arise from differential sensitivity at various life stages. It is important to determine critical developmental periods as larval stages of vertebrate development tend to be more sensitive than adult. Also, it is possible that effects from exposures may not manifest until a subsequent developmental stage, or even in the offspring of the exposed animal (Fort et al, 2007; Kavlock et al, 1996). Therefore to fully investigate EDC potential, it is necessary to look at *in vivo* systems at various critical developmental stages, preferably across multiple species to determine differential sensitivities.

1.2.4 HPA axis and Oxidative Stress during Metamorphosis

Stress is an important mediator of amphibian metamorphic plasticity. Environmental factors such as light, salinity and dissolved oxygen are important signals to regulate developmental timing and allow tadpoles to metamorphose before their aquatic environment dries up. As well as regulating TH synthesis and release in amphibians, Crh from hypothalamus stimulates corticotropes in the pituitary to synthesize proopiomelanocortin (Pomc), a prohormone that is converted by post-translational modifications and cleavage events into 4 different hormones including adrenocorticotropin (Acth; Figure 1.3). Acth then acts to stimulate the amphibian interrenal glands to produce corticosteroids including primarily corticosterone and to a lesser degree, aldosterone (Fort et al, 2007; Krain & Denver, 2004; Shi, 2000). During metamorphosis, the profile of circulating plasma corticosteroids is highest during premetamorphosis, then falls dramatically at prometamorphosis, only to increase in conjunction with TH profiles at metamorphic climax (Fort et al, 2007; Hayes, 1997; Krain & Denver, 2004).

There is evidence that corticoids have a dual function during metamorphosis. It has been observed in various amphibian species that administration of exogenous corticoids during early embryogenesis and premetamorphosis inhibits the onset of metamorphosis (Denver, 2009). Alternatively in the later stages of metamorphosis such as prometamorphosis and climax, corticoids have agonistic effects on T_3 signaling, increasing the rate or metamorphosis and thereby decreasing the metamorphic period (Denver, 2009; Fort et al, 2007; Hayes et al, 1993; Hayes, 1997; Krain & Denver, 2004). This could be an adaptive response to environmental cues allowing tadpoles to remain in their larval stages longer and increase their mass, or if metamorphosis is already initiated, to complete it quicker to become fully functional in a terrestrial environment (Denver, 2009).

Metamorphosis and stress responses are intrinsically linked, and hormones from either the HPT or HPA axis can modulate each other's response. Corticosterone potentiates the action of T_3 in various ways, including increasing the binding affinity of T_3 to Thrs (Kikuyama et al, 1993), prolonging T_3 bioavailability by increasing Dio2 activity (Denver, 2009), or synergistically increasing *thra* and *thrb* mRNA abundance with T_3 exposure (Bonett et al, 2010). Corticoids bind to the glucocorticoid receptor (Nr3c1) in the cytosol, which then forms a homodimer and is translocated into the nucleus where binding occurs at glucocorticoid response elements (GRE) within target gene promoter regions. Amphibian *nr3c1* has a TRE in its promoter region, and accordingly T_3 causes changes in *nr3c1* mRNA abundance in both natural and precocious metamorphosis, although the directionality of response is tissue specific. In the brain and intestine, *nr3c1* mRNA is reduced by increasing exogenous T_3, while in the tailfin it increases dramatically (Krain & Denver, 2004). Higher levels of *nr3c1* would help to potentiate the action of corticoids on gene targets with GREs.

The basic transcriptional element-binding protein/Kruppel-like factor 9 (Klf9) contains both a TRE and a GRE, allowing corticoids to modulate the T_3 response (Bonett et al, 2009; Furlow & Kanamori, 2002). Klf9 is a transcription factor that is involved in Thrb autoregulation (Bagamasbad et al, 2007), and is itself regulated by T_3 and corticosterone, demonstrating the complex cross-regulation between

hormonal signals (Bagamasbad & Denver, 2011; Bonett et al, 2009). Crosstalk between the HPT and HPA axes has also been described in rats (Helmreich et al, 2005) and zebrafish (Liu et al, 2011), with concurrent altered regulation of hormones and nuclear hormone receptors from both axes.

There is limited evidence for oxidative stress influencing the HPA axis. In a meta-analysis of research results, Costantini et al (2011) demonstrated that chronic stress and prolonged activation of the HPA via glucocorticoid administration was significantly correlated with ROS generation. Chronic stress decreases the functionality of various organ and regulatory systems in vertebrates, and is associated with decreased Darwinian fitness and increased disease susceptibility in the environment (Costantini et al, 2011). It is possible for ROS-induced oxidative stress to stimulate the HPA axis as well. ROS generated from hyperoxia increased the production of Crh, Acth, and corticosterone in rats. These effects of ROS were abolished with oral administration of the antioxidant vitamin E (Kobayashi et al, 2009).

While unregulated ROS and oxidative stress can be deleterious to cells, mitochondrial-derived ROS plays various important roles during the coordinated physiological changes of amphibian metamorphosis. During cellular respiration and production of ATP within mitochondria, small amounts of cytoplasmic ROS are generated (Boonstra & Post, 2004; Inoue et al, 2004). Apoptosis is a programmed physiological event in which a transition in mitochondrial membrane permeability generates ROS and subsequent oxidative DNA fragmentation and cell death (Inoue et al, 2004). Tailfin regression and intestinal remodelling are two major processes during amphibian metamorphosis that utilize apoptosis to degrade larval tissues while repurposing the nutrients for developing adult tissues (Inoue et al, 2004; Menon & Roman, 2007). Catalase is an enzyme that metabolizes intracellular H_2O_2, and therefore its observed T_3-induced decrease in activity and expression in tailfin allows ROS to increase to critical levels needed for programmed cell death (Hinther et al, 2010b; Kashiwagi et al, 1999). During metamorphosis, another role for ROS is in the synthesis of THs in the thyroid gland. Low levels of H_2O_2 are necessary in the Tpo-dependent incorporation of

iodine molecules onto thyroglobulin tyrosine residues, as outlined earlier (Kovacic & Edwards, 2010). ROS are also involved in reduction-oxidation (redox) signaling during cell cycle progression, important to all proliferating tissues. There is evidence that ROS act as second messengers in MAPK or tyrosine kinase signaling pathways by inhibiting the catalytic cysteine residue in protein tyrosine phosphatases (PTP; Boonstra & Post, 2004; Chiarugi et al, 2003). Transcriptional changes can be induced indirectly by activation of transcription factors such as c-Fos and c-Jun by AKT1 (Liu et al, 2002), or directly by redox sensitive DNA-binding receptors like NFKB1 that is involved in mediating cellular survival (Haddad et al, 2002). Depending on the level of ROS present, the effects on cell cycle can range from transient or permanent growth arrest to apoptosis, and very low levels of endogenous ROS have even been found to increase cell cycle progression (Boonstra & Post, 2004; Liu et al, 2002).

1.2.5 Sexual Development during Metamorphosis

After embryogenesis, tadpoles have bi-potential gonads that differentiate during metamorphosis into either ovaries or testes. Gonadal differentiation is coupled to metamorphic progression, although the timing is species-specific. In *X. laevis*, between premet stages NF46-55, potential ovaries and testes cannot be visually distinguished from each other (Kelley, 1996). However, sexual differentiation begins at NF52 (see Table 1.1; Nieuwkoop & Faber, 1994).

The immature gonads consist of an inner medulla and outer cortex regions. Germ cells migrate from cortical tissue to the medullary region to become spematogonia in males, or remain in the cortical tissue in females as oogonia. At NF53 and 54, germ cells divide while the ovaries or testes remain as compact structures. By the beginning of prometamorphosis at NF55 other structural components begin to appear, and visual differentiation between sexes becomes possible. In the testes, early seminiferous tubules develop and in the ovaries the central cavities appear within the regressing medullary tissue. In females, the central cavities have become very large at NF57 and the oocytes begin their

major growth period, continuing throughout and beyond metamorphosis. In males, by NF59 spermatocytes begin to appear in dispersed nests in the testes (Nieuwkoop & Faber, 1994). Therefore, sexual differentiation and gonadal development are part of many important physiological changes that occur during TH-dependent metamorphosis. Sexual differentiation and development are therefore coupled to metamorphic morphological endpoints.

Estrogens and androgens, primarily generated by the gonads, cause transcriptional responses through Esr and androgen nuclear receptor (Ar) respectively. Unlike Thrs, in the absence of hormone Esr and Ar associate with Hsp90 chaperones in the cytoplasm. Once hormone is present and bound to the nuclear receptors, the complex is transported to the nucleus where they form homodimers, bind to the DNA in promoter regions and increase the transcription of target genes. During *X. tropicalis* metamorphosis, *ar* and the two isoforms *esra* and *esrb* are up-regulated between NF34 and 46 (Duarte-Guterman et al, 2010). After NF52, these mRNA targets continue to increase in the gonad-mesonephros complex (GMC) until metamorphic climax (Duarte-Guterman & Trudeau, 2011). This shows that at these stages, tadpoles are competent to transcriptionally respond to signals from estradiol or testosterone.

While it is unclear to what extent TH-dependent metamorphosis and sexual differentiation are coupled, cross-talk between the two systems has been demonstrated. THs are required for *X. laevis* testicular differentiation as TH production inhibition with either thiourea or perchlorate caused female-biased sex ratios (Goleman et al, 2002; Hayes, 1997). Furthermore, exogenous administration of T_3 increased mRNA abundance for male sex-specific genes *ar*, *5α-reductase* and decreased female-related *esrb* abundance in the GMC (Duarte-Guterman & Trudeau, 2011). When premet tadpoles were administered exogenous estradiol or testosterone, metamorphosis was inhibited in *R. pipiens* (Richards & Nace, 1978) and *X. laevis* (see Figure 1.3; Gray & Janssens, 1990). Failure of sex steroids to elicit similar inhibition during *in vitro* organ cultures suggested regulation via the HPT axis by either down-regulating circulating TH levels or up-regulating proline mRNA (Gray & Janssens, 1990; Hayes, 1997; Shi,

2000). Therefore, TH-dependent metamorphosis may be intrinsically linked to sexual differentiation in amphibians, with hormones influencing either system.

1.3 Research Purpose and Hypothesis

nAg is an antimicrobial that is increasingly prevalent in consumer products and therefore has potential for both human and aquatic wildlife exposure. nAg has extensive toxicological data associated with high, cytotoxic doses, however the effects at low, environmentally relevant concentrations has not been thoroughly investigated. Initial results in our lab indicated that nAg has EDC potential at low concentrations in an *ex vivo* cultured bullfrog tailfin (C-fin) assay. Amphibian metamorphosis is an excellent model for EDC action as it is completely dependent on TH, incorporates co-ordination of multiple physiological processes, is sensitive to stress induction, and is the developmental period of initiation of amphibian sexual differentiation. TH metabolism and signaling is regulated both by the central nervous system as well as locally within tissues and cells, and therefore disruption in hormonal signaling requires a chronic *in vivo* exposure system. The first objective of this thesis was to determine the effects of nAg on TH-dependent metamorphic events at or below the concentration limits of North American water quality guidelines. A secondary objective was to investigate differential sex-biased transcription in the context of TH-dependent metamorphosis.

The effects of chronic environmentally relevant concentrations of nAg on the American bullfrog (*Rana catesbeiana*) tadpoles during metamorphosis are investigated in Chapter 2. Furthermore, the differential effects of nAg and its derivative, iAg are examined. This data represents my involvement in part of a larger research initiative. In Chapter 3, species- and stage-specific sensitivities to nAg are determined. The effects of nAg on *Xenopus laevis*, an amphibian with a shorter metamorphic period, during metamorphosis are examined. Potential biomarkers for nAg exposure are investigated. Chapter 4 outlines the development and testing of the XTC-2 cell line for use in mechanistic determination of nAg EDC action. Biomarkers of nAg exposure from Chapter 3 are tested in this *in vitro* assay.

The genetic sexing protocol in *X. laevis* was optimized and validated in Chapter 5. This protocol was then used to investigate potential sex-specific transcriptional markers during natural metamorphosis and in response to exogenous T_3 during the early stages of sex determination and gonadal differentiation.

2 The effects of chronic sublethal nanosilver exposure on *Rana catesbeiana* amphibian metamorphosis

The data presented in this chapter is part of a larger study. Exposures were performed at the Pacific Environmental Science Centre, Environment Canada, Vancouver, BC. Liver and brain RNA extractions and QPCR runs were performed by Vicki Rehaume and Austin Hammond. I would also like to thank Mitchel Stevenson, and Lauren Bergman for assistance in running the *eef1a* and *rps10* sets. FFF-ICP-MS was performed by Dr. Ehsanul Hoque in the laboratory of Dr. Chris Metcalfe, Trent University, Peterborough, ON, and nAg dissolution determined in the laboratory of Dr. Kevin Wilkinson, University of Montréal, QC. Otherwise, all data presented herein were collected and analyzed by me.

2.1 Introduction

Nanoparticles (NPs) are engineered in the nanoscale (<100nm) to have unique physicochemical properties from their larger-sized bulk counterparts that give them various industrial and commercial applications. Nanosilver (nAg) is one of the most widely used NPs due to its strong antimicrobial behaviour and is used in many products including medical supplies like wound dressings, catheters or contraceptives, and personal or household items including cosmetics, clothing, washing machines, and kitchen components (Woodrow Wilson Database, 2012, <www.nanotechproject.org>). Humans have the potential for exposure through direct contact with these materials, and aquatic species can be exposed through nAg leachate or discharge during the various product life-cycle stages including manufacture, transport and disposal in landfills (Musee, 2011).

An increasing number of studies have appeared in the literature describing general toxicity of nAg in eukaryotic *in vivo* and *in vitro* models (Kahru & Dubourguier, 2010). At high concentrations (mg/L) most studies describe inflammatory, antiproliferative, genotoxic, and cytotoxic consequences (AshaRani et al, 2009; Johnston et al, 2010) which may result in apoptosis or necrosis

(Ahamed et al, 2010a; Marambio-Jones & Hoek, 2010; Teow et al, 2011; Zhang et al, 2012). Furthermore, some studies have shown successful rescue of these deleterious effects using antioxidants to counter oxidative stress (Kawata et al, 2009; Kim et al, 2009a; Posgai et al, 2011). At relatively high, but non-cytotoxic concentrations (>100 µg/L), nAg has shown deleterious effects on reproduction in *Caenorhabditis elegans* (Roh et al, 2009), earthworms (Shoults-Wilson et al, 2011), and *Drosophila melanogaster* (Posgai et al, 2011), and development in zebrafish (Asharani et al, 2011; Zhao & Castranova, 2011).

It is possible for nAg to be oxidized and release Ag^+ ions (iAg) which are considered more toxic than elemental Ag (Drake, 2005). The small size of nAg results in an increased surface to volume ratio that causes higher iAg dissolution than the larger bulk colloidal silver. It is currently unclear whether the toxicity of nAg is due to unique, nano-specific effects from the complete NP, or whether it arises from released iAg (Johnston et al, 2010; von der Kammer et al, 2012). Some studies attribute all of the observed toxicity to iAg (Bouwmeester et al, 2011; Xiu et al, 2011; Yang et al, 2012), while others have described unique toxicities due to nanosized-Ag independent of iAg release (AshaRani et al, 2009; Carlson et al, 2008; Eom & Choi, 2010; Farmen et al, 2012; Griffitt et al, 2012; Griffitt et al, 2008; Hinther et al, 2010b; Kawata et al, 2009; Kim et al, 2009a; Navarro et al, 2008; Pokhrel & Dubey, 2012; Yang et al, 2012). It is even possible for nAg to act in a 'Trojan-horse' type mechanism where nAg are able to bypass barriers and deliver large amounts of iAg to their intracellular location (Park et al, 2010).

The toxicity of nAg has been well-studied at concentrations that cause overt toxic responses, however these concentrations are unlikely to be encountered in the aquatic environment that most wildlife species occupy. There are currently no accurate methods for differentiating between bulk silver, iAg, or nAg (natural or engineered) in environmental matrices, and therefore measuring environmentally relevant concentrations specific to nAg are dependent on advancing technology (Handy et al, 2012; von der Kammer et al, 2012). The

predicted environmental concentrations (PEC) of nAg range from 0.03 - 42.5 µg/L (Gottschalk et al, 2009; Mueller & Nowack, 2008; Musee, 2011).

The few studies that have investigated nAg effects in the low and sub- µg/L range have demonstrated or implied alterations in behaviour, reproduction, and/or development that have potential impacts on whole ecosystems. Predator detection and reproduction of Daphnia were significantly impacted by exposure to citrate-coated NP containing 2 µg/L total Ag (Pokhrel & Dubey, 2012). nAg induced disregulation of estrogen-responsive gene transcripts encoding vitellogenin, vitellogenin envelope protein beta, or choriogenin L proteins important in oocyte maturation in medaka (Pham et al, 2012) and rainbow trout (Gagné et al, 2012). Concentrations as low as 0.6 µg/L nAg disrupted regulation of thyroid hormone (TH)-responsive gene transcripts such as thyroid hormone nuclear receptor beta (*thrb*), and *Rana* larval keratin type 1 (*rlk1*) in cultured tailfin biopsies from *Rana catesbeiana* (North American bullfrog) premetamorphic tadpoles (Hinther et al, 2010b). This latter *in vitro* study implied that tadpole metamorphosis may be impacted by low dose exposure to nAg since this postembryonic developmental period is completely dependent upon TH.

Amphibians are environmental sentinels due to their sensitive, permeable skin, and dual life cycles in aquatic and terrestrial environments, and are keystone species in ecosystems, acting as both predator and prey. Amphibian metamorphosis is a complex developmental period where nearly every tissue undergoes proliferation, remodeling or apoptosis (Shi, 2000). Amphibians have no circulating TH during their premetamorphic stages, and can be induced to undergo precocious metamorphosis through exogenous administration of physiological concentrations of the bioactive form of TH, triiodothyronine (T_3). Regulation of TH synthesis, release and metabolism is controlled by the hypothalamo-pituitary-thyroid (HPT) axis with multiple levels of positive and negative feedback, and therefore *in vivo* studies are necessary to determine the potential of nAg and iAg to act as endocrine disrupting chemicals (EDCs) within whole animals.

The present study investigated the potential EDC effects of nAg at environmentally-relevant sublethal concentrations on tadpoles with an intact HPT axis. Premetamorphic *R. catesbeiana* tadpoles were chronically exposed *in vivo* for 28 d to nAg or iAg with or without exogenously-administered TH. Metamorphic stage progression, morphometrics and the levels of TH-responsive [thyroid hormone receptor alpha (*thra*); *thrb*; *rlk1*; carbamoyl phosphate synthetase (*cps*)] and stress-responsive [heat shock protein 30 (*hsp30*); catalase (*cat*)] gene transcripts were monitored.

2.2 Materials and Methods

Particle Characterization and Preparation

nAg was purchased from Northern Nanotechnologies (now known as Vive Nano, Toronto, ON; CAS 7440-22-4; Lot# AC0829LMPPTFD) with a proprietary polyacrylic acid (PAA) coating with carboxylic acid surface functionalization. Stock particle diameter was 10nm based on dynamic light scattering (DLS) and 2-6nm based on transmission electron microscopy (TEM), 99.1% purity, and at a concentration of 1500mg/L, according to manufacturer's specifications. The zeta-potential was previously determined as -41.14 mV ± 1.99 (Hinther et al, 2010b).

Actual Ag content in exposure water was determined with inductively coupled plasma mass spectrometry (ICP-MS; Elan DRCII, Perkin Elmer, Shelton, CT, USA). Dissolution of nAg into iAg in well water was examined at 12 µg/L nAg. Two samples were equilibrated for 24h and then passed through a preconditioned ultrafiltration membrane (3 kDa; PALL Corporation, Port Washington, NY, USA) to separate particulate and dissolved forms. Ag concentration in both retentate (nAg) and filtrate (iAg) was determined with ICP-MS (NexION; Perkin Elmer, Shelton, CT, USA).

Field flow fractionation online with ICP-MS (FFF-ICP-MS) was used to characterize the aggregation state and size distribution of nAg in exposure water. The FFF-ICP-MS method has previously been reported (Hoque et al, 2012), in brief, FFF was performed in the AF2000 Focus system (Postnova Analytics, Landsberg, Germany). In the FFF channel, a regenerated cellulose membrane

with a molecular weight cut-off of 10 kDa was used as the accumulation wall with a spacer thickness of 350 µm. ddH_2O water was used as the carrier fluid. The FFF system was interfaced with ICP-MS (Varian 820, Bruker Optics Ltd., Mississauga, ON) to detect eluted silver nanoparticles. Sample injection volume was 0.1 mL at 60 µg/L of stock nAg diluted in exposure water. The sizes of particles or aggregates in the exposure solutions were estimated from a calibration graph (i.e., nanoparticle size (10 to 60 nm) vs. retention time; n = 4; Figure 2.1C). nAg was added to vats of well water at nominal final concentrations (0.06 and 6 µg/L NP) which were then used to refill tanks after water changes. For the LoAg (0.06 µg/L) exposure, 1/100 working stocks from stock nAg concentrations were created. nAg was added directly to vats in a 1/250000 dilution, with 800 µl (stock or working stock) into 200 L well water.

Experimental Animals

The exposures were carried out by the staff at the Pacific Environmental Environment Centre (PESC) in Vancouver, BC using premet *R. catesbeiana* tadpoles between Taylor Kollros (TK; 1946) developmental stages IV-X which were wild-caught from the lower mainland of British Columbia. Animals were kept in 35 L tanks filled with well water ± treatment for the duration of the exposures. Water temperature was maintained at 20.41 ±0.07°C with 84.2 ±0.4% dissolved oxygen and pH of 7.78 ±0.01. The photoperiod was kept at 12/12hrs light/dark. The exposure was a static renewal system, and water was replaced every 2-6 d with prepared treatment water, after which tadpoles were fed algal pellets. Nitrogenous wastes were monitored and kept within non-toxic levels for ammonium (15 ±5 µg/L), nitrite (13 ±3 µg/L), and nitrate (71 ±18µg/L). Two animals were placed into each tank and followed individually throughout the experiment to enable a repeated measures design for morphological parameters. At the termination of the exposure, animals were euthanized with 0.1% (w/v) tricaine methanesulfonate (MS-222; Syndel Laboratories Ltd, Vancouver, BC) in well water buffered with 25 mM $NaHCO_3$. Animals used in the present study were treated and maintained in accordance with the guidelines of the Canadian

Council on Animal Care and the Animal Care Committee guidelines of the University of Victoria.

Exposure Setup

Two-28 day chronic exposures were performed: the first exposure was performed in March 2009 and involved immersion in 6 µg/L (HiAg) nominal Ag concentration and the second exposure was performed in October 2009 and involved immersion in 0.06 µg/L Ag (LoAg). The exposure setup was modified from the Organization for Economic Cooperation and Development (OECD) Amphibian Metamorphosis Assay (AMA) guidelines (2009). Immersion conditions in each exposure consisted of a well water control and two Ag concentration-matched treatments of either nAg or iAg (from $AgNO_3$; CAS: 7761-88-8; Fisher Scientific, Asheville, NC, USA, Cat#:351260100), a control for complete dissolution of nAg (Figure 2.1). On experimental day 4, all tadpoles received a 0.1% (v/w) intraperitoneal injection of either vehicle alone (100 nM NaOH final) or T_3 (10 nM final; 3,3′,5-triiodo-L-thyronine, CAS: 55-06-1; Sigma-Aldrich, Oakville, ON, Cat#:T2752-1G) according to the weight of each animal, resulting in 24 tadpoles per treatment group. At 48h post-injection (experimental day 6), tissues were collected from half of the animals within each of the 6 different experimental groups (see Figure 2.1, n=12 tadpoles/group). Liver, brain and tailfin were collected for transcript analyses. The remaining animals were monitored at the indicated timepoints for morphometric endpoints such as weight, tail (TL), snout-vent (SVL) and leg length (LL), and metamorphic progression defined by developmental TK stages until exposure termination on experimental day 28. Individual tadpoles were tracked so changes could be normalized to each tadpole's baseline, correcting for inter-individual variation. At experimental day 28, tailfin tissue was collected for transcriptional analysis (n=12 tadpoles/group). No mortalities were observed under any study condition. All collected tissues were tracked to individual animals and this tracking was maintained throughout the analyses.

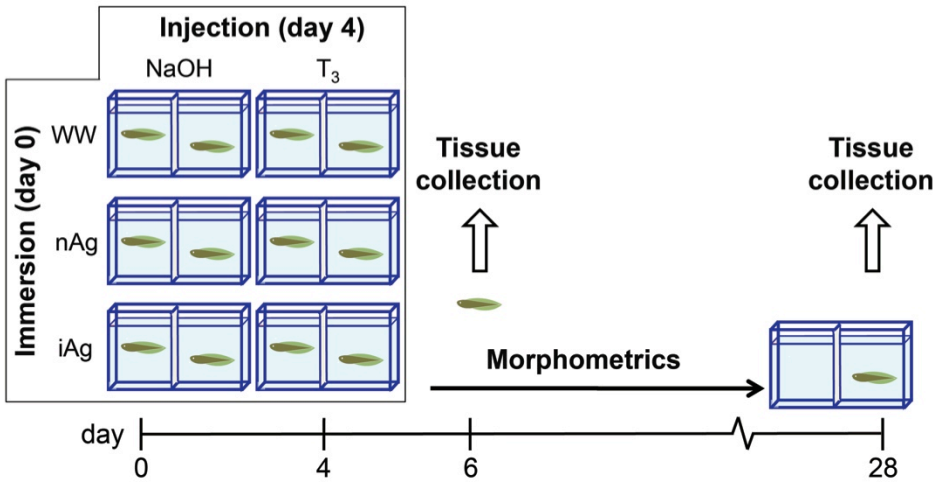

Figure 2.1 – Experimental treatments and setup for both exposures at 0.06 and 6 µg/L Ag. Tadpoles were immersed in well water (WW) alone or containing nAg or iAg on experimental day 0. On day 4, half of the tadpoles were injected with 10 nM T_3 and the other half with NaOH vehicle solution. On day 6, tissues were collected from half of the tadpoles in all of the treatment conditions (n=12) whereas the remaining animals were maintained in the immersion conditions and their morphology monitored until day 28 at which time tissues were collected from these animals (n=12 per treatment condition).

Quantification of Transcript Abundance

Tadpole liver, brain and tailfin tissues were preserved in RNAlater (Qiagen, Toronto, ON, Cat#:76106) after dissection, and stored at -20°C. RNA was extracted with TRIZOL reagent (Invitrogen, Grand Island, NY, USA, Cat#:15596-018) according to manufacturer's protocol. Prior to isopropanol precipitation 20µg of glycogen (Roche, Mississauga, ON, Cat#:10901393001) was added to samples to increase RNA yield. RNA pellets were resuspended in diethyl pyrocarbonate (DEPC)-treated RNase-free water, quantified using Nanodrop UV-Vis spectrophotometer (ND-1000, Thermo Scientific, Wilmington, DE, USA), and stored at -80°C. Complementary DNA (cDNA) was generated using 1 µg total RNA in the high capacity cDNA reverse transcription kit with RNase inhibitor (Applied Biosystems, Burlington, ON, Cat#:4374967) according to kit protocol. cDNA from brain and liver was diluted in RNase-free ddH_2O 1/40, and tailfin cDNA 1/20, and stored at -20°C.

Transcript levels were determined by quantitative real-time polymerase chain reaction (QPCR) on Stratagene MX3005P machines (Agilent Technologies, La

Jolla, CA, USA) using comparative cycle threshold analysis (ΔΔCt; Livak & Schmittgen, 2001). Target gene primer sequences, amplicon sizes, optimized thermocycle profiles, and quality control measures are listed in Table A.2 in Appendix A. Amplification efficiency and amplicon sequences were confirmed for all target primer pairs as suggested by the MIQE guidelines (Bustin et al, 2010). Biological samples were run in quadruplicate with a no-template control and an inter-plate standard to determine primer-dimer interactions and machine variation, respectively. One unit of Maxima™ Hot Start *Taq* DNA polymerase (Thermo Scientific, Rochester, NY, USA, Cat#:EP0602) was used in each reaction with 2 µl cDNA template with SYBR Green I (Molecular Probes Inc., Eugene, OR, USA) as the fluorophore. The threshold for each gene of interest was established within the window of linearity region during exponential amplification (Ruijter et al, 2009) and was constant across all plates for each gene. The cycle at which the target gene signal crosses the threshold (Ct) was normalized to the geometric mean of invariant transcript Cts for eukaryotic translation elongation factor 1 alpha (*eef1a*), ribosomal protein L8 (*rpl8*), and ribosomal protein S10 (*rps10*) to correct for cDNA input (see Table A.1 in Appendix A).

Statistical Analysis

Stage progression was tracked by individual and relative to each individual's initial starting stage on experimental day 0. The number of stages traversed was scored and contingency tables based upon the frequency of progression through 0, 2, 4, 6, or 8 stages (where applicable) were analyzed using Fisher's Exact test (www.quantitativeskills.com/sisa). To minimize inter-individual variation all other morphometric endpoints were normalized to each animal's baseline by the following equation:

$$\frac{Tn - T_0}{T_0}$$

where T_0 is the value at exposure initiation and Tn is the value at each subsequent time point. Morphometrics and QPCR results were not consistently

normally distributed or homoscedastic as determined by the Kolmogorov–Smirnov and Levene's test, respectively, therefore the non-parametric Kruskal-Wallis test (KW) was used at each time point across treatment groups with subsequent pairwise comparisons on statistically significant groups using the Mann-Whitney U (MW) test. Statistical significance was considered at p-value < 0.05. For pairwise comparisons, respective controls for the nAg and iAg immersion treatments were the well water negative controls within each injection type (NaOH vehicle or T_3).

2.3 Results

nAg Characterization in Exposure Medium

NP behavior can vary widely depending on the exposure system used, and therefore it is extremely important to determine what the distribution and concentration of NP is within each study (Handy et al, 2012). Stock nAg (Figure 2.2A) showed signs of slight aggregation over a range of 7.4-43.3 nm, with a peak maximum at 17 nm. This is slightly larger than the 10 nm diameter as specified by the manufacturer.

nAg showed a greater degree of polydispersity in the exposure water with two distinctly sized populations at 11.7 nm (range: 4.2-23 nm) and more prominently at 47.8 nm (range: 37.5-63.3 nm; Figure 2.2B). While a portion of nAg likely remained as single particles, this indicates that more had aggregated to some degree. A bimodal distribution in nAg size was also observed in the chronic exposure of sheepshead minnows (Griffitt et al, 2012), and the authors speculated that the smaller peak (around 3 nm) was possibly due to fragmentation of nAg. It should be noted that, due to instrument limitations, the concentration tested (60 µg/L) was 10-fold higher than the HiAg exposure (6 µg/L).

Ag content in nAg particles was determined to be 29.29% of total NP by weight by ICP-MS (Hinther et al, 2010b), which resulted in the iAg treatments having approximately 3x more total Ag present than the equivalent nAg concentration.

While it is unclear to what degree nAg was oxidized during the exposure, the Ag concentration in the iAg treatment would more than account for the complete dissolution of nAg. Actual exposure concentrations of Ag as measured by ICP-MS were 0.95 and 3.36 µg/L for nAg and iAg, respectively, in the HiAg (6 ug/L) exposure, and 0.09 and 0.12 µg/L for nAg and iAg, respectively, in the LoAg (0.06 µg/L) exposure. The dissolution of nAg at 12 µg/L was very low at 4.5% ±1, indicating most Ag within the nAg treatments remained in particulate form. Ag content in the well water control treatments was 0.045 and 0.055 µg/L in the LoAg and HiAg exposures, respectively.

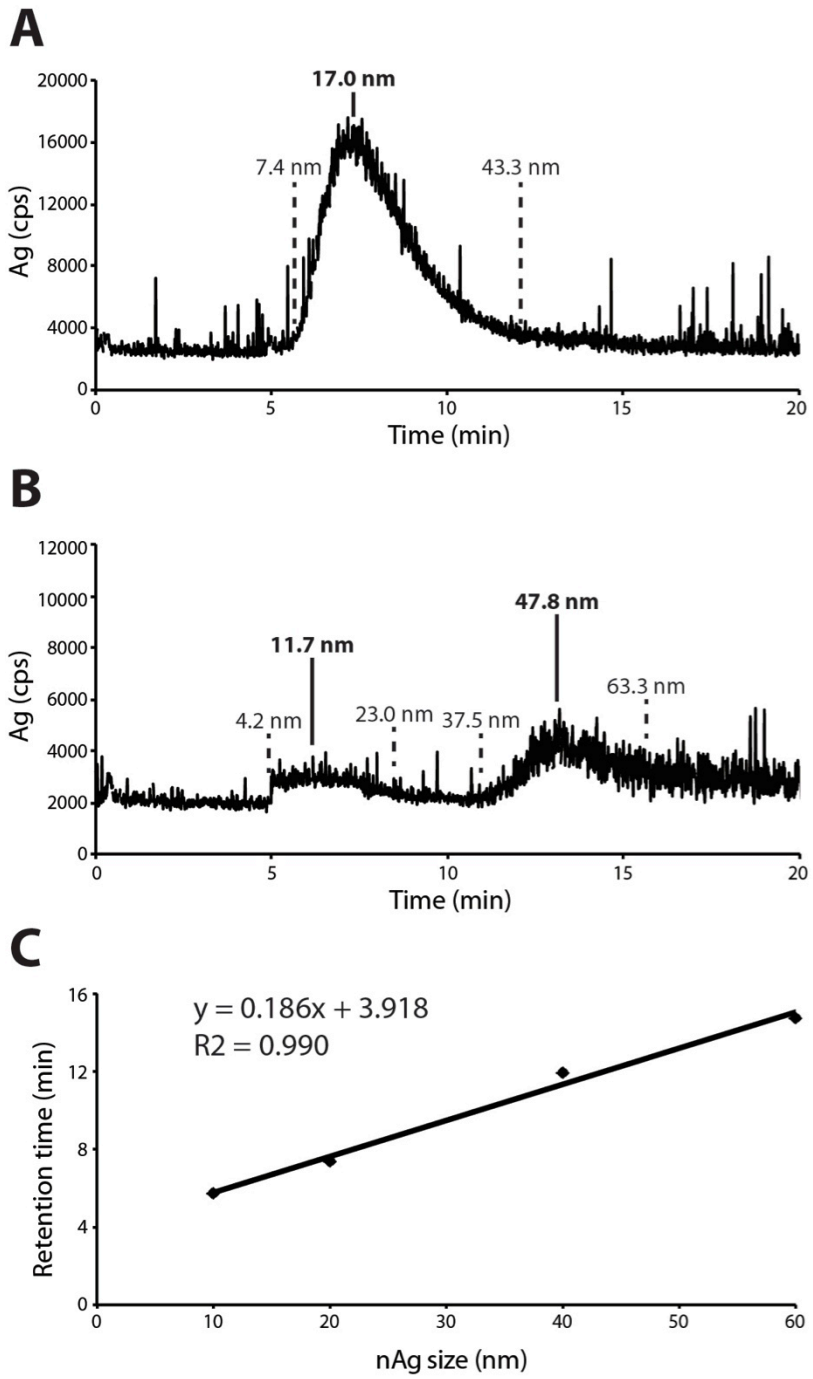

Figure 2.2 – FFF-ICP-MS separation of nAg in *R. catesbeiana* exposure water. A) stock nAg injected at 1500mg/L and **B)** nAg diluted to 60 µg/L in exposure water, detected at 420 nm with on-line UV-VIS spectrometry**. C)** Calibration curve used to determine nAg aggregate size based on retention times of known nAg standards (10-60 nm). (Partially adapted from Hoque et al, 2012).

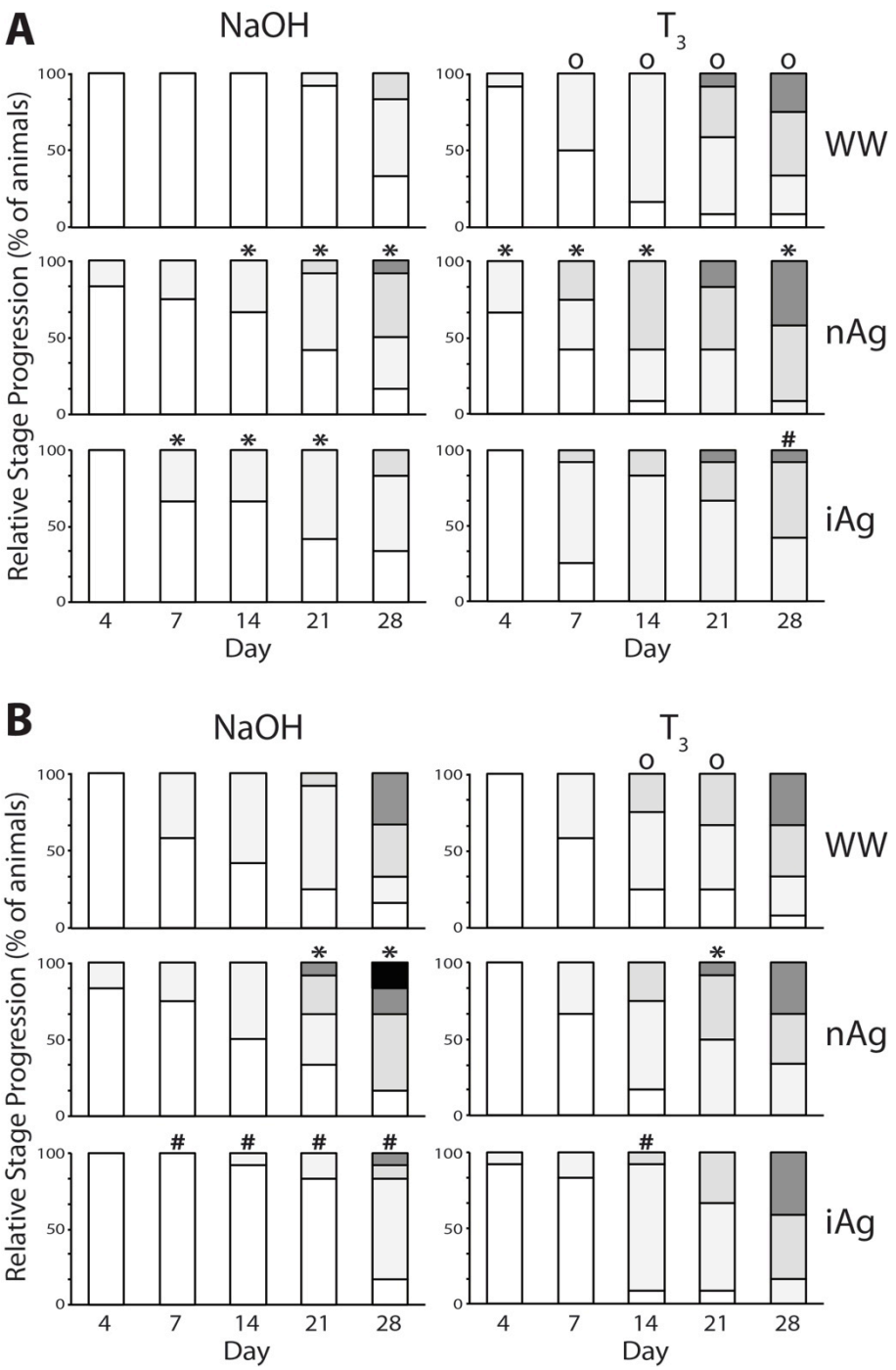

Figure 2.3 – Effects of nAg and iAg on individual stage progression through metamorphosis. Tadpoles were chronically immersed in either **A)** LoAg (0.06 µg/L Ag) or **B)** HiAg (6 µg/L Ag) with injection of either NaOH vehicle or 10 nM T_3 on experimental day 4. White bars represent no change in stage and each subsequently darker shade represents progression of an individual through 2 TK (Taylor & Kollros, 1946) stages up to 8 stages (black) with 12 animals per treatment. Significant acceleration (∗) or deceleration (#) compared with respective well water (WW) controls at concurrent time points is shown when p-value <0.05. Significant T_3-induced acceleration of metamorphosis is indicated by an open circle (o).

Morphology

The metamorphic timing was consistently accelerated by exposure to nAg (Figure 2.3A and B). Both 0.06 and 6 µg/L nAg accelerated natural and precocious metamorphosis compared to their respective controls, with a more significant acceleration was seen in the LoAg animals. The iAg did not have consistent effects on developmental timing. At 0.06 µg/L iAg, natural metamorphosis was accelerated while a delay was seen post T_3-injection compared with respective well water controls. At 6 µg/L iAg, stage progression was consistently delayed. By exposure day 28, all animals in both Hi and LoAg exposure sets had progressed on average to TK stage X, with a maximum of TK XIV, corresponding with the onset of prometamorphosis.

There was a differential sensitivity of tadpoles to T_3-injection to induce precocious metamorphosis between the two exposures. Over the 28 d experiment, control tadpoles injected with vehicle alone progressed through development at a faster rate in the HiAg exposure set compared to the LoAg exposure set (compare top left panels of Figure 2.3B to A). As a consequence, tadpoles in the LoAg exposure set had a stronger relative response to T_3 injection than those in the HiAg exposure set. T_3 alone increased the TL and LL in the LoAg exposure set, while a reduction of SVL was seen in HiAg exposure set tadpoles (Figure A.1, Appendix A). Weight was differentially influenced by T_3 in the two exposure sets, being increased and decreased in the LoAg and HiAg exposure sets, respectively.

Ag-induced effects on morphology were most evident during T_3-induced metamorphosis. At equivalent time points more perturbations were observed in the LoAg exposure set (Figure 2.4) than in the HiAg exposure set (Figure 2.5), consistent with the greater sensitivity to T_3 observed in the LoAg exposure set tadpoles. While nAg and iAg caused a similar decrease in SVL and weight, there were differential responses as well. nAg caused a greater decrease in TL than iAg, while LL was decreased due to iAg only.

Transcriptional Response

QPCR was used to determine the transcriptional response to Ag in three tissues at exposure day 6 (Figure 2.6A-C). Transcriptional responses to T_3 have been previously well-characterized, and mRNA abundance of *thra, thrb, rlk1* and *cps* all followed the expected pattern in liver (Figure 2.6A; Atkinson et al, 1996; Mukhi et al, 2010), brain (Figure 2.6B; Helbing et al, 2007a), and tailfin (Figure 2.6C; Helbing et al, 2007b; Hinther et al, 2010a), indicating the animals were sensitive and competent to respond to T_3-induced precocious metamorphosis.

Because tailfin tissue is a late responder to T_3 (Shi, 2000), it was also examined at exposure day 28 (Figure 2.6D). nAg and iAg caused differential perturbations in the TH responsive genes, *thra, thrb,* and *rlk1,* mostly in T_3-injected tadpoles. After 6 days of exposure to 6 µg/L nAg, the T_3 responses of *thra* and *thrb* were reduced in the liver and *rlk1* increased by approximately 4-fold in the brain. iAg caused a reduction in the *thra* T_3-response at both 0.06 and 6 µg/L in the liver. While there were no Ag-induced transcriptional changes in the tailfin at exposure day 6, both *thrb* and *rlk1* were affected after 28 days. At both 0.06 and 6 µg/L nAg, *thrb* abundance increased in precociously metamorphosing animals. Furthermore, in the LoAg exposure set, while both nAg and iAg perturbed the *rlk1* transcriptional response, only iAg caused an increase in *thrb* abundance.

No transcriptional perturbations were observed within the stress-responsive genes, *hsp30* and *cat* due to either silver exposure.

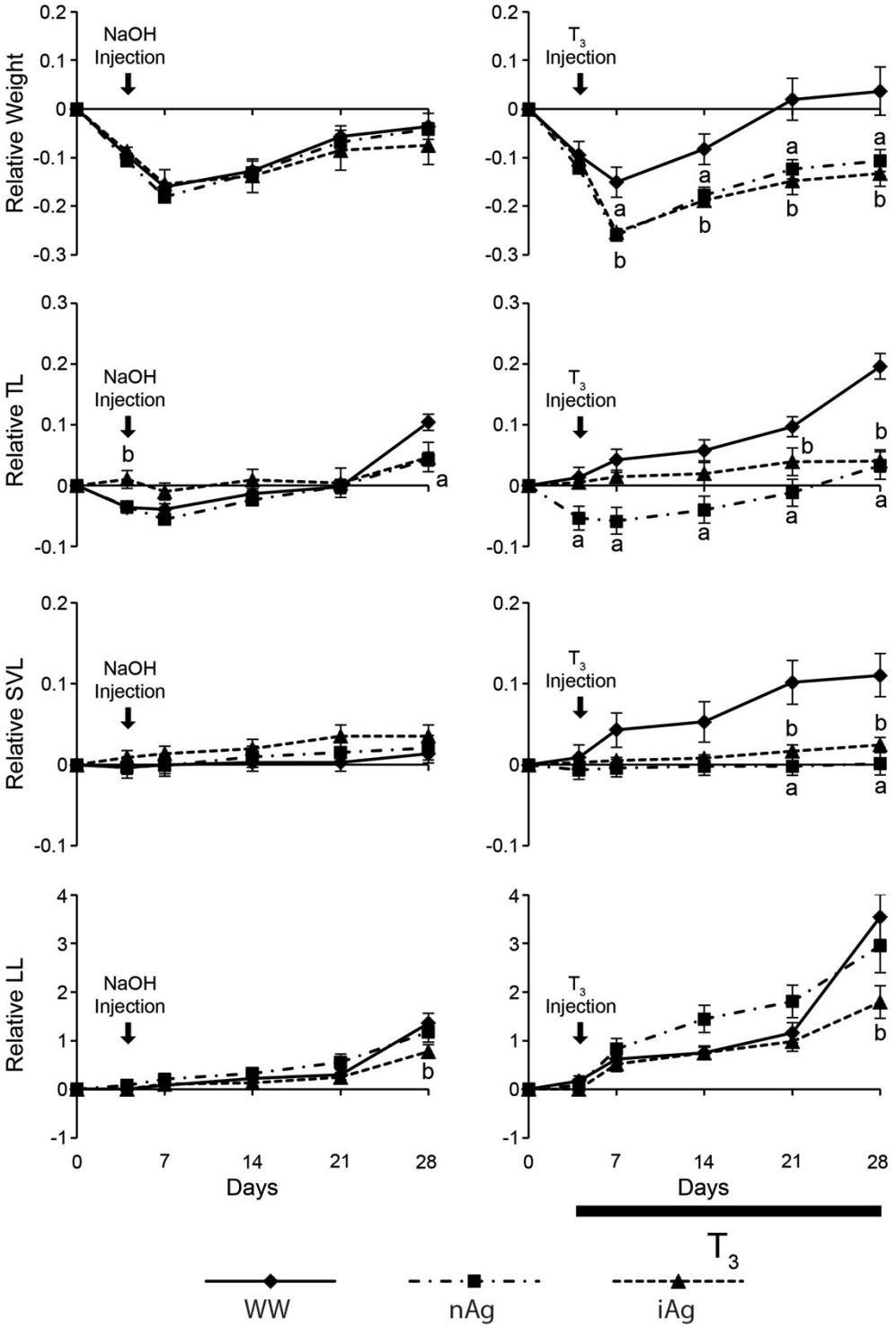

Figure 2.4 – Effect of LoAg (0.06 µg/L Ag) on weight, tail length (TL), snout-vent length (SVL), and leg length (LL). Mean relative values (±SEM) shown for individually tracked tadpoles throughout the 28 d chronic exposure after injection at exposure day 4 with either vehicle (NaOH) or T_3. Significant differences at each time point for nAg (a) or iAg (b) from the well water (WW) control were denoted when p-value <0.05.

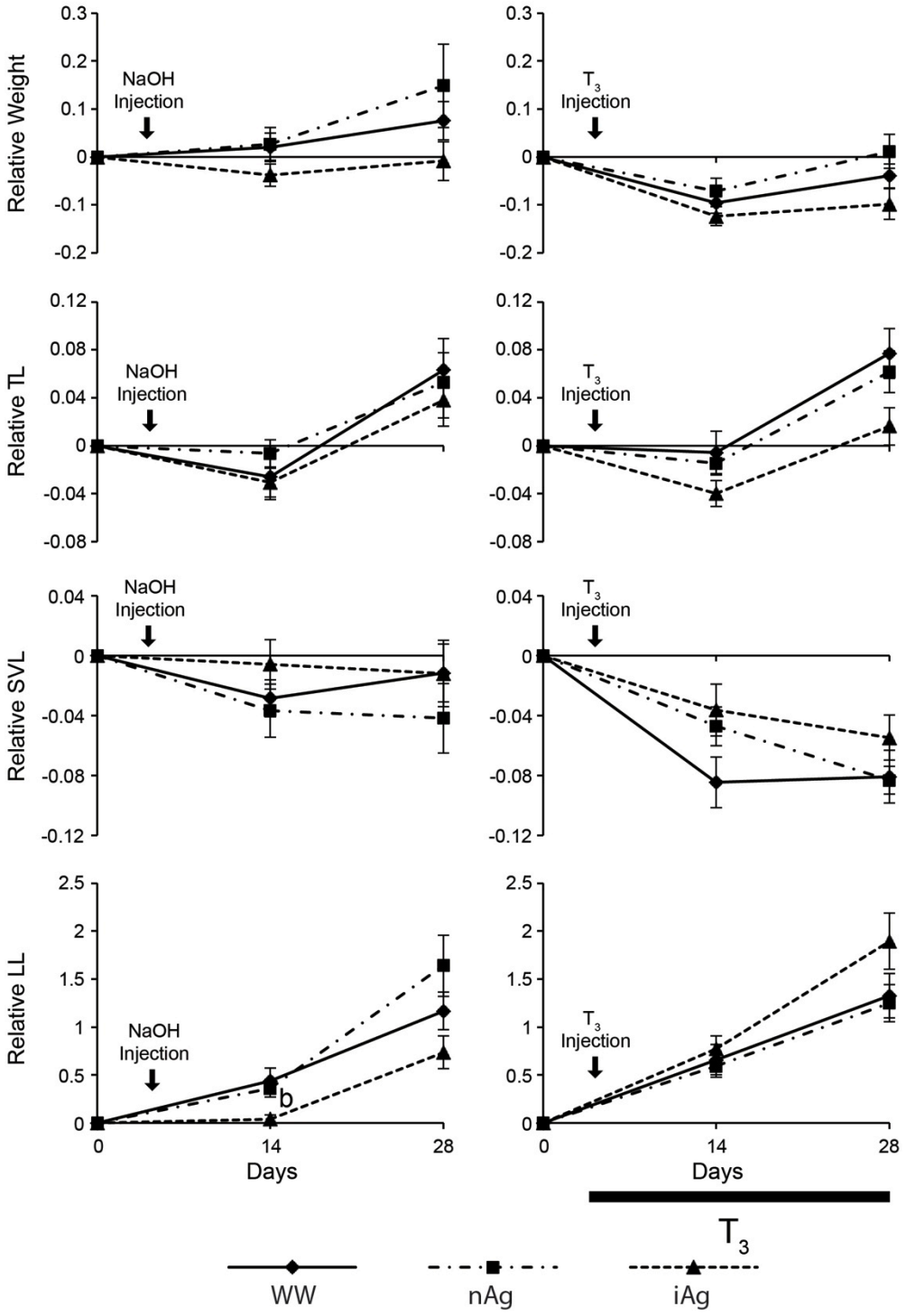

Figure 2.5 – Effect of HiAg (6 µg/L nAg) on weight, tail length (TL), snout-vent length (SVL), and leg length (LL). Mean relative values (±SEM) shown for individually tracked tadpoles throughout the 28 d chronic exposure after injection at exposure day 4 with either vehicle (NaOH) or T_3. Significant differences at each time point for nAg (a) or iAg (b) from the well water (WW) control were denoted when p-value <0.05.

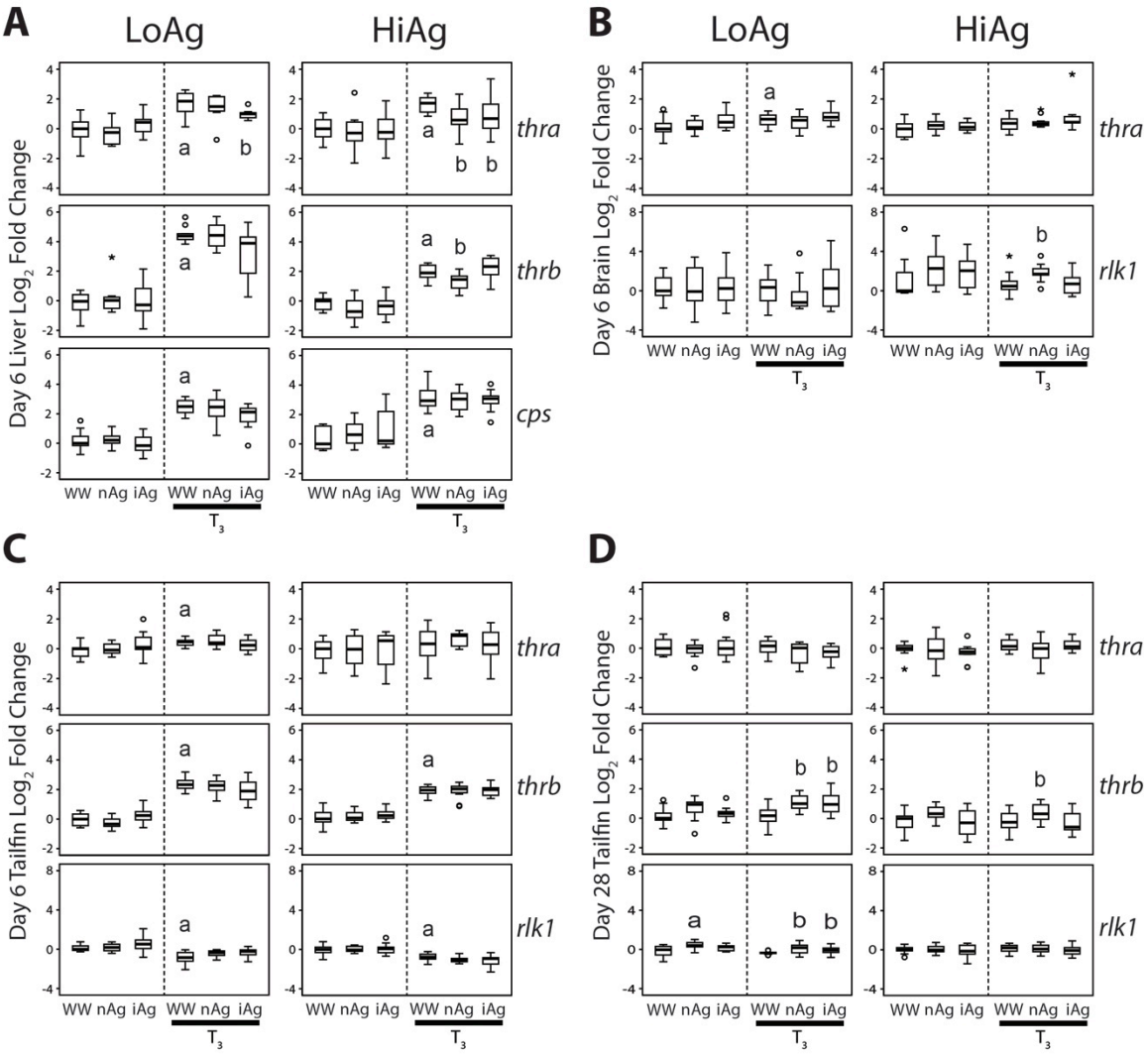

Figure 2.6 – Effects of nAg and iAg on transcript abundance in liver, brain and tailfin tissue. QPCR was used to determine differential transcript abundance in LoAg (0.06 µg/L Ag) and HiAg (6 µg/L Ag) exposures, after injection at exposure day 4 with either vehicle (NaOH) or T_3. Data from **A)** liver, **B)** brain and **C)** tailfin 48h after injection (experimental day 6) or **D)** tailfin at experimental day 28 were normalized to the geometric mean of invariant transcripts *rpl8*, *rps10* and *eef1a*, and are expressed as $\log_2$ relative fold change from NaOH well water (WW) control. Bars denote medians and boxes enclose the 25th and 75th percentile. Whiskers represent the remaining quartiles excluding outliers (°) and extreme values (*) beyond 1.5x and 3x box height respectively. Significance shown at p-value <0.05 compared with the NaOH WW control (a), or the T_3 WW control (b). *thra/b*: thyroid hormone receptor alpha/beta, *cps*: carbamoyl phosphate synthetase, *rlk1*: *Rana* larval keratin type 1.

2.4 Discussion

Differential T_3 sensitivity

A differential sensitivity between the two cohorts of tadpoles from each exposure was observed. Tadpoles in the LoAg exposure set had a stronger response to T_3-injection than those in the HiAg exposure set as was seen in both morphology and transcript changes. The HiAg and LoAg exposure sets were carried out in March and October respectively using wild-caught tadpoles. It is possible that seasonal differences between the tadpole populations may explain the differential sensitivity as it has been demonstrated to affect metamorphic timing in the species *Fejervarya limnocharis* (Indian rice frog) which has a relatively short metamorphic period (Kuan & Lin, 2011). Bullfrogs have a much longer larval phase from months to years and therefore seasonal timing is critical for their survival. With apparent inter-population influences on the extent of T_3-responsiveness, it is important to interpret the nAg response within the context of each exposure as the tadpoles may show a differential sensitivity to nAg as well.

Morphological Response to nAg

Clear acceleration of metamorphic timing was seen with nAg exposure in both natural and precocious metamorphosis, and tadpoles from the LoAg exposure set showed a stronger response. Accelerated metamorphosis can have deleterious effects on the survival of juvenile froglets as it has been associated with reduced immune response shortly after metamorphosis, which can increase susceptibility to pathogens (Gervasi & Foufopoulos, 2007). However, for the duration of both exposures the span of developmental stages in any treatment ranged between TK IV to TK XIV, spanning premetamorphosis into the onset of prometamorphosis. These stages are almost completely defined by hindlimb and toe differentiation and morphology (see Table 1.1, Chapter 1). As the time to complete metamorphosis could not be established during the 28 day exposure period, it is impossible to differentiate between overall acceleration of metamorphosis and tissue-specific effects on hindlimb growth and development. Investigating these effects on another amphibian species with a shorter

metamorphic period such as *Xenopus laevis* or *Pseudacris regilla*, would help determine whether nAg has EDC potential globally on the whole metamorphic regulation, or locally in a tissue-dependent manner.

nAg had an opposite effect from T_3 on SVL, TL and weight in the LoAg exposure set. Where T_3 increased growth, nAg inhibited it. Tailfin is typically a late responder, as it only starts to apoptose after metamorphic climax when T_3 concentrations are high (Shi, 2000). Weight and SVL are indicators of tadpole size and growth, and their increase is consistent with the prolonged feeding behaviour during early metamorphosis (Hourdry et al, 1996). This serves to add mass to tadpoles and leads to larger juvenile froglets after metamorphosis (Kuan & Lin, 2011). It is therefore possible that nAg effects on these parameters are not directly mediated by T_3 agonism or increased hormonal abundance, as the two responses differ.

Transcriptional profile is tissue specific

nAg altered transcriptional regulation in a tissue specific manner. The T_3-induced increase in *thra* was attenuated only in the liver, and was not altered in the brain or tailfin with nAg exposure. Furthermore, *thrb* responded in opposite ways between the liver and tailfin. *rlk1* was the only transcript with consistent responses, with increased expression in both the brain at experimental day 6 and tailfin at experimental day 28. Therefore, nAg seemed to affect the transcriptional regulation independently in each tissue. Furthermore, the profile of *thrb* and *rlk1* in the tailfin at experimental day 28 was consistent with a previous study using the C-fin assay (Hinther et al, 2010b).

It is important to note that as tadpoles were treated by immersion *in vivo*, each tissue could be exposed to nAg via different routes. For example, tailfin is in direct contact with nAg in the water column, while the brain and liver would only be exposed to nAg after uptake into the blood. Several studies have also indicated that the liver is the preferential tissue of nAg accumulation *in vivo*, given its role in filtering the blood of toxins (Choi et al, 2010; Johnston et al, 2010; Park et al, 2010; Scown et al, 2010; Yildirimer et al, 2011). The behaviour and

dissolution of nAg may differ when in the water and blood, and technological limitations have impaired determination of the relative contribution of iAg in tissue distribution (Johnston et al, 2010).

nAg had more transcriptional modifications when either exogenous or endogenous T_3 is present. In the tailfin, no transcriptional alterations due to either Ag type were seen until experimental day 28 when tadpoles were entering prometamorphosis, marked by the initiation of endogenous TH synthesis. Hinther et al (2010b) described alteration in transcript levels of *thrb* and *rlk1* in *R. catesbeiana* tailfin only after exogenous T_3 exposure. Also, brain and liver transcriptional alterations due to nAg were only seen in T_3-injected tadpoles. It is possible that nAg interferes with transcriptional machinery in the presence of T_3. The binding of T_3 to its nuclear hormone receptors induces conformational changes and alterations in associated protein complexes involved in transcriptional regulation, in a tissue specific manner (Shi, 2000). nAg could interfere with the changes induced by T_3 either directly by interfering in with receptor-cofactor interactions, or indirectly through (de)-phosphorylation events which alter nuclear receptor binding affinity to DNA. Therefore while assays like the C-fin and cell culture exposures are important for high-throughput screening, tissue specific differences highlight the importance of *in vivo* studies that incorporate the varied mechanisms of response within the whole body.

nAg-Induced Cellular Stress Events

nAg did not alter stress responsive transcript levels of *hsp30* and *cat* in any condition. This correlates with previous findings in the C-fin assay, where little or no stress response was detected in these two gene transcripts upon nAg exposure (Hinther et al, 2010b). However, the endpoints presented here are part of a larger research study, where metabolomics analysis was conducted on tadpole serum at experimental days 6 and 28. The metabolite data provide evidence of nAg-induced oxidative stress from the production of various antioxidants, and inflammatory responses demonstrated via prostaglandin synthesis and metabolism (unpublished data, Helbing, CC). At higher

concentrations oxidative stress is believed to be one of the major factors driving nAg toxicity (Johnston et al, 2010; Marambio-Jones & Hoek, 2010; Yildirimer et al, 2011). Furthermore, at similarly low concentrations of nAg to those used in the present study, stress-responsive transcriptional changes and lipid peroxidation were seen in *in vivo* rainbow trout exposures (Gagné et al, 2012). Therefore it is likely that some ROS is being generated even at these low concentrations. Furthermore, while *cat* and *hsp30* are useful in determining cellular stress events due to other toxicants (Hinther et al, 2011; Hinther et al, 2010b), it is possible that they do not represent the most sensitive gene transcripts to detect oxidative damage caused by low levels of nAg in metamorphosing *R. catesbeiana* tadpoles.

While there may be a degree of ROS produced from nAg in this exposure, it is unclear what deleterious effects, if any, it may cause. At low concentrations, ROS may even play a role in cell cycle regulation within cells. Endogenous ROS produced from mitochondrial respiration is involved as a second messenger in intracellular signaling such as mitogen activated protein kinase (MAPK) and tyrosine kinase pathways (Boonstra & Post, 2004; Chiarugi et al, 2003), and has been associated with cellular proliferative events (Boonstra & Post, 2004; Liu et al, 2002). Furthermore, low nAg concentrations have also been associated with cellular proliferation of human hepatoma cells (Kawata et al, 2009). In the present study, nAg-induced metamorphic acceleration was described, as defined by hindlimb growth and differentiation, a physiological process heavily reliant on cellular proliferation (Shi, 2000). While it was not possible to differentiate between hindlimb growth and overall acceleration of metamorphic timing, it is possible that ROS generated by nAg induced cellular proliferation causing accelerated hindlimb development. Further research is needed to determine whether the effects of nAg on the hindlimb were tissue-specific or a global phenomenon, and the role of ROS in that response needs verification.

Contribution of iAg to the nAg response

It is clear that iAg also has impacts on TH signaling, although not always corresponding with nAg effects. While nAg mostly accelerated stage progression, iAg had inconsistent effects, mostly causing a delay in progression. This was mirrored by the decrease seen in LL due to iAg exposure, in both LoAg and HiAg exposure sets. As discussed above, leg and foot-pad morphology are critical in defining the developmental stages of the tadpoles in these exposure sets, so it is unsurprising that a smaller LL correlates with the delay in metamorphic timing. However, no concurrent increase in LL was determined in nAg treated animals that were accelerated through metamorphosis, indicating that stage progression may be a more sensitive indicator of developmental perturbations than LL, especially when animals are individually tracked. This highlights the difference in response to the two types of Ag, and it is possible there are NP-specific effects extraneous to Ag dissolution.

nAg and iAg had a similar effect on weight, SVL and TL after T_3 injection in the LoAg exposure set. Size and growth are regulated strongly by feeding behaviour, which changes throughout metamorphosis as the digestive tract is remodelled (Hourdry et al, 1996). Therefore, both silver types may have an inhibitory effect on feeding behaviour, although this was not directly monitored. Similarities are also found in the transcriptional profile, as both silver types regulated target gene transcripts in the same direction. *rlk1* mRNA abundance was increased in the tailfin, while in the liver, the T_3 response of both *thr* transcripts was attenuated, although iAg affected only *thra,* not *thrb*. In general, there were more transcript perturbations by nAg than iAg.

Clearly there are both similarities and differences between the nAg and iAg responses. The similarities indicate that at least a portion of the effect due to nAg may be mediated by release of Ag^+ ions. This is in agreement with studies that attribute all effects of nAg to the liberated iAg (Bouwmeester et al, 2011; Xiu et al, 2011). However, the differences seen in hindlimb development indicate that there may be inherent effects due to the whole NP that can't be completely explained by the oxidized Ag alone. Therefore, the present study also concurs

with many studies which have identified NP specific effects (AshaRani et al, 2009; Carlson et al, 2008; Eom & Choi, 2010; Farmen et al, 2012; Griffitt et al, 2012; Griffitt et al, 2008; Hinther et al, 2010b; Kawata et al, 2009; Kim et al, 2009a; Navarro et al, 2008; Pokhrel & Dubey, 2012; Yang et al, 2012). Either way, iAg also plays a role in the perturbation of TH signaling.

Conclusions

nAg caused clear perturbations in T_3-mediated events including transcriptional disregulation and hindlimb differentiation, classifying it as an TH EDC. TH signaling is a well-conserved hormonal system and is integral to vertebrate development. There are many levels of TH regulation within the whole body, and further research is necessary to determine at which level nAg exerts it effects.

Coordination of physiological processes during metamorphosis is important to the survival and fitness of juvenile froglets. Amphibians are environmental sentinels, and the results presented in the present study in conjunction with alterations on reproductive potential and behaviour in vertebrates (Gagné et al, 2012; Pham et al, 2012) and invertebrates (Pokhrel & Dubey, 2012), show that further study is needed to determine the effects of low, environmentally relevant nAg concentrations on whole ecosystems.

3 The effects of chronic sublethal nanosilver exposure on *Xenopus laevis* metamorphosis

The exposures in this chapter were developed, executed, and analyzed by me with the following exceptions. FFF-ICP-MS was conducted by collaborators at Trent University, Peterborough, ON and ICP-MS was performed by scientists at the Pacific Environmental Science Centre, Environment Canada. nAg dissolution was determined by collaborators at the University of Montréal, QC.

3.1 Introduction

Nanoparticles (NPs) are manufactured substances defined as having at least one dimension in the nanoscale (<100nm), giving them unique physico-chemical from their bulk counterparts. Nanosilver (nAg) is the most widely used NP in consumer products due to its strong antimicrobial activity (Woodrow Wilson Database, 2012, <www.nanotechproject.org>). Potential exposure routes include direct contact in humans, and release into the environment during the manufacture, transport, use and disposal stages of product lifecycles (Marambio-Jones & Hoek, 2010). Although actual environmental concentrations are currently unavailable due to the difficulty in differentiating engineered versus naturally occurring Ag, predictive models estimate that environmental concentrations will range between 0.03 – 42.5 µg/L in European, African, and North American countries (Gottschalk et al, 2009; Mueller & Nowack, 2008; Musee, 2011). These concentrations bracket the maximum allowable Ag in water bodies according to the guidelines for the protection of aquatic life in Canada (0.1 µg/L; CCME 2007) and the USA (3.2 µg/L; NRWQC 2006b).

Many studies have investigated the toxicity of nAg at high concentrations (Kahru & Dubourguier, 2010). Cytotoxicity and genotoxicity can be caused by oxidative stress via reactive oxygen species (ROS) generation, inflammation and direct interaction of NPs with DNA, proteins and phospholipids (Arora et al, 2008; Asare et al, 2012; AshaRani et al, 2009; Bouwmeester et al, 2011; Comfort et al,

2011; Eom & Choi, 2010; Griffitt et al, 2008; Hsin et al, 2008; Kawata et al, 2009; Kim et al, 2009a; Lankoff et al, 2012; Lim et al, 2012; Nishanth et al, 2011; Park et al, 2010; Scown et al, 2010; Zanette et al, 2011; Zhang et al, 2012). Mitochondrial damage causing impaired cellular respiration is a target likely due to the evolutionary link to bacteria (Chaloupka et al, 2010; Marambio-Jones & Hoek, 2010).

Within mammalian *in vivo* exposures, nAg can become systematically available and preferentially accumulates in the liver (Johnston et al, 2010). In aquatic exposures, nAg accumulates in both the liver and/or gill tissue of Atlantic salmon (Farmen et al, 2012), brown trout (Scown et al, 2010), rainbow trout (Farkas et al, 2011a), and zebrafish (Griffitt et al, 2009). However, most of the research thus far has focused on toxic effects at lethal or high sublethal concentrations. Relatively few studies have determined the effects of nAg at environmentally-relevant concentrations that include disruption of hormone signaling pathways.

Endocrine disrupting chemicals (EDCs) have the potential to alter hormone signaling at very low concentrations (Vandenberg et al, 2012). Thyroid hormone (TH) signaling is highly conserved in vertebrates and is integral to post-embryonic development (Shi, 2000). Amphibians are excellent models to investigate potential EDC action as metamorphosis is completely driven by TH. The active TH, 3, 5, 3'-triiodothyronine (T_3), causes varied physiological changes in embryonic tissues from *de novo* synthesis of limbs and lungs, remodelling of internal organs, to resorption of tailfin and gills. Due to the temporal nature of TH production during metamorphosis, there may be developmental periods that are more sensitive to EDC action. TH acts to regulate transcription via thyroid hormone nuclear receptor (Thr)-retinoid X receptor (Rxr) dimers bound to thyroid response elements (TREs) in target gene promoters. The presence of endogenous THs, which peak during metamorphic climax, causes conformational changes which up or down-regulate target genes, often encoding transcription factors that can then regulate other genes changing the gene expression program.

At low, environmentally-relevant concentrations, there are indications that nAg acts as an EDC on TH signaling. Our lab discovered nAg-induced alteration in TH-responsive gene transcripts in American bullfrog (*Rana catesbeiana*) tadpole tailfin biopsies (Hinther et al, 2010b). Subsequently, we examined the EDC actions of nAg *in vivo* in a chronic 28 d exposure (see Chapter 2), since an intact hypothalamo-pituitary-thyroid axis is critical for TH regulation. Perturbations of TH-responsive gene targets were again seen in the liver and tailfin consistent with the response *ex vivo*. Furthermore, the metamorphic progression was accelerated by nAg as defined by hindlimb morphology, although differentiation between tissue-specific effects on hindlimb development and time to complete metamorphosis wasn't possible due to the long metamorphic period of bullfrog tadpoles.

The purpose of this chapter was to determine if the EDC actions are consistent within another amphibian species with a shorter developmental time, *Xenopus laevis* (African clawed frog). Moreover, the in-lab breeding advantage of *X. laevis* was used to produce tadpoles at high enough numbers to investigate potential stage-specific sensitivity to nAg. A chronic 28 d exposure was conducted with 3 low concentrations of nAg (0.018-1.8 µg/L Ag). Two exposure sets were conducted, the first with premetamorphic (premet) tadpoles before plasma T_3 is present [Nieuwkoop and Faber (NF; 1994) stage 51], the second with prometamorphic (promet) tadpoles with circulating endogenous T_3 (NF56). T_3 was used as a positive control for accelerated metamorphosis and to show tadpole competence to respond to external endocrine disrupting stimulus.

The liver transcriptional profile was determined with our in-house MAGEX cDNA microarray 48 h after initial exposure to gain insight into the mechanistic effects of nAg. Quantitative real-time polymerase chain reaction (QPCR) was used to validate targets identified by microarray as potential biomarkers of nAg exposure. Animals were monitored throughout the 28 d exposure for morphometric endpoints including leg length (LL), snout-vent length (SVL), tail length (TL) and weight. Furthermore, tadpoles were collected at the end of the

exposure and pooled for whole body Ag content analysis to determine the extent of nAg bioaccumulation.

We were able to confirm that nAg consistently displayed EDC action on amphibian TH-dependent metamorphosis, and had local, tissue-specific effects on hindlimb development.

3.2 Materials and Methods

nAg Characterization

The stock nAg used in this exposure was previously described in Chapter 2, Materials and Methods. nAg aggregation state in *X. laevis* exposure water was determined by FFF-ICP-MS. Furthermore, nAg behaviour in dechlorinated H_2O was compared with tadpole rearing water to examine the effect of buffer and salt addition on aggregation state. The actual concentration of nAg in the exposure water was determined by ICP-MS (Elan DRCII; Perkin Elmer, Shelton, CT, USA) from water samples collected as described in the "Exposure setup" section below. The extent of iAg dissolution in the tadpole rearing water was measured at concentrations of 0.25, 5 and 33 µg/L nAg, as described in Chapter 2.

Chemical Preparation

All working stocks were prepared as 1000x stock solutions and diluted into exposure water at each treatment renewal. T_3 (3,3′,5-triiodo-L-thyronine; CAS: 55-06-1; Sigma-Aldrich, Oakville, ON, Cat# T2752-1G) was prepared in dH_2O with NaOH to aid dissolution. Serial dilutions were performed to generate working stock solutions of 10 µM T_3 in 50 µM NaOH. NaOH was added to all treatments including the negative control at an equivalent final concentration of 50 nM NaOH. Working stocks for the negative control and the T_3 positive control were stored at -20°C, thawed prior to each water change, and sonicated along with the nAg working stocks as noted below.

nAg was diluted in dH_2O to 1000x the highest treatment concentration (1.8 mg/L Ag) and serially diluted 1/10 to the medium and lowest treatments.

Working stocks were stored at 4°C until treatment addition or renewal. To minimize NP aggregation, working stocks were sonicated in a water bath (Bioruptor UCD-200, Diagenode Inc., Denville, NJ, USA) for 10 min on low (30 sec on/off), a maximum of 2 h prior to addition to exposure water. Sonication decreased the average particle size and increased stability in the water column as determined by dynamic light scattering (DLS; ZetaPALS, Particle Sizing Software, Brookhaven Instruments Corp., Holtsville, NY, USA) and zeta-potential (ZetaPALS, PALS Zeta Potential Analyzer, Brookhaven Instruments Corp., Holtsville, NY, USA) respectively (data not shown). DLS and zeta-potential analysis were performed according to manufacturer's instruction.

Experimental Animals

Laboratory populations of *X. laevis* were housed at the Outdoor Aquatic Unit at the University of Victoria, BC. All animals were treated and maintained in accordance with the guidelines of the Canadian Council on Animal Care and the Animal Care Committee guidelines of the University of Victoria.

Mature adults were bred by injection of human chorionic gonadotropin (Sigma-Aldrich, Oakville, ON, Cat#CG10) at 500 and 1000 IU into males and females, respectively. Eggs and newly hatched tadpoles were kept in tadpole rearing water consisting of dechlorinated water treated with $NaHCO_3$ and synthetic sea salts (Instant Ocean sea salt, Aquarium Systems Inc, Mentor, OH, USA) to a pH of 7.4-7.8 and salinity of 0.4 ppt. A pump was used to circulate water and keep dissolved oxygen (DO) >90%. After initiation of feeding behaviour and throughout the exposures tadpoles were fed Nasco frog brittle (Nasco, Modesto, CA, USA; Cat#:SA05961), ground and suspended at 10% (w/v) in untreated tap water. Tadpoles were monitored until sufficient numbers reached the appropriate developmental stage for each exposure (n=200).

Conditions were based on the Organisation for Economic Co-operation and Development (OECD) guidelines for the Amphibian Metamorphosis Assay (AMA; Guideline 231, 2009). In brief, four replicate exposure tanks (2 L glass beakers) were used within each treatment for a total of 20 tanks/exposure. Ten tadpoles

were acclimated in each tank containing 2L tadpole rearing water for 24 h prior to treatment addition. Tadpole density was maintained at approximately 5 tadpoles/L, and water adjusted to 1.2L after removal of 4 tadpoles/tank on experimental day 2. Temperature was kept at 20.3 ±0.2°C with a photoperiod of 12/12 h light/dark. Glass pipettes were used as aerators to maintain high DO, prevent stagnation, and ensure treatments were thoroughly dispersed after chemical addition. Nitrogenous wastes were monitored throughout the exposure with Aquacheck strips (Nitrate/Nitrite test strips; Ammonium test strips; Elkhart, IN, USA) to prevent toxic concentrations. Animals were euthanized with 0.1% (w/v) tricaine methanesulfonate (MS-222; Syndel Laboratories Ltd, Vancouver, BC) in tadpole rearing water with 25 mM $NaHCO_3$.

Exposure Setup

The exposure setup was based on the OECD AMA guidelines for the testing of TH EDCs (OECD, 2009). Two 28 d exposure sets were conducted: one with premet and the other with promet tadpoles starting at NF51 and NF56, respectively. In each exposure, tadpoles were immersed in tadpole rearing water containing 1 of 5 treatments: negative control with 50 nM NaOH (Ctrl), T_3 positive control (10 nM T_3 in 50 nM NaOH), or 3 concentrations of nAg (0.018, 0.18 or 1.8 µg/L by Ag content), referred to here as Lo, Med or Hi nAg.

A semi-static exposure system was used, with 90% water changes every 2-3 d. Tadpole rearing water was prepared in bulk in an 80 gal tank and allowed to acclimate for at least 24 h prior to each water change. Treatment renewal occurred after water changes with a 1/1000 dilution of working stocks prepared as noted above. Statistical analysis was performed on measured H_2O parameters to ensure there were no tank effects among the 4 replicates within each treatment. No significant differences between tanks were observed and therefore data from all tanks was used in subsequent analyses. Fresh exposure water samples on experimental day 0 were taken to verify nominal Ag concentrations and old water samples after 3 d immersion were collected on experimental day 28 to determine loss of Ag from the water column.

After 48 h exposure, 16 animals from each treatment (4/tank) were collected for transcriptional analysis. Morphometrics were measured weekly for the 24 remaining tadpoles until experimental day 28. Tadpoles were individually sequestered in weigh boats and the developmental stage was directly determined under a dissecting microscope. Tadpoles were then transferred to transparent cell culture dishes and images taken with a digital camera (IXUS 75; Canon Inc.) using a ruler for an internal standard. Data for LL, SVL, and TL was subsequently extracted from photos using ImageJ64 software (National Institute of Health, USA, <http://rsb.info.nih.gov/ij>). To correct for differing body sizes, the LL was divided by the SVL of each animal.

On experimental day 28, the 6 remaining tadpoles from each tank were euthanized and pooled for whole body Ag content, with 4 pooled samples/treatment, and 3 samples within premet Ctrl and Hi nAg treatments (see results). Samples were stored at -20°C until homogenization (DIAX 600; Heidolph Elektro GmbH & Co., Kelheim, Germany), after which they were shipped to PESC (Vancouver, BC). Samples were prepared with an in-house method involving digestion with nitric acid and H_2O_2 before Ag content analysis with ICP-MS (Elan DRCII; Perkin Elmer, Shelton, CT, USA).

MAGEX cDNA Microarray

Animals collected on experimental day 2 were preserved whole in RNAlater (Qiagen,Toronto, ON, Cat# 76106) to prevent RNA degradation, with subsequent dissection of tadpole liver for mRNA quantification of 497 gene targets with the MAGEX cDNA microarray (Veldhoen et al, 2006). RNA extraction and quantification were performed as described in Chapter 2 Materials and Methods, and isolated RNA was resuspended in 20 µl diethyl pyrocarbonate (DEPC)-treated RNase-free water. Six samples per treatment were selected for microarray analysis based on RNA integrity as determined by ethidium bromide-stained agarose gel electrophoresis. cDNA synthesis, fluorescent labelling, wash protocol and hybridization have previously been described (Boone et al, 2013). In brief, the SMARTer PCR cDNA Synthesis Kit was used as per manufacturer's

protocol (Clontech Laboratories Inc., Mountain View, CA, USA) with subsequent purification of amplified cDNA with the GeneJET PCR Purification Kit (Fermentas, Burlington, ON). The DecaLabel DNA Labelling Kit was used to incorporate Cy3-dCTP (GE Healthcare Bio-Sciences Corp., Piscataway, NJ, USA) into cDNA according to the manufacturer's protocol (Fermentas, Burlington, ON). A universal DNA reference (UDR) including DNA sequences of all target probes on the MAGEX array was labeled with Cy5-dCTP (GE Healthcare Bio-Sciences Corp., Piscataway, NJ, USA). Labelled DNA was purified with the GeneJET PCR Purification Kit, and sufficient fluorophore incorporation was determined with the Nanodrop UV-Vis spectrophotometer (ND-1000; Thermo Scientific, Wilmington, DE, USA).

MAGEX microarray slides and coverslips were washed in coplin jars and prepared as previously described (Boone et al, 2013). Prior to hybridization, cDNA was denatured at 95°C and combined with labelled UDR in a hybridization solution including bovine serum albumin and A_{45} oligonucleotide to prevent non-specific binding. Hybridization was performed at 42 °C for 18 h in a Hybex Microsample Incubator (SciGene, Sunnyvale, CA, USA). Post-hybridization slides were washed, dried, and stored in a Scienceware autodessicator (Bel-Art, Pequannock, NJ, USA) before being scanned. A preliminary analysis of two test samples was conducted to determine the optimal spot signal and intensity at a PMT gain of 70% and laser level at 90% for both Cy3 and Cy5 channels. Images were collected with a 5 µm scan, and spot intensity levels were obtained via ImaGene Version 9 (BioDiscovery Inc., El Segundo, CA, USA) as per the manufacturer's protocol using the UDR to align the spot grid.

The universal floor for data was set at 2 robust standard deviations greater than the highest median background signal. Median signal intensities from triplicate spots on arrays were $\log_2$ transformed and normalized to the geometric mean of robust, non-T_3-responsive targets within each array to correct for inter-slide variation (Figure A.2, Appendix A).

QPCR

cDNA synthesis and QPCR analyses were performed on liver samples taken from each treatment group at the 48 h time point, as described in Chapter 2 Materials and Methods. Neat cDNA was diluted 1/20 for input into QPCR reactions with 1 unit of Immolase DNA polymerase (Bioline, Taunton, MA, USA, Cat#:BIO-21047). Primers for target transcripts were designed with either Primer Premier 5.0 (Premier Biosoft International, Palo Alto, CA, USA) for single products using Sybr green as fluorophore, or with Primer Express 3.0 (Applied Biosystems, Burlington, ON) for multiplexed targets with Taqman® (Invitrogen, Grand Island, NY, USA) probes. Primer/probe sequences, thermocycle profiles, quality control measures and other details are listed in Table A.2 in Appendix A. QPCR runs were performed as noted (Chapter 2, Materials and Methods). The comparative cycle threshold analysis (ΔΔCt; Livak & Schmittgen, 2001) was used to quantify relative amounts of transcripts in comparison with invariant normalizer genes ribosomal protein S10 (*rps10*) and eukaryotic elongation factor 1 alpha (*eef1a*; Table A.1, Appendix A).

Statistical Analysis

In all cases statistical significance was considered at p-value <0.05. Statistical analysis was conducted with either IBM SPSS 20 (Armonk, NY, USA) or the R statistical package version 2.15.0 (R Foundation for Statistical Computing, Vienna, Austria, www.r-project.org). H_2O parameters were collected at each water change for DO, pH, salinity, temperature and nitrogenous wastes. These parameters were not normally distributed so the non-parametric Kruskal-Wallis (KW) test was used to ensure there was no variation between the 4 replicate tanks. The developmental stages were grouped as denoted in Figure 3.3, and differences between treatments at the each time point were calculated with Fisher's Exact test (www.quantitativeskills.com/sisa/statistics/fiveby2).

The morphometric, microarray, and QPCR data were partially non-normal and therefore the non-parametric KW test was used across all treatments, followed by pairwise Mann-Whitney U (MW) comparisons if statistically significant.

Microarray data was compared before and after normalization with Intraclass correlation and Cronbach's alpha to confirm low levels of inter-slide variation.

The microarray targets included in the hierarchical cluster were significantly different from the Ctrl in either exposure. Cluster analysis was performed with Pearson's correlation on uncentered $\log_2$ transformed median values with Gene Cluster 3.0 software (de Hoon et al, 2004).

3.3 Results

nAg Characterization

It is extremely important to characterize the behaviour of NPs in each exposure system tested, as the aggregation state is influenced by various components of water chemistry. For the purpose of comparative studies in NP research, the minimum recommended analyses include actual exposure concentration and particle size and distribution (Handy et al, 2012). The experimental medium can influence NP properties and more thorough characterization is needed for the purposes of risk assessment (Nowack et al, 2012). The stock nAg used for this experiment has previously been shown to have slight aggregation (see Figure 2.1A, Chapter 2). The addition of $NaHCO_3$ and synthetic sea salts to tadpole rearing water did not affect the size and distribution of nAg in the exposure system (Figure 3.1A and B). There were two distinct populations around 8 nm and 35 nm in diameter, in a similar pattern to that reported previously during exposure of *R. catesbeiana* tadpoles to nAg in well water (see Figure 2.1B, Chapter 2). It is likely that the smaller population represents single nAg particles, while the larger is aggregated to some degree, ranging between 28 and 47 nm in diameter. It should be noted that these aggregate sizes are still relatively small, and some nAg types are manufactured within that size range (Hoque et al, 2012).

The amount of iAg dissolution from nAg in the tadpole exposure water between the range of 0.25-33 µg/L nAg was on average 34% ±7.9. This is slightly higher than the dissolution of nAg in well water from Vancouver (see Chapter 2). While the addition of sea salt and $NaHCO_3$ did not significantly affect the amount of iAg

released (data not shown), other parameters such as DO content, pH, and nAg preparation (sonicated or not) could account for these differences.

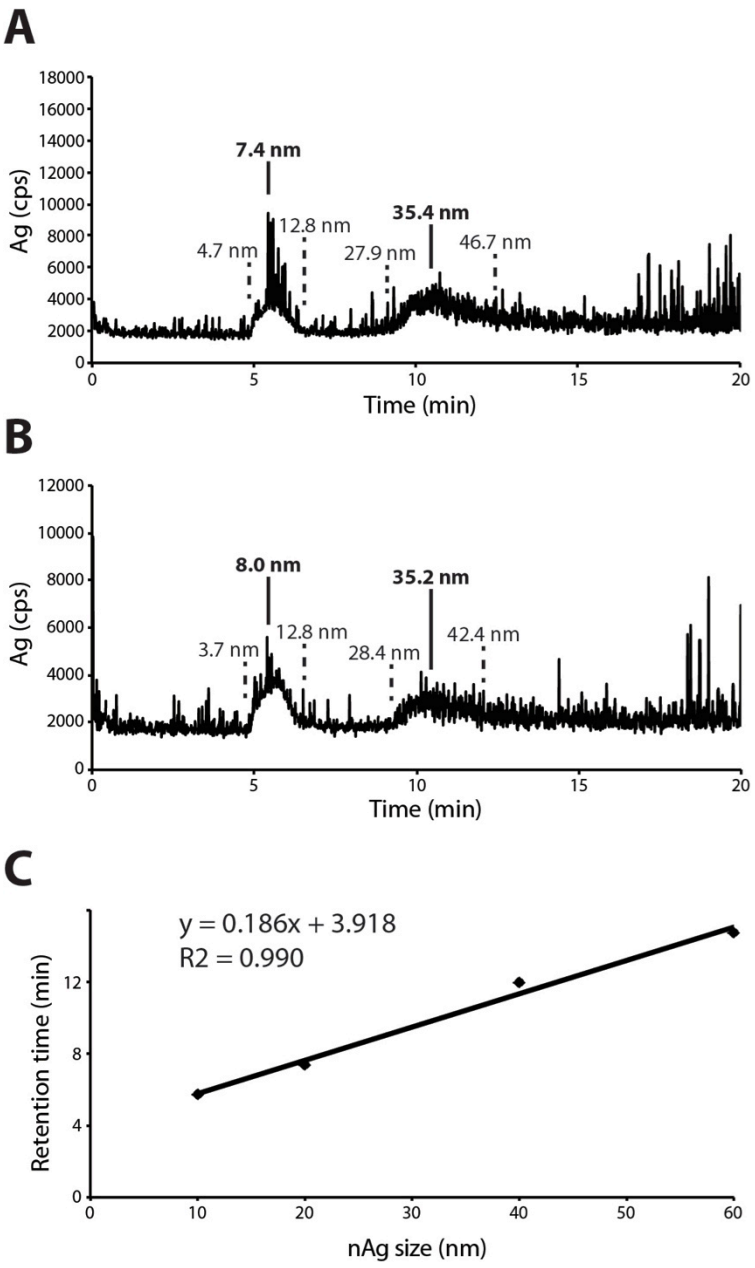

Figure 3.1 – Effect of *X. laevis* tadpole rearing water on nAg aggregation determined by FFF-ICP-MS separation. nAg was diluted to 60 µg/L with either **A)** dechlorinated water or **B)** synthetic sea salt and $NaHCO_3$ treated dechlorinated water. Ag was detected at 420 nm with on-line UV-VIS. **C)** Calibration curve used to determine nAg aggregate size based on retention times of known nAg standards (10-60 nm). (Partially adapted from Hoque et al, 2012).

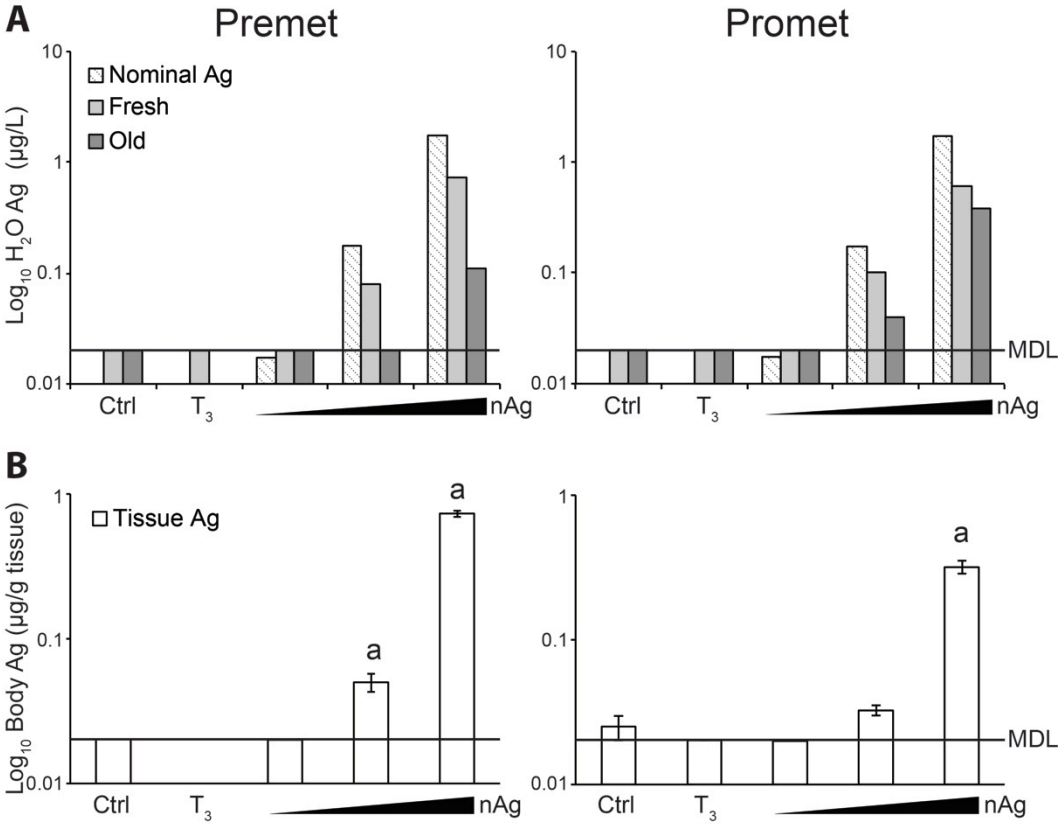

Figure 3.2 – Ag concentration in *X. laevis* exposure water and tissue samples determined by ICP-MS. A) Ag concentration in premet and promet exposure water for 0.018-1.8 µg/L nominal Ag (hatched). Actual concentrations were determined for fresh exposure water at experimental day 0 (light grey), and older exposure water at experimental day 28 (dark grey), with a minimum detection limit (MDL) of 0.02 µg/L. One tank/treatment was measured at each timepoint. **B)** Mean (±SEM) Ag concentration in premet and promet whole bodies after 28 d exposure to Lo, Med or Hi nAg treatments. Six animals/tank were pooled to satisfy volume requirements, giving 4 samples per treatment, and 3 samples in premet Ctrl and Hi nAg. Significance relative to the negative control (Ctrl) is denoted with an (a) when $p < 0.05$.

H_2O and whole body Ag content

Measured H_2O Ag concentrations were below the minimum detection limit (MDL; 0.02 µg/L Ag) for the control, T_3, and Lo nAg (0.018 µg/L Ag nominal) treatments (Figure 3.2A). In the Med nAg and Hi nAg treatments the freshly prepared H_2O was on average 45 ±4.8% of the nominal Ag in both exposures. This range of Ag detected in H_2O was similar to that found in the bullfrog *in vivo* exposure (See Chapter 2, Results), indicating that either the concentration was less than stated by the manufacturer, or the initial concentration of NP in the

stock solution was less than 1500 mg/L. Since the Lo nAg working stocks were serially diluted from the higher treatments, it is highly probable that there is nAg present, just below the instrument detection limit.

No mortalities due to nAg treatment were observed in either exposure. However, one tank (6 tadpoles) from both the premet Ctrl and Hi nAg treatments was removed from the exposure after experimental day 14 due to a contamination event. Therefore only three replicates were available for tissue Ag content analysis in premet Ctrl and Hi nAg treatments. Biological uptake of the administered Ag was evident through a reduction of Ag in the water column 3 d post-administration and accumulation in tadpole tissues. Ag concentration in the old exposure water was 8.9 ± 2.6% of nominal in the premet exposure, and 22.4 ± 0.6% in the promets (Figure 3.2A, dark grey bars). Tadpoles in the premet exposure accumulated more Ag over 28 days than the promets. Premet Ag tissue content was approximately 600-1000x the measured Ag concentration in H_2O, with promets having 500x as much (Figure 3.2B).

Response to T_3

Positive controls are essential in low dose endocrine studies to verify that animals are sensitive to external stimuli (vom Saal & Welshons, 2006). Tadpoles in both the premet and promet exposure were competent to respond to endocrine disruption, as seen by their sensitivity to T_3. The metamorphic timing was accelerated in both exposures (Figure 3.3), becoming lethal in premets after 14 d due to asynchronous tissue development (Figure 3.3A). Only three mortalities occurred in the promets, two after 2 d, and one after 21 d. The differential stage-sensitivity was likely due to promets already having circulating T_3 that allowed sensitive, early-responding tissues to develop properly. The morphometrics demonstrated a strong response to T_3, as expected (Figure 3.4A, B). In Ctrl animals, TL and SVL increased gradually before decreasing after 21 d and between 7 and 21 d in premets and promets, respectively. T_3 caused a decrease in both metrics much earlier in the exposures, as well as increasing the rate of LL/SVL growth in both exposures. T_3-treated promets had decreased weight on

experimental day 28 indicative of less accumulated body mass before tissue remodelling and resorption (Figure 3.4B). Liver mRNA also displayed consistent sensitivity to T_3-dependent transcriptional regulation (Figure 3.6A), with a generally similar pattern to their natural metamorphic profile with endogenous T_3 (Figure 3.6B). Responsive transcripts include thyroid hormone receptors alpha and beta (*thra, thrb*), cyclin-dependent kinase inhibitor xic1 (*cdknx*), Ftz-F1-related orphan receptor A (*nr5a2*), insulin-like growth factor 2 (*igf2*), and cytoplasmic beta actin (*actb*).

Morphometrics

As one tank from both the Ctrl and Hi nAg premet treatments was removed, only 18 animals instead of the full 24 are represented in those treatments from experimental day 21 onwards in all morphometric endpoints. nAg did not alter the rate of metamorphosis at any concentration tested or in either exposure (Figure 3.3). However, other morphometric endpoints were altered, especially by Lo nAg (0.018 µg/L) treatment. At both experimental day 2 of the premet exposure and day 28 of the promet exposure, Lo and Med nAg significantly increased the relative LL/SVL ratio (Figure 3.4A). Lo and Hi nAg also increased the SVL in the premet tadpoles, although the direction was opposite to the response to T_3. Weight at experimental day 28 did not fluctuate in response to nAg in either exposure (Figure 3.4B).

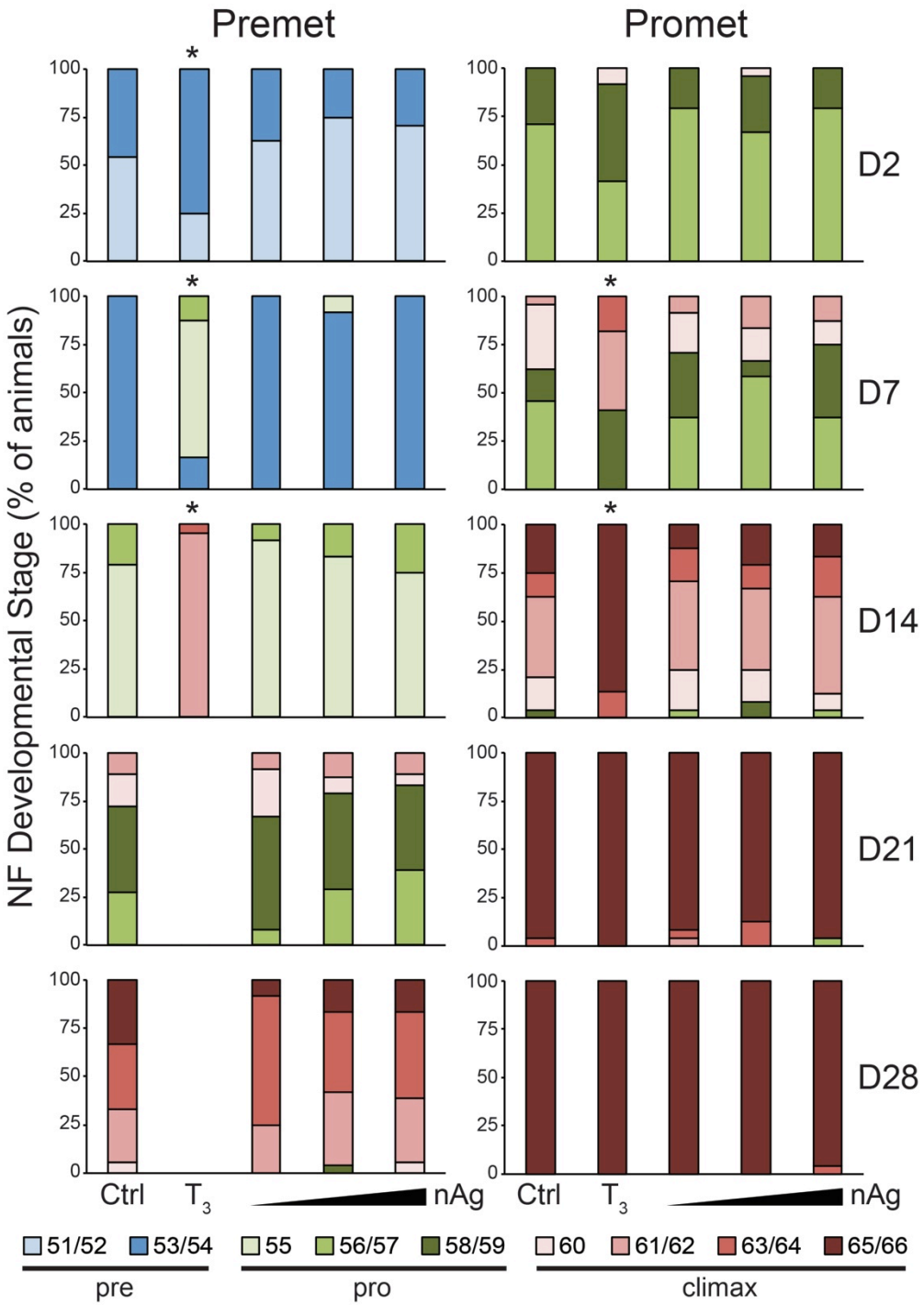

Figure 3.3 – Effects of nAg on natural metamorphic timing. Premet (NF51) and Promet (NF56) tadpoles were exposed for 28 days to 0.018-1.8µg/L nAg. Each subsequently darker shade represents further development, with blue, green and red denoting premet, promet and metamorphic climax stages respectively. Forty animals/treatment are represented at experimental day 0 (D0), with 24 at D2 onwards. After D14, 18 tadpoles are in both premet Ctrl and Hi nAg treatments. Significant acceleration (*) with respect to Ctrl at concurrent time points is denoted when $p < 0.05$.

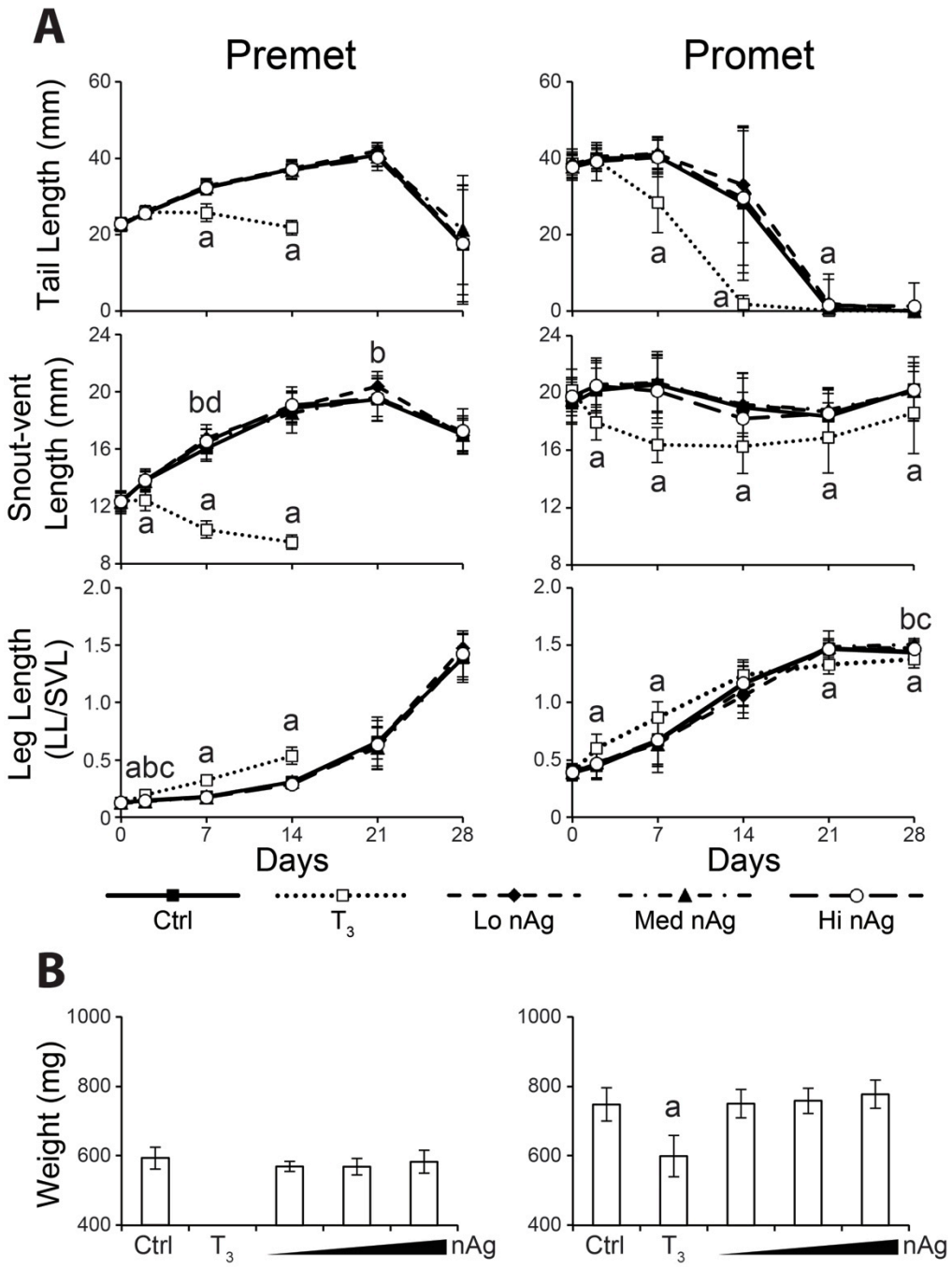

Figure 3.4 – Effects of nAg on tadpole morphology. Premet and promet tadpoles were chronically exposed to 0.018-1.8µg/L nAg for 28 days. Mean (±SEM) values shown for **A)** TL, SVL and LL/SVL ratio, measured weekly and **B)** weight determined after 28 d. Significance with respect to Ctrl at each time point denoted for T_3 (a), Lo nAg (b), Med nAg (c), or Hi nAg (d) when p-value <0.05. See Figure 3.3 for animal numbers.

MAGEX Microarray

Microarray analysis was performed with the in-house, cross-amphibian species MAGEX cDNA array. The transcript profiles of 497 targets were examined in the liver at experimental day 2 in a subset of 6 animals out of 16 per treatment. More transcripts were perturbed in the promet exposure (12 up, 4 down), than the premet (3 up, 4 down), with no overlapping targets responding in both exposure sets. Hierarchical clustering of these targets was performed and 3 clusters were highlighted based on high correlation of response pattern (Figure 3.5). Seven genes that were increased in response to nAg in the promet exposure were correlated (R^2=0.778) including negative regulator Id2 (*id2*), *actb*, matrix metalloproteinase 9 (*mmp9*), eosinophil peroxidase (*epx*), myeloperoxidase (*mpo*), Na+/K+ transporting ATPase beta subunit (*atp1b3*), and *nr5a2*. Two of these, *epx* and *mpo*, are peroxidases involved in responding to oxidative stress. The increased abundance of these two transcripts was very strongly correlated with *mmp9* (R^2=0.981), which has previously been shown to be up-regulated in response to H_2O_2 induced ROS generation (Yoo et al, 2002). Two gene transcripts whose abundance was reduced with nAg exposure in the promets were also strongly correlated (R^2=0.955), namely cyclin-dependent kinase inhibitor (*xicl*), and *cdknx*. It should be noted that their sequences on the cDNA microarray are highly similar (92.1% identity) so their similar profile could be due to cross hybridization. While there were no strongly correlated clusters of up-regulated targets in the premet exposure, two gene transcripts, c-myc I (*myc*) and *igf2*, were reduced by nAg (R^2=0.884). Biological functions of correlated clusters are noted in Table 3.1.

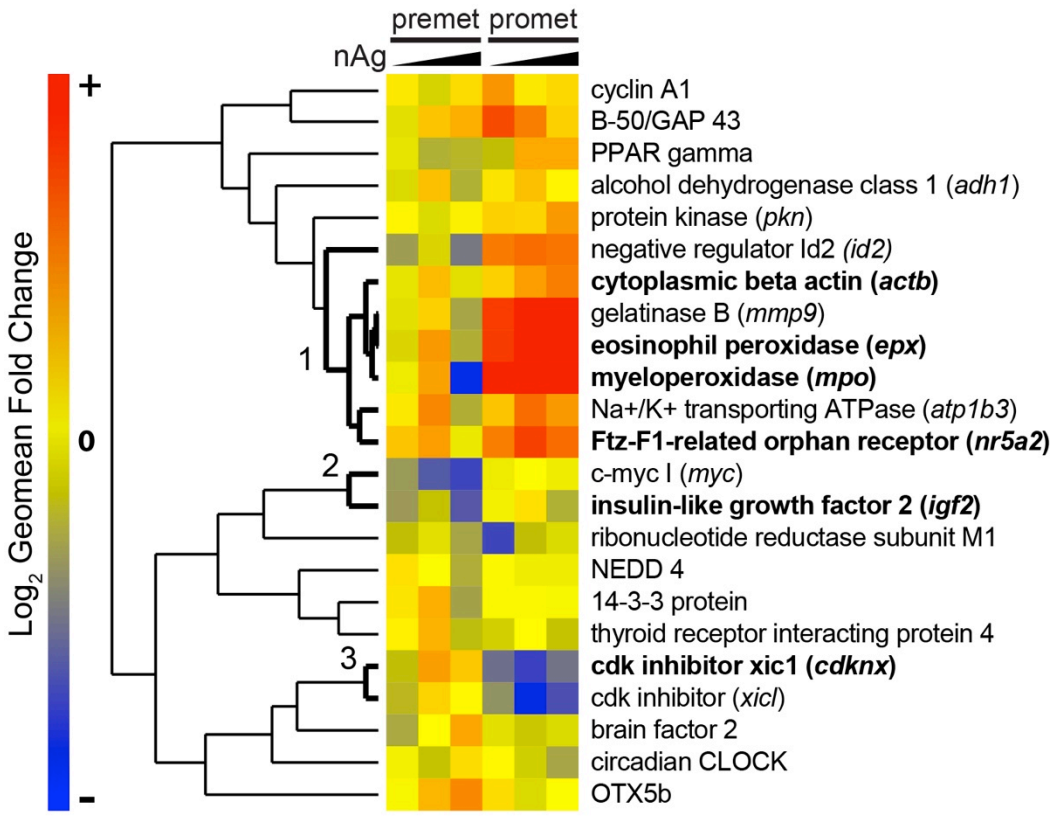

Figure 3.5 – Hierarchical cluster of nAg responsive genes from MAGEX cDNA microarray. Transcriptional response in premet and promet tadpole liver exposed *in vivo* to Lo, Med, and Hi nAg (0.018-1.8 µg/L Ag) for 48 h. Signal intensity from significant nAg responsive genes (p-value <0.05) was normalized to robust, non-T_3-responsive probes. Log_2 transformed geometric means of 6 animals per treatment are shown indicating fold change from each control. Genes of interest (GOIs) for potential nAg exposure biomarkers are in bold, and three clusters (1,2,3) were identified based on strong correlation (R^2>0.75).

Table 3.1 – Gene Ontology of nAg responsive gene clusters.

NF Stage	Cluster Group	Correlation Coefficient	Target	Gene Ontology	p-values[a]		
					Lo nAg	Med nAg	Hi nAg
53	2	0.884	*myc*	regulation of transcription, DNA-dependent		0.041	0.004
53	2	0.884	*igf2*	nervous system development	0.009		0.002
57	1	0.778	*id2*	myotube cell development	0.026	0.009	0.009
57	1	0.778	*actb*	protein binding		0.004	0.004
57	1	0.778	*mmp9*	proteolysis	0.041	0.004	0.002
57	1	0.778	*epx*	response to oxidative stress	0.041	0.002	0.002
57	1	0.778	*mpo*	response to oxidative stress	0.004	0.002	0.002
57	1	0.778	*atp1b3*	ATP biosynthetic process		0.015	0.041
57	1	0.778	*nr5a2*	regulation of transcription, DNA-dependent	0.015	0.004	0.004
57	3	0.955	*cdknx*	cell cycle arrest	0.009	0.002	0.015
57	3	0.955	*xicl*	cell cycle arrest		0.002	0.026

a = p-values for pairwise comparison with Ctrl of premet (NF53) or promet (NF57) exposures

QPCR

RNA quality was determined by RNA gel electrophoresis and geometric mean Cts of normalizer genes. Samples with any RNA degradation were only found in the Hi nAg treatments. 6 and 8 samples were removed from QPCR analysis in the premet and promet exposures, respectively. The observed degradation was possibly due to nAg within in the tissues interfering with the preservation solution, RNAlater. No degradation was observed in subsequent *in vitro* experiments where RNA was directly extracted without use of RNAlater (data not shown). However, it is important to note that exposure to low concentrations of nAg (1.8 µg/L Ag) can impact RNA preservation, highlighting the importance of RNA quality assurance with QPCR analysis.

Six genes of interest (GOIs) were chosen for QPCR validation based on strong statistical significance ($p<0.01$, KW) and pronounced nAg response patterns (*epx*, *mpo*, *cdknx*, *actb*, *nr5a2*, *igf2*). The transcript profiles were consistent between microarray and QPCR analysis using the same 6 samples (Figure A.3, Appendix A), validating the microarray. Furthermore, the microarray-based response profiles held over all 16 animals per treatment by QPCR analysis, showing that these represent reliable nAg responses (Figure 3.6A). The dynamic range of QPCR measured responses was larger than the microarray, highlighting the differential sensitivities of these two techniques. *nr5a2* was the only transcript to show nAg-induced response in both exposure sets, having slightly less and strongly increased abundance in the pre- and promet exposure sets, respectively. *Thra* and *thrb* transcripts were also examined as they had previously been shown to respond to nAg in the liver of bullfrog tadpoles exposed to nAg (see Figure 2.6A, Chapter 2). Both receptor transcripts increased during natural metamorphosis, although *thra* was not quite significant at $p=0.06$. Furthermore, while both were responsive to exogenous T_3, only *thra* was reduced in premets exposed to nAg.

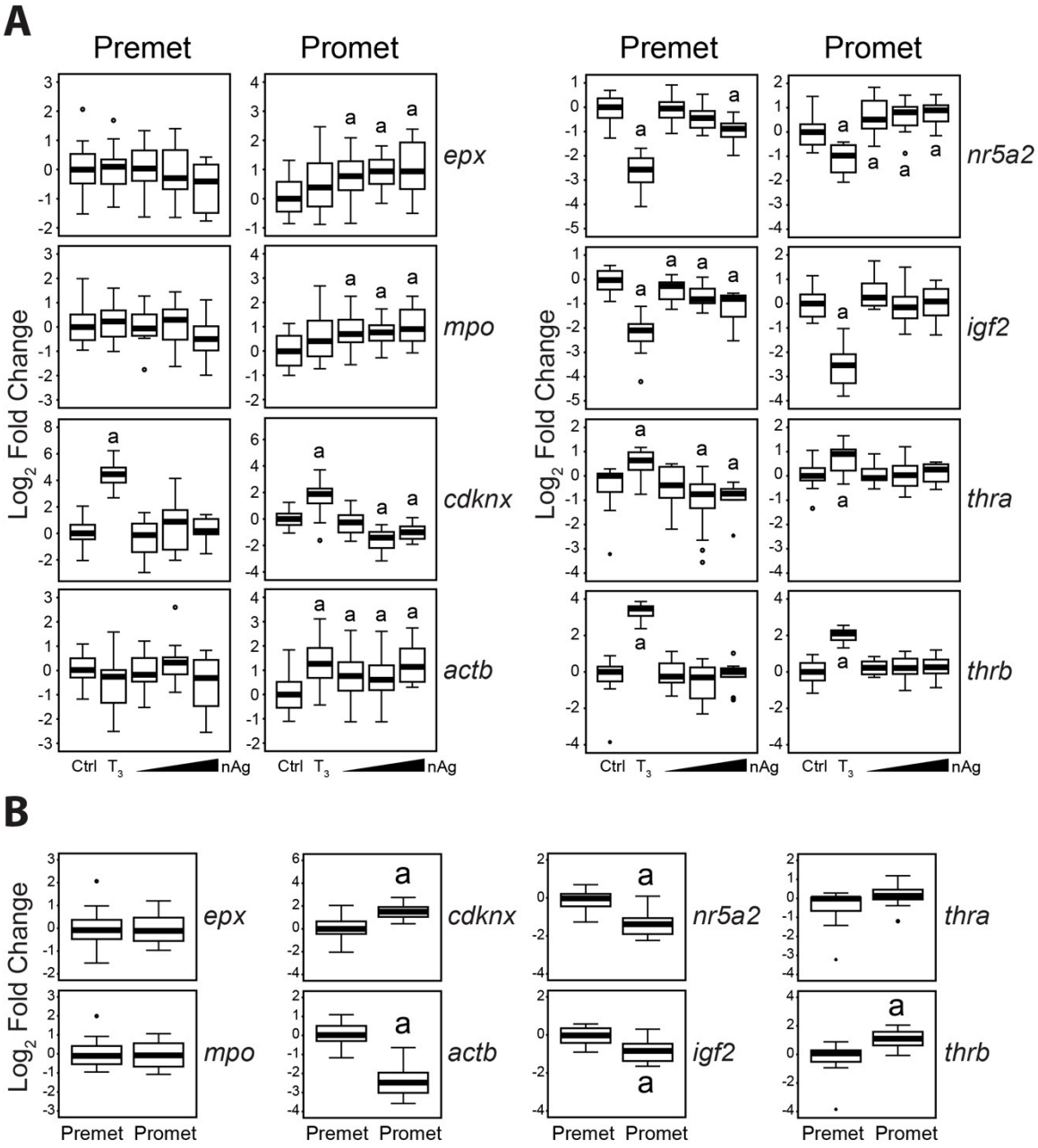

Figure 3.6 – QPCR determination of nAg- and T_3-response gene mRNA abundance in premet and promet *X. laevis* liver. Target abundance in liver from 16 animals/treatment after 48 h exposure to 0.018-1.8 µg/L nAg **(A)** and in negative controls from premet and promet exposure sets **(B)**. Data were normalized to the geometric mean of invariant transcripts *rps10* and *eef1a* and expressed as $\log_2$ relative fold change from the respective negative controls. Significance ($p<0.05$) is denoted for pairwise comparison to the negative control (a). See Figure 2.6 for boxplot details. Within the Hi nAg treatment, 6 and 8 animals were removed from premet and promet analyses, respectively, due to poor RNA quality.

3.4 Discussion

H_2O and Tissue nAg Content

There are many possible routes of loss of nAg from the water column during the exposure. nAg reduction between water changes has also been observed in another aquatic chronic exposure with brown trout (Scown et al, 2010). Ag can be oxidized into iAg in the presence of DO (Liu & Hurt, 2010), which then precipitates as AgCl when Cl^- ions are present. nAg can also precipitate when aggregates become too large for colloidal suspension. NPs associate with mucous on tadpole epithelium, which then sloughs off and sediments (Handy et al, 2012). NPs also associate with organic molecules such as food proteins (Fabrega et al, 2011) and therefore can either be taken up by the tadpoles or settle to the tank bottom. These are all likely phenomenon to occur in the environment as well.

Bioaccumulation occurs when a substance is absorbed at a greater rate by an organism than the rate at which it is lost. While nAg associated with food still present in the intestinal tract undoubtedly contributed to the observed Ag tissue concentrations, it is unlikely to completely account for all measured Ag. Tissue silver was 500-1000x higher than that measured in the exposure water, and accumulated in a dose-dependent manner (see Figure 3.2B).

There are several exposure routes for nAg internalization. First, nAg can be taken up by contact with the gill and skin epithelium. Several studies have demonstrated increased Ag content in fish gills after nAg exposure (Farkas et al, 2011a; Farmen et al, 2012; Griffitt et al, 2009; Scown et al, 2010). Unlike fish, direct uptake of nAg through the epidermis is also possible in amphibians due to their semi-permeable skin. Second, nAg can also be taken up via ingestion of either nAg associated with food particles, aggregated NPs, or biofilms. Larger aggregates increased the potential for NP ingestion in other filter feeders such as mussels and oysters (Fabrega et al, 2011) and a degree of nAg aggregation was seen in the current exposure. The exposure tanks were not sterile and therefore biofilms were present on surface of glassware during the exposure despite water changes. Fabrega et al (2009) demonstrated that nAg accumulates in biofilms

which tadpoles are likely to ingest. After ingestion, nAg can cross the intestinal lining and enter the blood stream (Bouwmeester et al, 2011) where it can cross the blood-brain and blood-testes barrier with implications on behaviour and reproduction (Braydich-Stolle et al, 2010; Johnston et al, 2010). Indeed, in a study at similarly low concentrations, Pokhrel and Dubey (2012) demonstrated that nAg disrupted *Daphnia* predator-prey interactions and reproductive potential. Any liberated iAg could also be taken up into tissues via membrane ion transporters, similar to uptake of Na^+ and Cu^+ and could bioconcentrate in organisms (Fabrega et al, 2011). Concentrations above 2 µg Ag/g tissue caused sterility in clams in the San Francisco Bay in the 1980s, after a release of iAg to the environment (Brown et al, 2003). Tissue concentrations reported here were only slightly less and were obtained from very low environmentally-relevant exposure concentrations. It would therefore be of interest to investigate the effects of nAg on reproductive potential in amphibians.

The extent of nAg accumulation is dependent upon the developmental stage. Greater accumulation was observed in premet vs promet tadpoles. It is possible that this is due to prolonged feeding behavior of the younger animals. Tadpoles stop feeding when they reach the later stages of prometamorphosis as their intestines completely remodel to adjust to the different food sources of adult frogs. Furthermore, while tadpoles filter feed continuously, froglets eat sporadically with periods of fasting between meals (Hourdry et al, 1996). By the end of the 28 day experiment, most tadpoles in the promet exposure were froglets, while only 10-25% of premets completed metamorphosis.

Morphology and Metamorphic Timing

One objective of this research was to determine whether the nAg-induced increase in stage progression seen in *R. catesbeiana* was a tissue-specific effect on hindlimb growth and development, or an overall acceleration of metamorphosis. Here we show that exposure of *X. laevis* to low, environmentally-relevant concentrations of nAg resulted in an increased LL/SVL ratio in both premet tadpoles and froglets from the promet exposure. At the

same time, no alterations in metamorphic timing were observed as determined through stage progression. These results suggest that nAg directly affects the hindlimb, and not other morphological changes during metamorphosis such as emergence of forelimbs, eye repositioning, or tail regression. T_3 mediates toe differentiation in premet tadpole stages and hindlimb length in promets throughout metamorphic climax (after NF58; Shi, 2000). Therefore, nAg induced an increase in T_3-mediated hindlimb development and growth in both *R. catesbeiana* and *X. laevis* in 28 d chronic exposures.

The SVL was slightly larger in the Lo and Hi nAg treatments, which is opposite to the T_3-induced SVL decrease. In the bullfrog study, nAg also perturbed the SVL in the opposite direction from the T_3 control (see Figure 2.4, Chapter 2). This may indicate that nAg-induced effects on SVL are not mediated through T_3-specific pathways. Tadpole size and growth are heavily influenced by feeding behaviour during metamorphosis (Hourdry et al, 1996), so it is possible that nAg alters the feeding behaviour of premet tadpoles. Promet tadpoles had reduced feeding behaviour as they progressed through metamorphic climax that could account for the lack of changed SVL. We observed that premets accumulated more Ag than promets, likely mediated by feeding activity (see discussion above). Therefore, closer examination of nAg effects on the brain or behavioural patterns at these low concentrations is warranted.

In both exposures, more pronounced morphological effects were observed in the lowest nAg treatment (0.018 µg/L) relative to the control. Low dose stimulatory effects have also been noted with respect to nAg exposure in human hepatoma cells (Kawata et al, 2009), and among various other NPs (Iavicoli et al, 2010). Non-monotonic dose responses are common when hormonal regulation is disrupted by EDCs (Vandenberg et al, 2012). It is also possible that nAg causes a hormetic response where low doses can trigger opposite responses from high ones (Kendig et al, 2010). These results highlight the importance of empirically determining the effects of nAg at environmentally relevant concentrations.

Transcriptional Response to ROS

One main mechanism of nAg action is through oxidative stress and intracellular damage from ROS production (AshaRani et al, 2009; Marambio-Jones & Hoek, 2010; Yildirimer et al, 2011; Zhang et al, 2012). Within the promet exposure set, there was evidence of ROS involvement. The response patterns of *epx*, *mpo*, and *mmp9* to nAg were highly correlated, and all three transcripts are directly linked with ROS generation. *Epx* and *mpo* encode heme-containing peroxidases involved in both detoxification and production of ROS in phagolysosomes. While their primary function is the breakdown of phagocytosed substances, they are a secondary regulator of ROS, after catalase, superoxide dismutase, and glutathione peroxidase in immunocompromised states (Schaffer & Bronnikova, 2012). *Epx* transcripts were also increased in *R. catesbeiana* liver after chronic *in vivo* nAg exposure (Chapter 2, unpublished data). *Epx and mpo* also were responsive to nAg in the brain of nAg-exposed mice, although contrary to the results of the present study, their abundance decreased (Rahman et al, 2009), possibly illustrating tissue and species differences.

Mmp9 transcripts, identified by the microarray analyses, have previously been shown to be responsive to ROS generation. In murine macrophages, Yoo et al (2002) noted that *mmp9* transcripts were increased by ROS produced from exogenous H_2O_2 mediated by nuclear factor kappa B (*Nfkb1*). Furthermore, in human monocytes, *MMP9* transcripts were increased in response to ROS generated from cobalt NPs via activation of AP-1 and protein tyrosine kinase (Wan et al, 2008). Gagné et al (2012) also described oxidative stress responses of transcripts in rainbow trout exposed *in vivo* to low concentrations of nAg comparable to those used in the present study. The response of these targets potentially indicates nAg-induced ROS generation even at very low, sublethal concentrations.

On the other hand, none of the above targets were changed in premet tadpoles exposed to nAg. In fact, Igf2 has a protective role against ROS, and its transcript was decreased upon nAg treatment. Igf2 inhibited H_2O_2-induced reduction in total blastocyst count and inner cell mass during embryogenesis of C3B6F1 mice

(Kurzawa et al, 2004). Therefore, premet tadpoles either had an alternative method to cope with potential ROS generation, or were less competent to respond transcriptionally. The second scenario could be problematic considering their increased capacity to accumulate nAg relative to promet tadpoles.

While there may be a degree of ROS produced from nAg at the low concentrations used in the present study, it is unclear what deleterious effects, if any, this may cause. At low concentrations, ROS can have physiological roles in cell cycle regulation. Endogenous ROS produced from mitochondrial respiration act as second messengers in intracellular signaling of mitogen activated protein kinase (MAPK) and tyrosine kinase pathways (Boonstra & Post, 2004; Chiarugi et al, 2003). ROS also promote cell cycle progression via growth factor receptors NFKB1 and AP-1, and has been associated with cellular proliferative events (Boonstra & Post, 2004; Liu et al, 2002). Low nAg concentrations have also been associated with cellular proliferation of human hepatoma cells (Kawata et al, 2009). In the current study, the transcript encoding Cdknx, a protein involved in cell cycle arrest, was decreased due to nAg exposure. This was also observed in bullfrog liver (Chapter 2, unpublished data), and indicates progression of cellular division. Furthermore, as discussed above, nAg promotes hindlimb growth and differentiation, a physiological process heavily reliant on cellular proliferation (Shi, 2000). It is therefore possible nAg-induced ROS mediates the proliferation of the hindlimb during development. However, the involvement of ROS in hindlimb development was not tested in this exposure, and requires further investigation.

TH-responsive transcriptional targets

The mRNA abundance of *thra* and *thrb* increased as expected with exogenous and endogenous T_3. This response is well characterized in many tissues and has previously been described in the liver of *X. laevis* (Fairclough & Tata, 1997), and *R. catesbeiana* (See Figure 2.6A, Chapter 2; Chen & Atkinson, 1997; Helbing et al, 1992). Furthermore, T_3 induced a strong response in *cdknx*, *igf2*, *nr5a2*, and *actb* during both precocious and natural metamorphosis. *Cdknx* was

also found to be up-regulated in response to exogenous T_3 in the tailfin of *R. catesbeiana* (Veldhoen et al, 2006). In contrast with the current response in liver, *igf2* increased with T_3 treatment in the brain of *X. laevis* (Helbing et al, 2011). Although the T_3-responsiveness of *nr5a2* during metamorphosis has not previously been reported, it is known to be expressed during early embryonic development of *X. laevis* pancreas and liver (Hayata et al, 2009). It is noteworthy that *actb* mRNA was altered both as metamorphosis progressed and by exogenous T_3 as it is often used as a normalizer gene in QPCR analysis. It is therefore important to monitor potential biological responses of normalizers within experimental assays.

Of the above targets, five transcripts were sensitive to nAg treatment, although their response often did not match that of T_3. In the premets, the mRNA abundance of both *igf2* and *thra* was decreased with nAg exposure. In the liver of *R. catesbeiana* tadpoles, both nAg and iAg were able to attenuate the T_3-induced induction of *thra* as well (see Figure 2.6A, Chapter 2). *Cdknx* and *actb* were only responsive to nAg in the promets, while *nr5a2* was decreased by nAg in premets, and increased in promets. There may not be a clear link between TH and nAg responsiveness, but many targets involved in TH-signaling were perturbed by nAg exposure.

It is interesting to note that there are more nAg-induced transcript abundance changes in the presence of T_3. Promet tadpoles have endogenously circulating T_3, and had more transcriptionally changed targets (16 vs 7 in premets), including most of the strongest responders including *epx* and *mpo* mRNAs. In the bullfrog, most transcript abundance perturbations occurred in T_3-injected compared to vehicle-injected premet tadpoles (Figure 2.6, Chapter 2). Furthermore, in the bullfrog C-fin assay, transcripts only changed levels in the presence of exogenous T_3. Many TH responsive genes have thyroid response elements (TREs) in their promoter region where Thr-Rxr complexes regulate gene expression in the absence and presence of T_3. A possible mechanism of nAg disregulation could include interference with transcriptional machinery, particularly during the change in cofactor association that occurs with increased

T_3 abundance (see Figure 1.6, Introduction). Alternatively, nAg could alter phosphorylation events that influence Thr-DNA binding kinetics (Chen et al, 2003; Nicoll et al, 2003; Tzagarakis-Foster & Privalsky, 1998). However, both of these possibilities require independent verification, as they were not directly tested here.

X. laevis tadpoles have developmental stage-dependent sensitivity to nAg exposure. While premet tadpoles accumulated more nAg in their tissues and had an increased SVL, promets showed more transcript disregulation and stronger responses. Furthermore, most of the nAg-altered gene transcripts identified by microarray or QPCR were only responsive at one developmental stage. The liver is a TH-responsive organ and undergoes extensive genetic reprogramming during metamorphosis (Mukhi et al, 2010) which could explain the differential nAg-induced transcript profiles. Griffitt et al (2008) saw a stage-specific sensitivity between zebrafish juveniles and adults to iAg, although none was observed for nAg. However, the behaviour of nAg in their exposure system may differ from the current one, where less than 35% of nAg dissolved into iAg. The results presented here demonstrate that prometamorphosis is a sensitive life stage to TH-disruption from nAg.

Conclusions

In conclusion, nAg displayed EDC activity on amphibian metamorphosis at environmentally-relevant concentrations. nAg accelerated T_3-mediated differentiation and growth of the hindlimb and perturbed the levels of TH-responsive transcripts. The stage-dependent differences seen in gene transcripts suggest that prometamorphosis may be particularly sensitive to nAg effects. Furthermore, 7 transcripts were identified with consistent responses that are potential markers for nAg exposure. The concentrations at which nAg perturbed TH-signaling and displayed evidence of ROS generation are within or below the regulations in Canada and the USA for the protection of aquatic life (NRWQC 2006b; CCME 2007) and therefore these guidelines may need to be reconsidered.

4 The effects of nanosilver on *Xenopus laevis* XTC-2 cells

The experiments in this chapter were developed, executed, and analyzed by me with the following exceptions. FFF-ICP-MS was conducted by collaborators at Trent University, Peterborough, ON and ICP-MS was performed by scientists at the Pacific Environmental Science Centre, Environment Canada. nAg dissolution was determined by collaborators at the University of Montreal, QC.

4.1 Research Purpose

The purpose of the present study was to optimize an *in vitro* assay to elucidate the components and mechanisms of nanosilver (nAg) interference with the thyroid hormone (TH) transcriptional response, as outlined in the Chapter 3 Discussion. While *in vivo* assays are essential to verify the endocrine disrupting chemical (EDC) effects on animals with an intact hypothalamo-pituitary-thyroid (HPT) axis, *in vitro* assays allow increased experimental manipulation such as the combined use of various agonists and inhibitors. This assay would enable determination of the relative contribution of nAg components, specifically comparing the effects of the whole nanoparticle (NP) with the dissolved Ag ion (iAg) and the polyacrylic acid (PAA) coating. This assay would also allow examination of the involvement of nAg-generated ROS in TH-signaling disruption. The 7 transcriptional biomarker candidates that showed a consistent and strong response in Chapter 3 were tested to determine if they were sensitive to nAg in a cell culture setting. Given that these targets are involved in ubiquitous cellular functions such as cell cycle regulation, oxidative stress response and hormonal signaling, it is reasonable to assume that the TH-sensitive *Xenopus laevis* tadpole “fibroblast-like” cell line (XTC-2; Pudney et al, 1973) would be similarly responsive.

Preliminary results with XTC-2 cells indicated that nAg altered the levels of mRNAs encoding thyroid hormone nuclear receptors alpha and beta (*thra, thrb*; unpublished data). However, significant variation in the *thrb* response to TH indicated that subpopulations of different cell types might be present in the cell

line. XTC-2 cells were isolated and subcultured to obtain monoculture cell lines derived from single cells. The TH-responsiveness of four new monocultures was tested using *thrb* transcript responsiveness as a readout, and the subcultured cell line with the strongest and tightest response (XTC-2 K4-2) was selected for testing of the biomarkers of nAg exposure. XTC-2 cells were exposed to nAg (0.018-18 µg/L) for 24 h in the absence and presence of 10 nM T_3 and changes in transcript levels were determined with quantitative real-time polymerase chain reaction (QPCR). While the biomarker candidates were generally non-responsive to nAg in XTC-2 K4-2 monoculture, the assay remains a valuable tool for testing other TH disrupting EDCs in the future.

4.2 Materials and Methods

nAg characterization

Stock nAg with PAA coating was provided by Vive Nano (Toronto, ON, Canada; CAS:7440-22-4; Lot#:RL101111A). According to manufacturer's specifications, the particle diameter was 1-5 nm by transmission electron microscopy (TEM), and 4.9 nm by dynamic light scattering (DLS) at a concentration of 720 mg/L by Ag content. At 2.5 mg/L total NP in 70% Leibowitz-15 (L-15) cell culture medium as prepared below, nAg had an average diameter of 28.17 ±0.32 nm with DLS (ZetaPALS, Particle Sizing Software, Brookhaven Instruments Corp., Holtsville, NY, USA) and zeta-potential of -7.39 ±3.06 mV (ZetaPALS, PALS Zeta Potential Analyzer, Brookhaven Instruments Corp., Holtsville, NY, USA).

Samples of culture medium prepared at the two highest nominal concentrations (1.8 and 18 µg/L Ag) as well as from the NaOH control were sent to the Pacific Environmental Science Centre (PESC, Vancouver, BC) for actual Ag content analysis by inductively-coupled plasma mass spectrometry (ICP-MS). Samples were prepared for analysis as in Chapter 2, Materials and Methods.

The effect of 10% (v/v) foetal bovine serum (FBS) on aggregation state of nAg in L-15 cell culture medium was determined with field flow fractionation online with ICP-MS (FFF-ICP-MS). Samples were prepared and analyzed as noted in

Chapter 2, Materials and Methods. The extent of iAg dissolution in L-15 cell culture medium was measured at concentrations of 8 and 29 µg/L nAg, as described in Chapter 2. nAg lot# AC0829LMPPTFD as used in Chapter 2 and 3 was used in FFF-ICP-MS and dissolution tests for direct comparison with nAg behaviour in other exposure systems.

Chemical Preparation

All stocks were prepared at room temperature and all dilutions into culture medium were prepared in a class II type A2 biological safety cabinet (BSC; Labgard ES NU-425, NuAire, Plymouth, MN, USA) using aseptic technique. 1000x stocks of T_3 (3,3′,5-triiodo-L-thyronine; CAS: 55-06-1; Sigma-Aldrich, Oakville, ON, Cat# T2752-1G) were prepared by dissolution in dH_2O with NaOH vehicle with subsequent dilutions for a final concentration of 10 µM T_3 in 50 µM NaOH. A final concentration of 50 nM NaOH was present in all treatments, including the negative control. 1000x NaOH stocks were prepared in dH_2O at 50 µM. 2x stocks of NaOH or T_3 were prepared by a 1/500 dilution of 1000x stocks into T_3 stripped L-15 medium prepared as below, at a concentration of 100 nM NaOH or 20 nM T_3 in 100 nM NaOH respectively.

A 2000x nAg stock was created in autoclaved dH_2O at a concentration of 36 mg/L Ag content. All nAg dilutions were followed by a 1 min vortex to ensure complete dispersion. A 2x stock of the highest nAg treatment was prepared by a 1/1000 dilution of the 2000x stock into T_3 stripped L-15 medium at a concentration of 36 µg/L Ag. Subsequent 2x nAg stocks were prepared by 1/10 serial dilutions in T_3 stripped L-15 medium for final concentrations of 3.6, 0.36 and 0.036 µg/L Ag.

XTC-2 cell culture

Parental stock XTC-2 cells were obtained from Robert Denver's lab at the University of Michigan. All XTC-2 cell culture manipulations were performed in the BSC. Cells were cultured in air at 25°C in 70% strength Leibovitz's L-15 media (Gibco, Invitrogen, Grand Island, NY, USA, Cat#:41300-039) with 10 mM HEPES (Sigma–Aldrich, Oakville, ON, Cat#:H4034) and adjusted to pH 7.5.

Medium was sterilized with a 0.2 µm pore filter (Sarstedt Inc., Montreal, QC, Cat#:83.1827) and supplemented with 10% (v/v) heat inactivated FBS (HyClone, Logan, UT, USA, Cat#:SH30071.03) and 2 mM L-glutamine (Gibco, Invitrogen, Grand Island, NY, USA, Cat#:25030-081). Heat inactivation was achieved by heating FBS to 55°C for 30 min.

Monoculturing

At confluence, cells were harvested by washing 2x with sterile Mg^{2+}-free medium (MFM), followed by addition of 0.05% (w/v) trypsin (Gibco, Invitrogen, Grand Island, NY, USA, Cat#:15090-046) in sterile Ca^{2+}- and Mg^{2+}-free media (CMFM) containing 0.5 mM EDTA. Single cells were isolated by plating cells at a density of 5 cells/10 cm diameter culture dish (Sarstedt Inc., Montreal, QC, Cat#:83.1802). Cell numbers and morphologies were monitored until individual colonies reached sufficient size to be isolated with 150 µL trypsin solution added to cloning cylinders (Fisher Scientific, Bel-Art Products, Wayne, NJ, USA, Cat#:07-907-10) sealed to plates with sterile white petroleum jelly. Colonies were plated in Primaria 24-well plates (Falcon BD, Mississauga, ON, Cat#:353847) and grown with subsequent splitting into Primaria 6-well plates (Falcon BD, Mississauga, ON, Cat#:353846) and finally 10 cm culture dishes. Colonies for TH response testing were chosen based on unique and homogeneous cell morphology and overall robust growth and maintenance.

Exposure Setup of TH and nAg Response Tests

XTC-2 cells were plated in 6-well plates at a density of 4.8×10^4 cells/mL medium, with 6 replicate wells per treatment. After 24 h, plates were washed 3x with MFM before addition of T_3 stripped L-15 medium, prepared as noted above except with 10% (v/v) charcoal/dextran treated FBS (Hyclone, Logan, UT, USA Cat#:SH30068.03). After 2 days the plates were washed 1x with MFM before addition of exposure treatments. For the monoculture TH response tests, the 1000x NaOH and T_3 stocks were diluted 1/1000 into T_3 stripped L-15 medium for final concentrations of 50 nM NaOH or 10 nM T3 in 50nM NaOH respectively. For the nAg exposure treatment placement was randomized among wells in

different plates. The 2x stocks of the 4 nAg treatments were diluted ½ with 2x NaOH or 2x T_3 in NaOH for final concentrations of 0.018, 0.18, 1.8 and 18 µg/L nAg ± 10nM T_3. The negative and T_3 controls were prepared by a ½ dilution of 2x NaOH or T_3 stocks into T_3 stripped L-15 medium to generate final concentrations of 50 nM NaOH and 10 nM T_3 in 50 nM NaOH, respectively. XTC-2 cells were incubated with respective treatments for 24 h before being harvested into 1 ml of TRIzol reagent (Ambion, Mississauga, ON, Cat#:15596018). Lysed cells were stored at -80°C until RNA extraction.

Transcript Analysis

Total RNA extraction and cDNA synthesis were performed as described in Chapter 2 Materials and Methods. Isolated RNA was resuspended in 20 µL RNase-free water, quantified with a NanoDrop UV-Vis spectrophotometer (ND-1000, Thermo Scientific, Wilmington, DE, USA) and cDNA was diluted 1/20 prior to QPCR analysis. Primer/probe sequences, thermocycle profiles, quality control measures and other primer details are listed in Table A.2 in Appendix A. The comparative cycle threshold analysis (ΔΔCt; Livak & Schmittgen, 2001) was used to normalize transcriptional abundance of targets to the invariant *rpl8* transcript in TH response tests, and the geometric mean of *rpl8*, *rps10* and *eef1a* in the nAg exposure (see Table A.1, Appendix A).

Statistical Analysis

Analysis was performed using IBM SPSS 20 (Armonk, NY, USA). The $\log_2$ transformed relative abundance of most transcripts was not normally distributed as determined by the Shapiro-Wilk test, so non-parametric statistics were used. The Kruskal-Wallis test was used across all treatments, and if significant within either the NaOH or T_3 treated groups, pairwise analysis was conducted with the Mann-Whitney U test. Statistical significance was considered to be $p < 0.05$.

4.3 Results

nAg Characterization in L-15 Culture Medium

Water chemistry has a significant effect on nAg behaviour, and therefore it is important to properly characterize it in each exposure system tested. Handy et al (2012) recommend, at a minimum, the verification of actual NP concentration with some indication of particle distribution in each aqueous environment. Cell culture medium is a complex mixture of buffers, salts, vitamins and amino acids with the addition of fetal bovine serum (FBS) for necessary growth factors needed to maintain and grow cells. The distribution of nAg in medium without added FBS (Figure 4.1A) was similar to its distribution in previously characterized aqueous exposure systems (See Chapter 2, Figure 2.1B, and Chapter 3, Figure 3.1B), with two subpopulations of nAg size. The smaller group likely represents individual nAg particles at around 8.1 nm, and ranges between 4.2 and 20.9 nm. The relatively larger second peak size indicates a greater degree of aggregated nAg than in previous aqueous exposures, however FBS acts as a dispersant to decrease the polydispersity of nAg in the L-15 medium (Figure 4.1B). The FFF-ICP-MS results show that the majority of nAg present is around 6 nm in size, with significantly less in the larger size range compared to medium without FBS. The stock nAg has previously been shown to have slight aggregation (see Chapter 2, Figure 2.1A), so it is interesting that FBS is capable of reversing most of that aggregation. This dispersive action has previously been described for FBS (Farkas et al, 2011a) and bovine serum albumin (BSA; Handy et al, 2012) in culture systems, and therefore indicates that the XTC-2 cells are exposed to relatively evenly-distributed nAg particle sizes in contrast to other aqueous exposure systems (Chapters 2 and 3).

The amount of iAg dissolution from nAg in the L-15 cell culture medium between the range of 8-29 µg/L nAg was on average 5.7% ±5.2. This low iAg content reflects the stability of nAg in the culture medium. The concentration of nAg in the exposure system as determined by ICP-MS was 119.3% ± 1.1 of the nominal based on total Ag content. The Ag content in the negative control was less than the limit of detection (0.02 µg/L Ag).

The nAg batch (lot# AC0829LMPPTFD) used in Chapter 2 and 3 was used for comparisons with previous exposure systems. While the iAg dissolution and FBS-mediated dispersion was indicative of the behaviour of the current XTC-2 exposure nAg batch (lot# RL101111A), it was not directly tested.

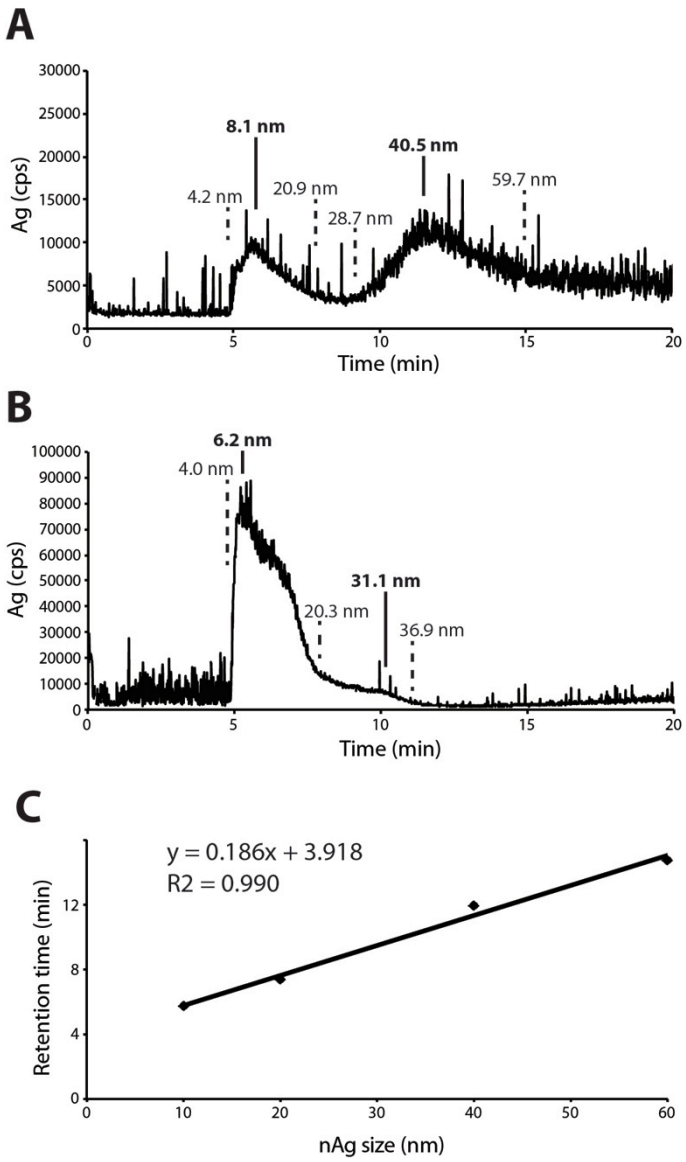

Figure 4.1 – Effect of FBS on nAg behaviour XTC-2 L-15 culture medium determined by FFF-ICP-MS separation. Stock nAg was diluted to 60 µg/L with either **A)** 70% L-15 culture medium or **B)** 70% L-15 culture medium +10% FBS. Ag was detected at 420 nm with on-line UV-VIS. **C)** Calibration curve used to determine nAg aggregate size based on retention times of known nAg standards (10-60 nm). (Partially adapted from Hoque et al, 2012).

Monoculture Validation

Thrb transcript levels were used as an indicator of the T_3 transcriptional response as it is an auto-regulated direct response gene with a thyroid hormone response element (TRE) in its promoter (Shi, 2000). In the stock XTC-2 cells, the *thrb* response to T_3 was highly variable between culture wells ranging from 35- to 140-fold greater than the negative control (Figure 4.2A; n=12). The response in each monoculture line was much tighter than the stock (Figure 4.2B; n=6/monoculture). Furthermore, the strength of the *thrb* induction between each monoculture varied between a median of 40- and 80-fold greater than the control. The XTC-2 K4-2 line was used for further nAg testing as it had the largest and tightest response to T_3.

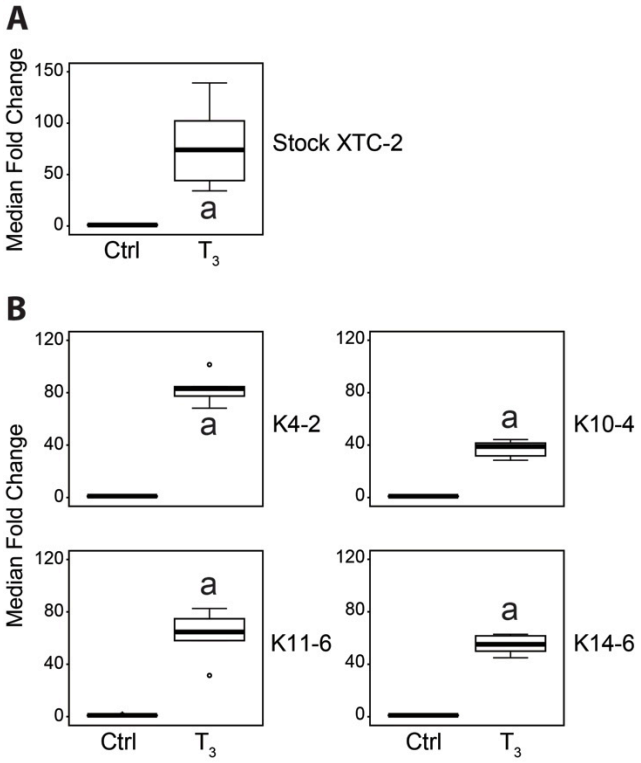

Figure 4.2 – *thrb* mRNA response to T_3 in parental stock and monocultured XTC-2 cells. XTC-2 cells were exposed to 10 nM T_3 for 24 h. *Thrb* transcript abundance as determined by QPCR in **A)** stock cells (n=12/treatment), and **B)** 4 monocultures of XTC-2 cells (n=6/treatment). Data was normalized to the invariant *rpl8* transcript and expressed as median fold change from the negative control (Ctrl). Statistical significance denoted at p-value <0.05 (a). See Figure 2.6 for boxplot details.

Examination of T_3 and nAg responses

Eight transcripts were examined which had previously demonstrated nAg responsiveness (see Figure 2.6 Chapter 2, and Figure 3.6 Chapter 3; Hinther et al, 2010b). The specific transcripts were: *thra* and *thrb*, cyclin-dependent kinase xic1 (*cdknx*), Ftz-F1-related orphan receptor A (*nr5a2*), insulin-like growth factor 2 (*igf2*), cytoplasmic beta actin (*actb*), eosinophil peroxidase (*epx*) and myeloperoxidase (*mpo*). Four targets (*cdknx*, *actb*, *igf2*, *thra*) that had well characterized *in vivo* responses to endogenous and exogenous T_3 in *X. laevis* liver (see Figure 2.6, Chapter 2) did not respond to T_3 in the XTC-2 cells (Figure 4.3). Two targets did show a response to T_3 (*thrb, nr5a2*), although no nAg-induced changes were detected. Only 1 target (*cdknx*) responded significantly to nAg ($p=0.025$), but only at 0.18 µg/L nAg in the presence of 10 nM T_3.

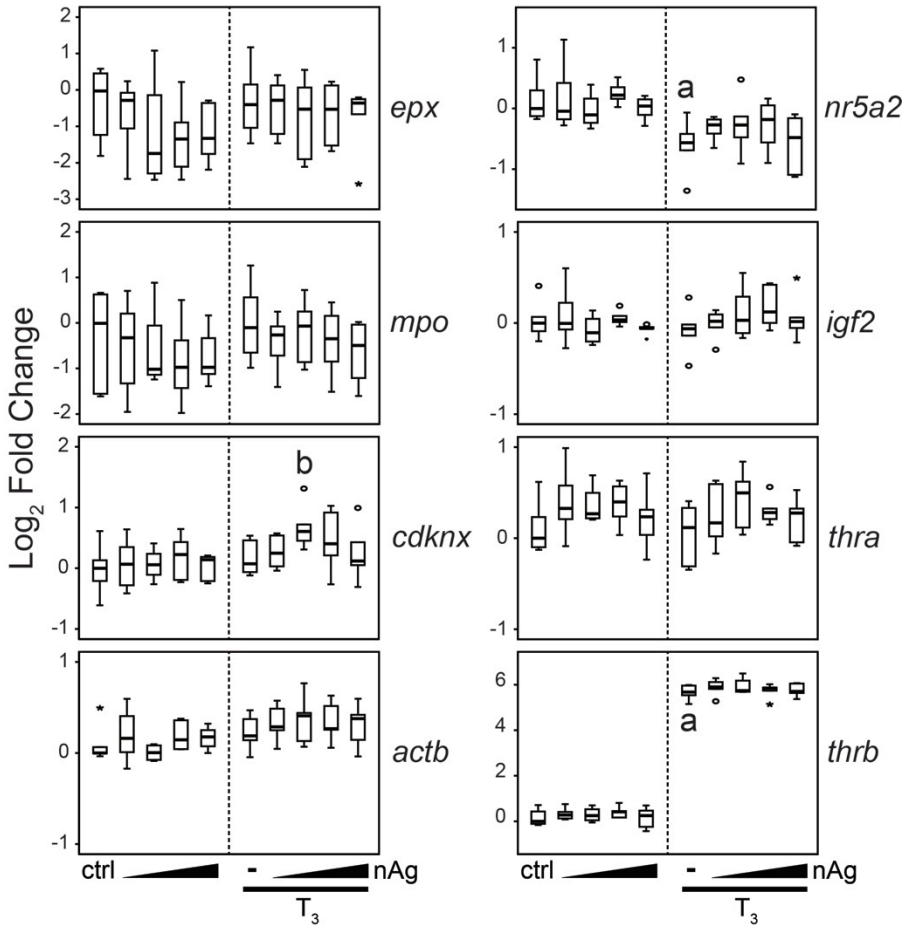

Figure 4.3 – Effect of nAg on XTC-2 K4-2 cells. XTC-2 cells were exposed to nAg (0.018-18 µg/L Ag) for 24hrs in the absence and presence of 10nM T_3. Transcriptional abundance was determined by QPCR for nAg-responsive targets from *in vivo X. laevis* exposures, and normalized to the geometric mean of invariant transcripts *eef1a, rpl8,* and *rps10.* Data is represented as log_2 fold change from the negative control (ctrl). Significance from ctrl (a) or T_3 control (b) denoted at $p<0.05$. See Figure 2.6 for boxplot details.

4.4 Discussion

Monocultures

XTC-2 cells were originally prepared from a whole tadpole body with the internal organs removed, and the resultant cells were described as both fibroblast-like and epithelial (Pudney et al, 1973). XTC-2 cells have previously been subcultured due to the heterogeneity of stock cells (Snoek et al, 1990). The morphology of individual monocultured cell lines also ranged between fibroblast-like and epithelial. Furthermore, while the selected monocultures all responded to TH using *thrb* transcript as the readout, the strength of response varied, with a two-fold difference between strongest and weakest responding monoculture (K4-2 and K10-4 respectively). Therefore, it is clear there were multiple subpopulations of cells within the original stock and that the monoculturing procedure was effective in reducing TH-response variation.

Effect of T_3 and nAg on transcript levels

Eight transcripts were tested for responsiveness to T_3 and nAg based upon previous *in vivo* and *in vitro* data (see Chapters 2 and 3). While *thrb* and *nr5a2* transcripts showed responsiveness to T_3 consistent with that observed in *X. laevis* pre- and prometamorphic tadpoles (see Figure 3.6, Chapter 3), none of the other transcripts were altered by T_3. During metamorphosis, tissues are induced by endogenous T_3 to undergo varied physiological responses from apoptosis to cellular proliferation (Shi, 2000), so tissue-specific TH-responsiveness may account for some of this disparity. While *thrb* transcript levels are also increased in most amphibian tissues including brain (Helbing et al, 2007a; Helbing et al, 2011), intestine (Shi & Brown, 1993), tailfin (Helbing et al, 2011; Veldhoen et al, 2006), and liver (Chapters 2 and 3; Chen & Atkinson, 1997; Fairclough & Tata, 1997; Helbing et al, 1992), the TH-response of other transcripts are dependent on the tissue being examined. For example, *igf2* transcript levels increased in the brain (Helbing et al, 2011) and decreased in liver (see Figure 3.6, Chapter 3). While *cdknx* mRNA abundance was increased in both tailfin (Veldhoen et al, 2006) and liver (Chapter 2 and 3) with TH administration, it was not altered in the

present study. Furthermore, other gene transcripts that were T_3-responsive in *X. laevis* liver (*actb, thra*; Chapter 3) or *Rana catesbeiana* brain, liver and tailfin (*thra*; Chapter 2) were not T_3-responsive in the XTC-2 cells. Therefore, the tissue-specific nature of TH-dependent transcription may explain the differential transcript response in XTC-2 cells.

We previously identified several biomarker candidates for responsiveness to nAg exposure (Chapter 3). These candidates encoded proteins that function in a wide variety of cell types and tissues. With the exception of *cdknx*, none of the seven transcripts found to be affected by nAg *in vivo* (*epx, mpo*, *cdknx, actb, igf2, nr5a2, thra*) were affected in XTC-2 cultured cells. nAg slightly increased the abundance of *cdknx* in XTC-2 cells, however, in contrast, *cdknx* transcripts were consistently reduced in the prometamorphic tadpole liver (see Figure 3.6). Therefore, the responsiveness of this cell line differs substantially from intact liver and tail fin biopsy tissue.

There are several reasons that could account for the lack of nAg-induced response as compared to the *in vivo* exposures (Chapter 2 and 3) and the *ex vivo* C-fin assay (Hinther et al, 2010b). First, tissue origin may influence responsiveness. Like the differential responsiveness seen with TH, nAg appears to exert differential tissue effects at the molecular level (see Chapter 2, Discussion). Therefore, the difference between hepatic and fibroblast-like cell types may preclude similarity in nAg responsiveness. Second, a contributing factor may be differences inherent in cell culture vs tissue systems. The present assay is an *in vitro* system lacking the complexity of the multiple cell types within organs or whole animals present in the C-fin assay (Hinther et al, 2010a) and *in vivo* exposures. There may be key signaling events between tissue layers that influence the effects of nAg on transcript signaling that are not present in the homogeneous cell line. Third, there may be differences due to the properties of the nAg itself. We found that FBS has a dispersive action on nAg in the exposure medium, which differs from the slight aggregation seen in the *in vivo* exposures (Chapter 2, Figure 2.1B; Chapter 3, Figure 3.1B). Previous studies have indicated that smaller nAg sizes are associated with greater toxicity such as

cell death and decreased metabolic activity (Lankoff et al, 2012). In contrast, in the present study fewer transcriptional responses were observed with more dispersed particles than previously (Chapter 2 and 3). However, the nAg used in the present study was from a different batch, and perhaps differences in the proprietary manufacturing process accounted for the lack of transcript response.

The absence of a characteristic transcript profile from nAg-exposed XTC-2 cells meant that further mechanistic investigations were not possible. However, as the XTC-2 K4-2 cell line is now optimized and responds well to T_3 in *thrb* and *nr5a2*, it can be used to investigate the TH disrupting effects of other potential EDCs.

Although nAg did not change the levels of transcript candidates tested herein, the effects on many other transcripts in TH signaling were not determined. Future research could include microarray or RNA-seq analysis of the transcriptome to identify nAg responsive targets specifically within the context of these cells allowing mechanistic investigation into the elements responsible for its endocrine disrupting capacity in the broader perspective of cellular processes.

5 Sex-biased TH responsiveness of the *Xenopus laevis* tadpole liver during pre- and prometamorphosis

The data in this chapter was obtained from exposures performed in Chapter 3, with subsequent sexing, and sex-specific transcriptional analysis. Preliminary genomic sexing on tailfin tissue was performed by Stacey Maher and Saadia Vawda. The *actb* and *xdm-w* primers were designed by Nik Veldhoen, and the *xdm-w* primers were initially assessed by Melissa Cabecinha. Otherwise, all data presented herein were collected and analyzed by me.

5.1 Introduction

During amphibian metamorphosis, thyroid hormone (TH) induces modifications in nearly all tissues within the developing frog. The onset of TH synthesis in the thyroid gland differentiates pre- (premet) and prometamorphic (promet) tadpoles, lacking and having circulating TH, respectively. In *Xenopus laevis*, the African clawed frog, sex determination and subsequent gonad differentiation and development initiates prior to metamorphosis and is coupled with distinct developmental stages, although it is not directly dependent on TH (Hayes, 1998). Larval bipotential gonads differentiate into ovaries or testes in a process that begins in premets at Nieuwkoop and Faber (NF) stage 52 (Nieuwkoop & Faber, 1994). Gonads and secondary sex organs continue to develop throughout and past metamorphosis, terminating when frogs reach sexual maturity, between approximately 6-10 months for males and 12-24 months for females (Kelley, 1996). While histological analysis can demonstrate early gonadal differentiation defined by germ cell localization and tissue reorganization, determination of phenotypic sex by visual examination of gonads is impossible before the onset of prometamorphosis at NF55 (Kelley, 1996).

Although sex chromosomes are indistinguishable from autosomal chromosomes, in most amphibians sex determination is under genetic control, as with birds and mammals (Hayes, 1998). As in birds, *X. laevis* employ a ZZ/ZW

sexing system, determined through breeding tests using estrogen- and androgen-induced sex reversal (Chang & Witschi, 1956). As opposed to the XX/XY system, heterogametic individuals are female (ZW) and males are homogametic (ZZ). While the sex determining genes remain unknown in most amphibian species, in *X. laevis* the newly identified *xdm-w* gene is specific to the W chromosome and therefore can be used to determine the genetic sex of individuals (Yoshimoto et al, 2008). The Xdm-w protein possesses a doublesex-mab3 (DM) domain containing a zinc finger-like DNA-binding motif with high similarity to the doublesex- and mab3-related transcription factor 1 (Dmrt1) protein (Yoshimoto et al, 2008) which is involved in testicular formation during sexual development in many vertebrates (Kettlewell et al, 2000; Nanda et al, 2002; Raymond et al, 1999; Raymond et al, 2000). However, the transactivation domain within the C-terminal region of Dmrt1 in *X. laevis* is absent from Xdm-w. Furthermore, contrary to Dmrt1, Xdm-w is essential for proper ovarian development. Overexpression of Xdm-w in transgenic male (ZZ) tadpoles caused increased expression of the aromatase enzyme that converts testosterone to estradiol, as well as the development of ovotestes containing both ovarian and testicular gonadal tissue (Yoshimoto et al, 2008). Therefore while the *xdm-w* gene is a paralog of *dmrt1*, it has a unique function in female gonadal development. Moreover, normal females possess the *xdm-w* gene while males do not, thereby providing a means for genetically sexing *X. laevis* at any stage.

Endocrine disrupting chemicals (EDCs) can either mimic hormones or otherwise alter their metabolism, activity or signaling pathways. As sex steroids are involved in gonadal differentiation and development, EDCs can alter gonadal morphology. For example, estrogenic EDCs such as ethinylestradiol (EE2) can cause gonadal malformations such as ovotestes, as well as complete sex reversal of ZZ males into phenotypic females. Using the northern leopard frog (*Rana pipiens*), Hogan et al (2008) determined that the initial stages of gonadal differentiation during premetamorphosis are critical periods of sensitivity to EE2 action, and the feminized gonads persisted throughout development even after

EE2 was removed. Furthermore, gonadal malformations due to EDC action can persist until sexual maturity and decrease the reproductive potential of adult *X. tropicalis* frogs (Pettersson et al, 2006). As it is desirable to examine the effects of EDCs during the initial, sensitive stages of gonadal differentiation, amplification of the *xdm-w* gene provides a means to quickly determine the genetic sex of individuals when visual differentiation is not possible. This tool would be even more powerful in conjunction with transcriptional markers that are EDC-responsive and possibly even representative of the phenotypic sex. In this manner, perturbations in normal signaling pathways could be monitored, and sex-reversal determined relatively early in development.

Triiodothyronine (T_3) is the active form of TH that drives amphibian metamorphosis. While T_3 is not involved in initial sex differentiation, there is evidence it is necessary for male gonadal development. When TH production is inhibited with either perchlorate or thiourea, a female-biased sex ratio is observed in developmentally-arrested *X. laevis* tadpoles (Goleman et al, 2002; Hayes, 1997). Administration of the TH production inhibitor propylthiouracil to adult female zebrafish increased the plasma concentrations of the female sex hormones, luteinizing hormone (LH) and follicular stimulating hormone (FSH; Liu et al, 2011). Furthermore, when exogenous T_3 was administered to *X. tropicalis* premet tadpoles in the initial stages of sexual differentiation (NF52-54), the mRNA abundance of male sex-specific genes such as androgen receptor (*ar*) and 5-alpha-reductase 1 and 2 (*srd5a1, srd5a2*) were strongly increased in the gonad-mesonephros complex (Duarte-Guterman & Trudeau, 2011). Concurrently the female-specific gene estrogen receptor beta (*esr2*) mRNA was decreased. Therefore, there is compelling evidence that THs are involved in gonadal development, particularly playing a masculinizing role during amphibian metamorphosis. However, how this is accomplished remains poorly understood.

Even less is understood regarding the role of genetic sex upon the TH-mediated response in the liver. It is clear that this organ displays sex-specific transcript profiles in sexually differentiated adults. This sexual bias affects transcripts involved in a variety of biological functions from sexual reproduction,

lipid metabolism and thyroid hormone receptor activation to transcription and chromatin organization (Zhang et al, 2011). For example, it is well known for its role in producing vitellogenin (Vtg) in females, a yolk protein in egg-laying animals that is subsequently transported to the ovaries and into maturing oocytes post-metamorphosis in *X. laevis* (Rabelo et al, 1994). In human adult liver, over 1200 transcripts have been described that are differentially regulated between the sexes. However, what is unclear is to what extent transcript differences occur in tadpoles at early stages of sexual differentiation and to what extent responsiveness to THs may be influenced by sex during pre- and prometamorphic stages since TH induces extensive gene-switching in the liver during metamorphosis (Mukhi et al, 2010).

In the present study, we first asked whether or not sex-bias in liver transcript profiles is evident in tadpoles during pre- and prometamorphosis in *X. laevis* tadpoles and whether developmental progression, which correlates with gonadal differentiation and increased TH levels, influences sex-bias in the tadpole liver transcriptome. Second, we asked whether or not there are sex-specific transcriptional responses to exogenous administration of physiological concentrations of T_3.

While the majority of transcripts investigated demonstrated no sex-bias at these stages, some notable exceptions were detected with implications that TH-responsiveness may be influenced by genetic sex in non-gonadal tissue.

5.2 Materials and Methods

Exposure setup

Preparation and execution details for chemical preparation, experimental animals, exposure setup, MAGEX cDNA microarray and QPCR are described in Chapter 3. In brief, sixteen *X. laevis* premet or promet tadpoles each were immersed in 10 nM T_3 for 48 h. Negative control animals were immersed in the 50 nM NaOH solvent alone. After 48 h, tadpoles were euthanized in tricaine methanesulfonate and preserved in RNAlater with subsequent dissection of liver

for RNA extraction and QPCR and microarray transcriptomics analysis. The heart was collected for gDNA extraction to determine genetic sex of each animal.

Genetic sexing protocol

Genomic DNA (gDNA) was extracted with the DNeasy Blood and Tissue Kit (Qiagen, Toronto, ON, Cat#:69506) with RNase A digestion (Qiagen, Toronto, ON, Cat#:1018048) from premet (NF53) and promet (NF57) heart tissue, as per manufacturer's protocol. gDNA was eluted into 150 µl Buffer AE, and quantified with the Nanodrop UV-Vis spectrophotometer (ND-1000, Thermo Scientific, Wilmington, DE, USA). Neat gDNA was diluted to a constant 10 ng/µl in diethyl pyrocarbonate (DEPC)-treated RNase-free water of which 2 µl was used for quantitative real-time polymerase chain reaction (QPCR) sex determination. Primer sequences, thermocycle profiles, quality control measures and other details are listed in Table A.2 in Appendix A. All samples were run in duplicate. Sex specificity of *xdm-w* primers was verified on sexually dimorphic adult male and female *X. laevis* frogs. gDNA was extracted as above from biopsies taken from toe webbing of 3 males and 3 females, and 1.5% agarose gel electrophoresis was used to confirm specificity and predicted amplicon size of *xdm-w* primers (Figure 5.1A). The cytoplasmic beta actin gene (*actb*) was used as a gDNA control. Determination of sex was made in 2 ways. As the *xdm-w* primers caused non-specific amplification in males, a cut-off was given on the difference in the cycle to cross the threshold (dCt) from *actb*. If the dCt was greater than 2.5 then samples were denoted male, otherwise they were female. These calls were checked against the *xdm-w* dissociation curve from the QPCR runs. Female samples had an amplification product which peaked at 88.5°C, while males had non-specific product melt temperatures around 77°C (Figure 5.1C). Gel electrophoresis with a 1.5% agarose gel was used to confirm QPCR primer product sizes from 4 female and male samples (Figure 5.1B) whose sex was determined as above.

Statistical analysis

Statistical analyses were performed with R statistical package version 2.15.0 (R Foundation for Statistical Computing, Vienna, Austria <www.r-project.org>). Non-parametric rank-based statistical models were used, as some data did not meet normality or homoscedastic requirements, as determined by Shapiro-Wilks and Levene's tests respectively. The Kruskal-Wallis test (KW) and 2-way robust ANOVA (raov R function, rfit package) were used on both QPCR and microarray data where KW was used to evaluate the influence of sex within each developmental stage and robust ANOVA for all other comparisons. Significance in ANOVA models was represented by the interaction between both factors (either sex+treatment or sex+developmental stage). Post-hoc analysis of significant groups was performed with pairwise Kruskal-Wallis tests. Statistical significance in all cases was considered at $p\text{-value} < 0.05$.

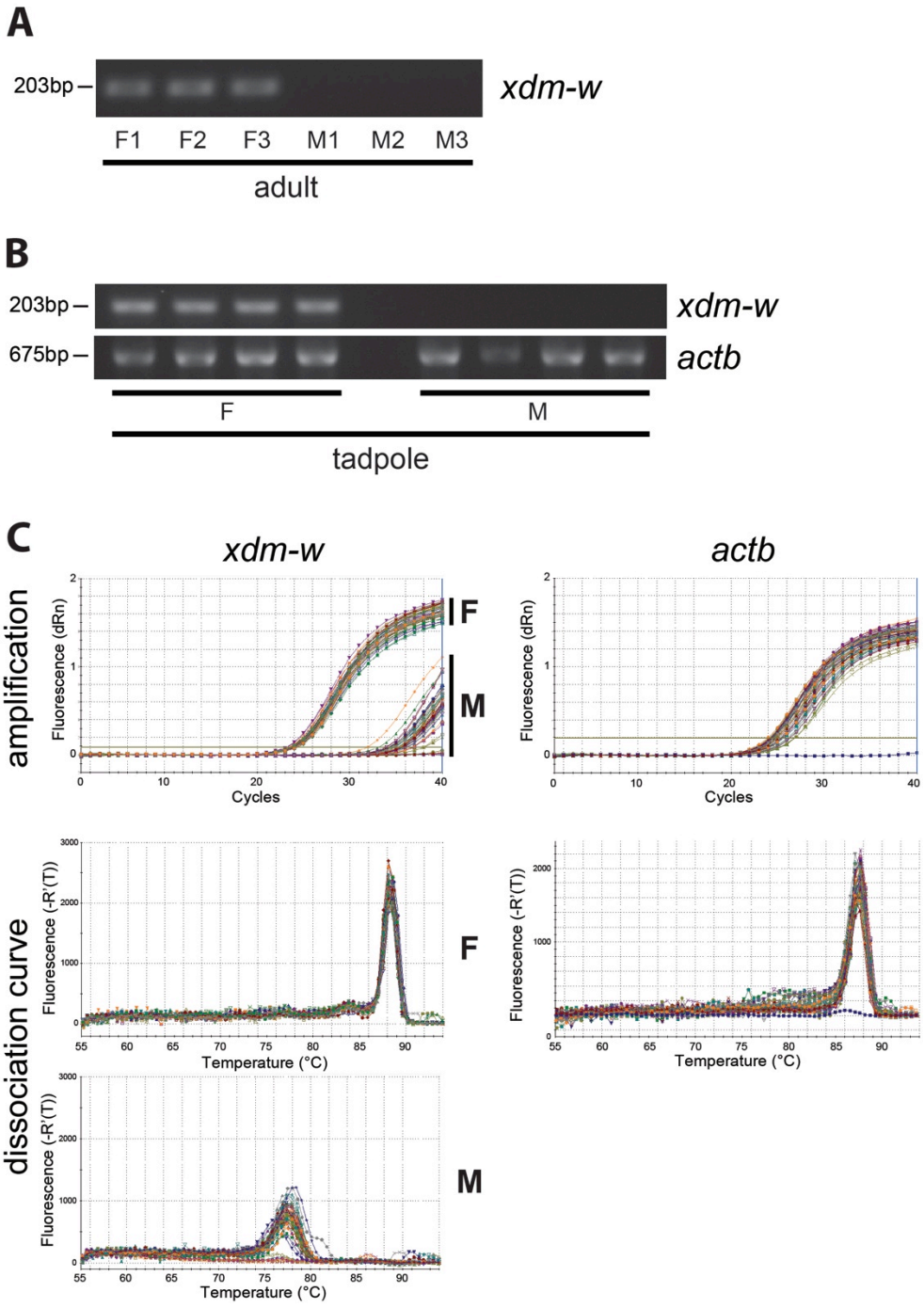

Figure 5.1 - Determination of genetic sex by QPCR amplification of female-specific *xdm-w* gene. A) Validation of *xdm-w* primer specificity and amplicon size on adult tissue with 1.5% agarose gel electrophoresis. The *xdm-w* gene was amplified only in heterogametic females (ZW). **B)** Sex determination of visually undifferentiated tadpoles (NF53) via *xdm-w* amplification in heart gDNA. *actb* was the gDNA input control, and gel electrophoresis performed as in A). **C)** QPCR amplification and dissociation curves showing distinct specificity for *xdm-w* in females (F).

5.3 Results and Discussion

Genetic Sexing Protocol

The genetic sexing protocol was a successful and reliable tool to determine the sex of tadpoles during the early stages of gonadal differentiation. Preliminary testing in our lab using gDNA extracted from tailfin was problematic possibly due to cross-contamination from skin cells off other tadpoles. The heart was then used as the pericardial cavity allows greater protection from cross-contamination during dissection. The sex ratio across all animals at each stage was approximately 50% (Figure 5.2), as expected (Chang & Witschi, 1956). Therefore, we have successfully sexed pre- and promet tadpoles using a QPCR based analysis with 2 independent verification methods (dCt threshold and dissociation curve analysis) which precludes the necessity of gel electrophoresis, saving time and resources.

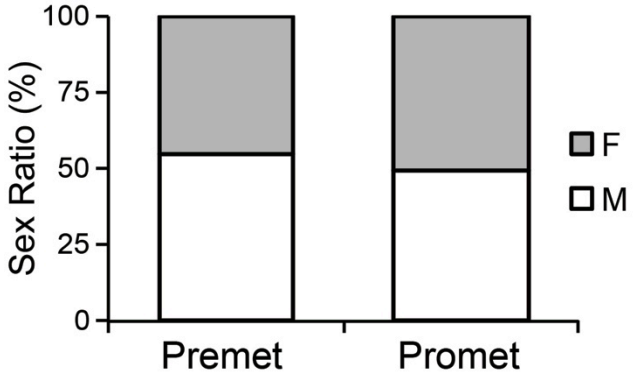

Figure 5.2 – Sex ratio of *X. laevis* tadpoles at premet (NF53) or promet (NF57) stages as determined by the genetic sexing protocol. F: female, M: male.

TH-responsive and sexually-biased gene transcripts in premet and promet tadpole livers

We first investigated the mRNA profile of male and female tadpoles to see if there were sex-biased targets at specific stages of development: premetamorphosis (NF53), and prometamorphosis (NF57). QPCR was used to determine the abundance of transcripts previously demonstrated to be responsive to T_3 in *X. laevis* during precocious and natural metamorphosis (see

Figure 3.6A and B respectively, Chapter 3), including thyroid hormone receptor alpha or beta (*thra, thrb*), cyclin dependent kinase xic1 (*cdknx*), insulin-like growth factor 2 (*igf2*), Ftz-F1-related orphan receptor A (*nr5a2*), and cytoplasmic beta actin (*actb*). While the natural profile of these targets during metamorphosis was maintained by both male and female tadpoles, no sex-specific differences were observed (Figure 5.3A). At these stages there are likely endogenous sex-steroids in circulation due to their role in gonadal development (Hayes, 1998; Kelley, 1996). Therefore, the lack of a sex-bias implies these targets are not likely sensitive to endogenous sex-steroid secretions.

Using the in-house MAGEX cDNA microarray, we were able to identify three transcripts that did show a sex-bias in liver between males and females (Figure 5.3B): 17-beta hydroxysteroid dehydrogenase type 5/aldo-keto reductase family 1 member C3 (*akr1c3*), vitellogenin (*vtg*) and SRY-box 9 (*sox9*). All three targets have a higher mRNA abundance in males than females in premet tadpoles. This difference was attenuated in a*kr1c3* and *vtg* by NF57. Vtg is produced in the liver and regulated by estrogen via the estrogen nuclear receptor (Esr; Bagamasbad & Denver, 2011). As such it is a well-known estrogenic EDC biomarker, often indicative of feminizing effects on male individuals.

While *sox9* transcript abundance in males was not altered between NF53 and NF57, females showed a significant increase in abundance. This implies there is a sex- and stage-specific sensitivity of *sox9* during natural metamorphosis. Therefore, there is evidence of sex-biased transcript levels during the early stages of TH-dependent metamorphosis, which correspond with gonadal differentiation.

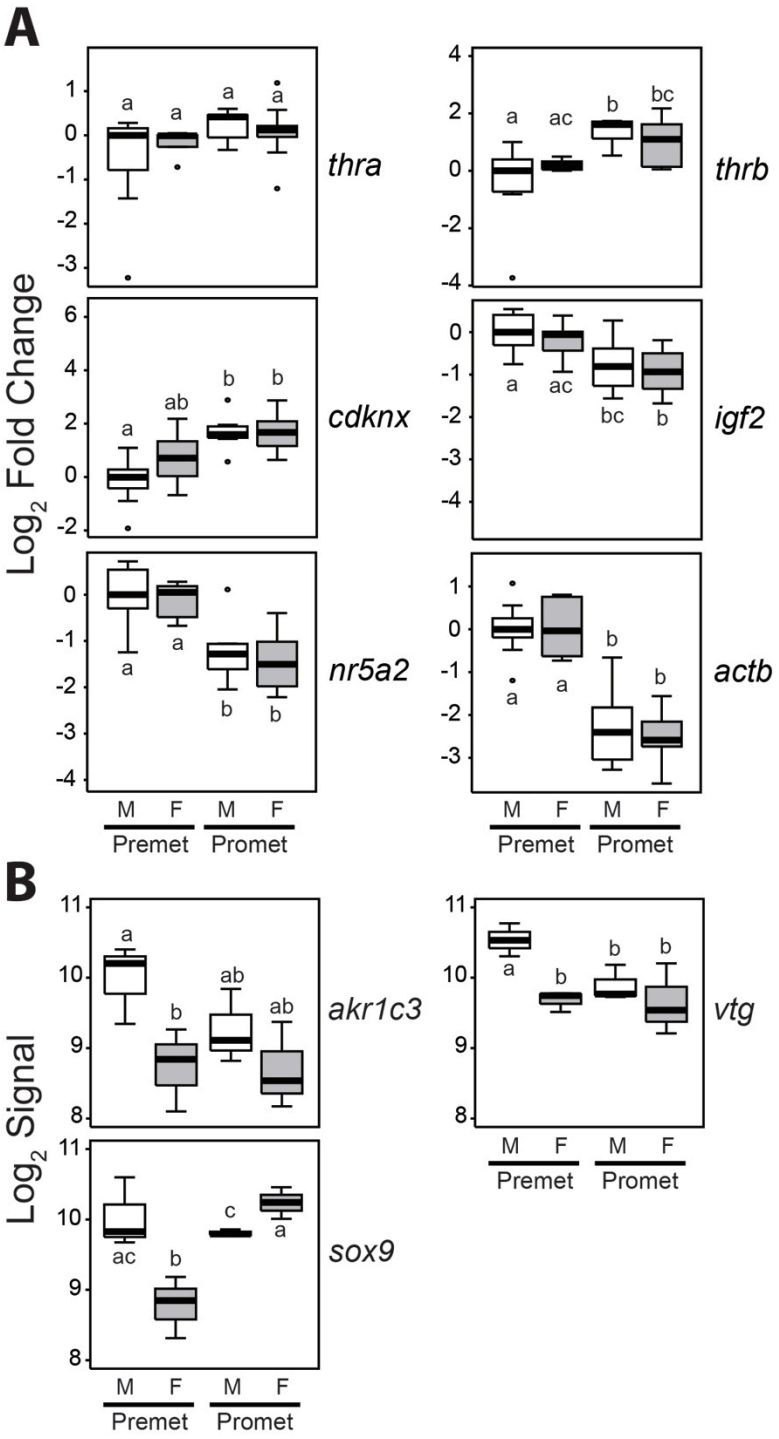

Figure 5.3 – Male (M) and female (F) liver transcript levels at premet (NF53) and promet (NF57) stages. A) QPCR analysis of TH-responsive targets with 5-11 animals/group, normalized to *eef1a* and *rps10* invariant transcripts, $\log_2$ transformed and expressed relative to the premet M group. **B**) Log_2 signal intensity of targets identified by microarray analysis, normalized to robust, non-TH-responsive probes, with 3 animals/group. Pairwise significant differences at $p<0.05$ denoted with different letters between groups. See Figure 2.6 for boxplot details.

Sex-specific transcript response during TH-induced metamorphosis

We next investigated whether sex has an influence on TH-signaling in premet and promet tadpoles, using T_3 to induce transcriptional changes. Transcriptional cross-talk has only previously been investigated with respect to the influence of endogenous or exogenous TH on sex-related genes in the gonad (Duarte-Guterman & Trudeau, 2011), brain (Duarte-Guterman & Trudeau, 2010), or whole embryonic tissues (Duarte-Guterman et al, 2010), with tadpoles of unknown sex. Herein we specifically ask how sex can influence TH-signaling in extra-gonadal liver tissue.

There were no observed sex-specific responses to T_3 in TH-responsive targets (Figure 5.4A). Male and female tadpoles both responded to T_3 as expected at premet and promet stages (see Figure 3.6A, Chapter 3). This result further indicates that these targets are probably not regulated by the endogenous sex steroids involved in gonadal differentiation. By extension, this suggests that these targets won't be responsive to estrogenic or androgenic EDCs. It is important to know there are not sex-specific differences when using these targets in TH-signaling studies, as the sex of tadpoles during TH EDC assays is often not investigated. Furthermore, these targets would be useful when investigating complex mixtures such as sewage wastewater. Effluent may contain TH-disrupting, estrogenic and androgenic compounds (Li et al, 2011), so disruption of the above targets could be attributed to the presence of TH EDCs specifically.

A differential response to T_3 was noted in sex-biased targets. In premets, exogenous T_3 caused a decrease of *vtg* and *sox9* mRNA abundance in males and an increase in females (Figure 5.4B). The increase of female premet *sox9* abundance was consistent with the increase in females during natural development, suggesting that T_3 is at least partially involved in the sex-specific regulation of *sox9* during metamorphosis.

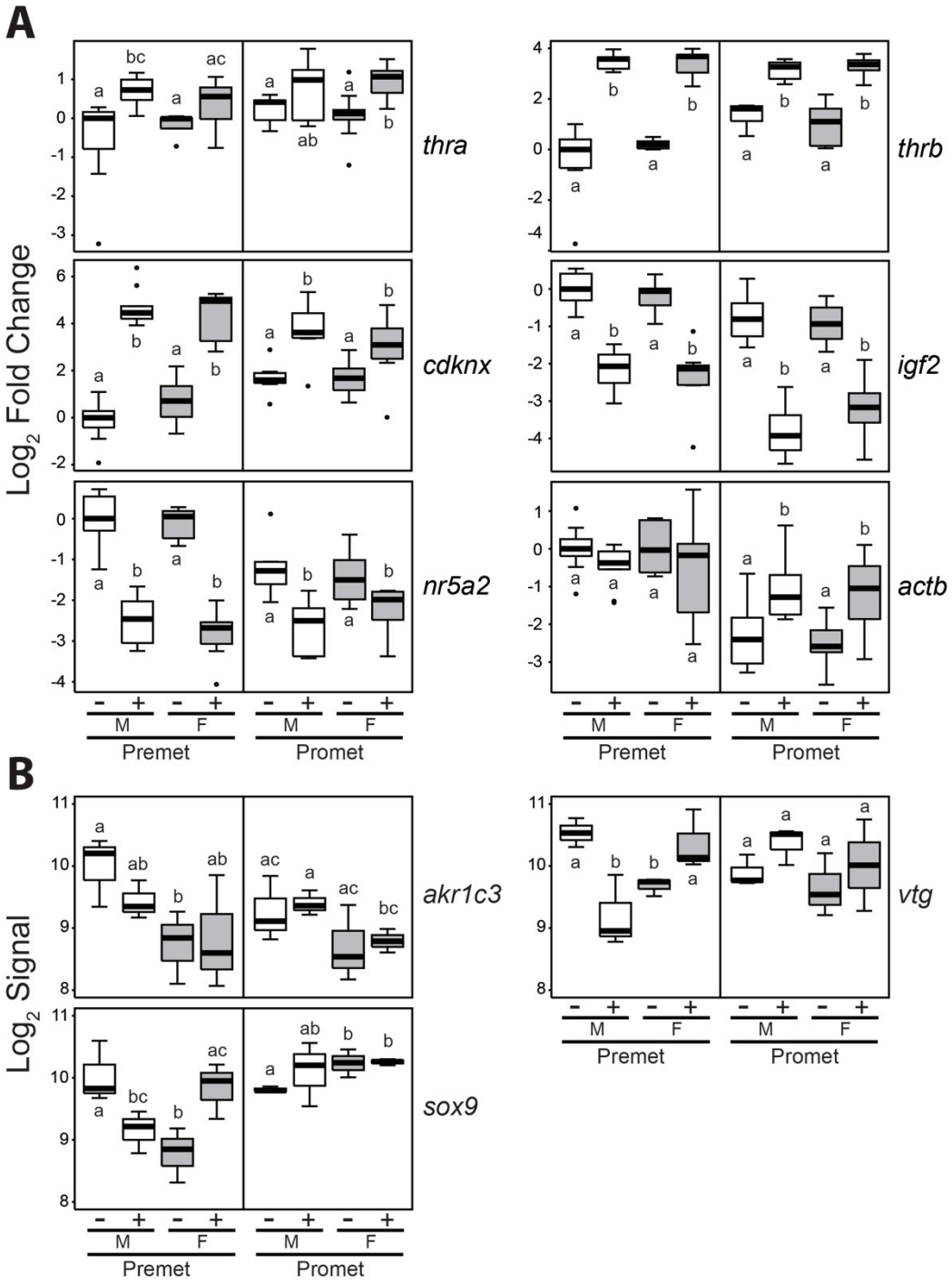

Figure 5.4 – TH-induced liver mRNA response of male (M) and female (F) tadpoles at premet (NF53) and promet (NF57) stages. Tadpoles were exposed to NaOH vehicle (-) or 10 nM T_3 (+) for 48 h. **A**) QPCR analysis of TH-responsive targets with 5-11 animals/group, normalized to *eef1a* and *rps10* invariant transcripts, log_2 transformed and expressed relative to the premet M group. **B**) Log_2 signal intensity of targets identified by microarray analysis, normalized to robust, non-TH-responsive probes, with 3 animals/group. Within each box, pairwise significant differences at $p<0.05$ denoted with different letters between groups. See Figure 2.6 for boxplot details.

The Sox9 protein is a transcription factor containing a high mobility group box (HMG-box) domain, and is related to the SRY protein. Whereas in mammals, birds and reptiles, Sox9 is associated with testicular development, being increased in testes and decreased in ovaries, in amphibians and fish *sox9* is consistently expressed in both testicular and ovarian tissue (reviewed in El Jamil et al, 2008). While there is no current information on the presence or role of Sox9 in the liver of adult or larval amphibians, *sox9*-positive progenitor cells in mammalian livers are involved in its development during organogenesis, regeneration after injury and maintaining progenitor cells in an undifferentiated state (Furuyama et al, 2011). Therefore, *sox9* potentially plays a sex-specific role in liver development during metamorphic changes from a larval to adult tissue.

Premet tadpoles displayed a sex-specific response to T_3 in *vtg* mRNA abundance. Premetamorphosis corresponds with the early stages of gonadal differentiation in *X. laevis*, and there is evidence that T_3 plays a role in testicular development (Duarte-Guterman & Trudeau, 2011; Goleman et al, 2002; Hayes, 1997; Liu et al, 2011). Therefore, T_3 also likely plays a role in sex-specific *vtg* regulation during early premet stages in tadpole liver.

The sex-specific response of *vtg* to exogenous T_3 did not match its profile during natural metamorphosis where there was an attenuation of any sex-bias by NF57. This indicates that other factors are involved in its transcriptional regulation during promet stages outside of T_3. Previously Rabelo et al (1994) also described a lack of *vtg* transcript changes in response to T_3 in promet *X. laevis* tadpoles (NF56-58), although the sex of these tadpoles was not determined. As well, at metamorphic climax (NF60-64), a strong potentiation of estrogen-mediated *vtg* induction by T_3 was observed, likely in both males and females. Here we describe a sex-specific sensitivity in *vtg* transcript levels to T_3 during premetamorphosis which could not have been previously determined without sensitive sexing techniques.

Although all tadpoles need to respond to T_3 to progress through metamorphosis, there is differential T_3-response of *vtg* and *sox9*, dependent on their sex. This implies that although most TH-responsive targets investigated

with QPCR or microarray analysis did not show a sex-bias, it is possible for certain targets to have sensitivity to both TH and endogenous sex-steroids.

While not significant in all cases, there was a trend in *akr1c3* mRNA towards greater abundance in males than females during natural and precocious metamorphosis (Figure 5.4B). This could indicative of a sex-bias in the liver that is consistent throughout multiple developmental stages. While this observation needs independent verification with QPCR analysis and with further developmental stages, if the sex-bias persists *akr1c3* could be a useful tool when examining estrogenic or androgenic EDCs.

akr1c3 is a member of the aldo-keto reductase superfamily involved in steroidogenesis, and is overexpressed in many cancers, including breast and prostate. The Akr1c3 enzyme specifically reduces androstenedione into testosterone, estrone into estradiol, and dehydroepiandrosterone into androstenediol (Byrns et al, 2011). In adult humans, the Akr proteins in the liver function to metabolize sex steroids and prevent against circulating steroid excesses (Penning et al, 2000), and Akr1c3 was specifically implicated as the enzyme responsible for low-level testosterone production in the adrenal glands (Nakamura et al, 2009). Therefore, the increased concentration of *akr1c3* in male liver could either be a potential source of extra-gonadal androgen steroidogenesis, or could act as a regulatory mechanism on circulating androgen concentrations in male tadpoles.

In conclusion, the genetic sexing protocol has been used successfully to investigate the role of sex on TH-signaling in extra-gonadal tissue. Herein we have established that sex can have an impact on TH-signaling in the liver, especially during the early gonadal differentiation stages of premet tadpoles. However, the “classic” TH-response gene transcripts do not show sex-bias. Therefore, when using transcript profiles to study TH EDCs, it is important to keep in mind that targets can potentially respond in a sex-specific manner, which is often overlooked when the sexes are not independently examined.

6 Conclusions

This thesis presents a thorough investigation into the TH endocrine disrupting capacity of nAg at environmental concentrations. The high production volume and use in consumer products means that nAg is invariably an environmental contaminant exposed to aquatic wildlife species during sensitive life stages such as amphibian metamorphosis. Three frog models were used to investigate nAg effects, including an *in vivo* exposure with *R. catesbeiana*, and both *in vivo* and *in vitro* exposures with *X. laevis*, using T_3 as an agonist to induce precocious metamorphosis.

The results of this thesis show consistent evidence of TH EDC action over multiple studies and species. The hindlimb growth and development was accelerated in both *R. catesbeiana* and *X. laevis* tadpoles during the premet stages of metamorphosis, as well as at the conclusion of metamorphosis in *X. laevis*. Furthermore, distinct tissue-specific TH-dependent transcriptional pertubations were noted. In the liver, *thra* mRNA was consistently reduced by nAg in both species. In *R. catesbeiana* tailfin, *thrb* and *rlk1* mRNA abundances were increased in both the *in vivo* study presented here and the initial *ex vivo* C-fin assay prior to this research (Hinther et al, 2010b). Furthermore, one of the major mechanisms for nAg toxicity at higher concentrations is through the production of ROS. Here data were presented indicating ROS could be generated, even at these low concentrations. A transcriptional response to ROS was observed via an increase in *mpo, epx* and *mmp9* transcripts in liver during prometamorphosis in *X. laevis.*

Here we also demonstrated that nAg bioconcentrates to a significant degree within tadpoles during chronic exposures throughout metamorphosis. To investigate how bioavailable nAg would be to juvenile and adult frogs after metamorphosis, it would be beneficial to determine elimination rates after nAg exposure. Furthermore, data was presented across morphological and transcriptional endpoints that the dissolution of nAg into iAg didn't account for all

of the observed effects. This indicates that at least a portion of the effects were NP-specific.

While the XTC-2 monocultures had a much tighter response to T_3 than the original stock cells, the nAg biomarkers determined from *in vivo* exposure were not responsive in the cell line. Further mechanistic insight into nAg's TH-disrupting capabilities could be determined by either creating a stable hepatocyte cell line, or by utilizing primary hepatocyte cultures. In this way, the response of the 7 biomarkers of nAg exposure could be validated. Alternatively, transcript markers for nAg exposure could be obtained by performing a microarray analysis on the XTC-2 K4-2 cells. Once a characteristic transcriptional response was found, mechanistic investigation into the relative contribution of ROS in TH signaling would be possible with ROS generators and inhibitors. Additionally, it would be possible to delve into the response to dissolved iAg with Ag chelators, or even the contribution of the PAA surface coating by exposure to the shells on their own. Therefore, a great deal of information could be gleaned through the combined use of *in vitro* cultures with valid transcriptional biomarkers of exposure.

Due to the timely discovery of a sex-linked gene for *X. laevis*, we were able to investigate the possibility that sex-bias may exist in liver during early gonadal differentiation stages and with respect to TH-dependent metamorphosis. Chapter 5 of this thesis outlined the work done to optimize the genetic sexing protocol for QPCR determination, which was deemed successful. Further work is still needed to test three mRNA targets on a larger sample size to validate their sex-bias during the critical stages of gonadal differentiation and natural and T_3-induced metamorphosis. As such, these targets are potential endpoints for disruption of hormonal signaling by EDCs.

While many studies have investigated the toxicity of nAg, almost none have examined the potential for endocrine disruption, particularly at environmentally-relevant concentrations. Here we present novel and compelling evidence that nAg is a TH EDC. This observation is important to all vertebrates as TH and its nuclear receptors are extremely well-conserved, and TH is involved in a variety

of important physiological and biochemical processes including fetal brain and bone maturation, moulting in birds, homeostasis, mitochondrial respiration and lipid metabolism (Tata, 2006). Disruption of TH-signaling by nAg has implications not only for the health of aquatic species, but also for all vertebrates exposed to nAg, including humans. The current Canadian guidelines for silver in the drinking water (no limit; CCME, 2008) and for the protection of aquatic life (0.1µg/L Ag; CCME, 2007) are above or within the range of observed effects seen within this thesis (0.018-6 µg/L nominal nAg). Therefore, not only are new nano-specific regulations needed to cover effects different from bulk or iAg, the allowable limits clearly need to be revisited.

Bibliography

(2006a) *National Drinking Water Regulation*. Offices of Water and Science & Technology. US Environment Protection Agency. Washington, DC.

(2006b) *National Recommended Water Quality Criteria.* Offices of Water and Science & Technology, US Environmental Protection Agency. Washington, DC.

(2007) *Canadian Water Quality Guidelines for the Protection of Aquatic Life*. Environment Canada. Canadian Council of Ministers of the Environment: Ottawa, ON.

(2008) *Guidelines for Canadian Drinking Water Quality Summary Table*. Federal-Provincial-Territorial Committee on Drinking Water of the Federal-Provincial-Territorial Committee on Health and the Environment. Ottawa, ON.

(2012) Woodrow Wilson Database: The Project on Emerging Nanotechnologies <http://www.nanotechproject.org> [Accessed Oct 22 2012].

Ahamed M, AlSalhi MS, Siddiqui MKJ (2010a) Silver nanoparticle applications and human health. *Clinica Chimica Acta* **411:** 1841-1848

Ahamed M, Karns M, Goodson M, Rowe J, Hussain SM, Schlager JJ, Hong Y (2008) DNA damage response to different surface chemistry of silver nanoparticles in mammalian cells. *Toxicology and Applied Pharmacology* **233:** 404-410

Ahamed M, Posgai R, Gorey TJ, Nielsen M, Hussain SM, Rowe JJ (2010b) Silver nanoparticles induced heat shock protein 70, oxidative stress and apoptosis in *Drosophila melanogaster*. *Toxicology and Applied Pharmacology* **242:** 263-269

Arakawa H, Neault JF, Tajmir-Riahi HA (2001) Silver(I) complexes with DNA and RNA studied by Fourier transform infrared spectroscopy and capillary electrophoresis. *Biophys J* **81:** 1580-1587

Arora S, Jain J, Rajwade JM, Paknikar KM (2008) Cellular responses induced by silver nanoparticles: In vitro studies. *Toxicology Letters* **179:** 93-100

Arora S, Rajwade JM, Paknikar KM (2012) Nanotoxicology and in vitro studies: The need of the hour. *Toxicology and Applied Pharmacology* **258:** 151-165

Asare N, Instanes C, Sandberg WJ, Refsnes M, Schwarze P, Kruszewski M, Brunborg G (2012) Cytotoxic and genotoxic effects of silver nanoparticles in testicular cells. *Toxicology* **291:** 65-72

AshaRani PV, Hande MP, Valiyaveettil S (2009) Anti-proliferative activity of silver nanoparticles. *BMC Cell Biology* **10:** 65

Asharani PV, lianwu Y, Gong Z, Valiyaveettil S (2011) Comparison of the toxicity of silver, gold and platinum nanoparticles in developing zebrafish embryos. *Nanotoxicology* **5:** 43-54

Atkinson BG, Helbing C, Chen Y (1996) Reprogramming of gene expression during amphibian metamorphosis. In *Metamorphosis: postembryonic reprogramming of gene expression in amphibian and insect cells*, Gilbert LI, Tata J, Atkinson BG (eds), pp 539-566. San Diego: Academic Press

Bagamasbad P, Denver RJ (2011) Mechanisms and significance of nuclear receptor auto- and cross-regulation. *General and Comparative Endocrinology* **170:** 3-17

Bagamasbad P, Howdeshell KL, Sachs LM, Demeneix BA, Denver RJ (2007) A Role for Basic Transcription Element-binding Protein 1 (BTEB1) in the Autoinduction of Thyroid Hormone Receptor. *J Biol Chem* **283:** 2275-2285

Bakand S, Hayes A, Dechsakulthorn F (2012) Nanoparticles: a review of particle toxicology following inhalation exposure. *Inhal Toxicol* **24:** 125-135

Bassett J, Harvey CB, Williams GR (2003) Mechanisms of thyroid hormone receptor-specific nuclear and extra nuclear actions. *Mol Cell Endocrinology* **213:** 1-11

Benn TM, Westerhoff P (2008) Nanoparticle silver released into water from commercially available sock fabrics. *Environ Sci Technol* **42:** 4133-4139

Blaustein AR, Wake DB, Sousa WP (1994) Amphibian Declines - Judging Stability, Persistence, and Susceptibility of Populations to Local and Global Extinctions. *Conserv Biol* **8:** 60-71

Bonett RM, Hoopfer ED, Denver RJ (2010) Molecular mechanisms of corticosteroid synergy with thyroid hormone during tadpole metamorphosis. *General and Comparative Endocrinology* **168:** 209-219

Bonett RM, Hu F, Bagamasbad P, Denver RJ (2009) Stressor and Glucocorticoid-Dependent Induction of the Immediate Early Gene Kruppel-Like Factor 9: Implications for Neural Development and Plasticity. *Endocrinology* **150:** 1757-1765

Boone MD, Hammond SA, Veldhoen N, Youngquist M, Helbing CC (2013) Specific time of exposure during tadpole development influences biological

effects of the insecticide carbaryl in green frogs (*Lithobates clamitans*). *Aquat Toxicol***:** Accepted

Boonstra J, Post JA (2004) Molecular events associated with reactive oxygen species and cell cycle progression in mammalian cells. *Gene* **337:** 1-13

Bouwmeester H, Poortman J, Peters RJ, Wijma E, Kramer E, Makama S, Puspitaninganindita K, Marvin HJP, Peijnenburg A, Hendriksen PJM (2011) Characterization of Translocation of Silver Nanoparticles and Effects on Whole-Genome Gene Expression Using an In Vitro Intestinal Epithelium Coculture Model. *ACS Nano* **5:** 4091-4103

Braydich-Stolle LK, Lucas B, Schrand A, Murdock RC, Lee T, Schlager JJ, Hussain SM, Hofmann MC (2010) Silver Nanoparticles Disrupt GDNF/Fyn kinase Signaling in Spermatogonial Stem Cells. *Tox Sci* **116:** 577-589

Brown CL, Parchaso F, Thompson JK, Luoma SN (2003) Assessing Toxicant Effects in a Complex Estuary: A Case Study of Effects of Silver on Reproduction in the Bivalve, *Potamocorbula amurensis*, in San Francisco Bay. *Human and Ecological Risk Assessment: An International Journal* **9:** 95-119

Buchholz DR, Paul BD, Fu L, Shi YB (2006) Molecular and developmental analyses of thyroid hormone receptor function in *Xenopus laevis*, the African clawed frog. *Gen Comp Endocrinol* **145:** 1-19

Bustin SA, Beaulieu JF, Huggett J, Jaggi R, Kibenge FS, Olsvik PA, Penning LC, Toegel S (2010) MIQE precis: Practical implementation of minimum standard guidelines for fluorescence-based quantitative real-time PCR experiments. *BMC Mol Biol* **11:** 74

Byrns MC, Jin Y, Penning TM (2011) Inhibitors of type 5 17 beta-hydroxysteroid dehydrogenase (AKR1C3): Overview and structural insights. *Journal of Steroid Biochemistry and Molecular Biology* **125:** 95-104

Cao X, Kambe F, Yamauchi M, Seo H (2009) Thyroid-hormone-dependent activation of the phosphoinositide 3-kinase/Akt cascade requires Src and enhances neuronal survival. *Biochemical Journal* **424:** 201-209

Carlson C, Hussain SM, Schrand AM, Braydich-Stolle LK, Hess KL, Jones RL, Schlager JJ (2008) Unique cellular interaction of silver nanoparticles: size-dependent generation of reactive oxygen species. *J Phys Chem B* **112:** 13608-13619

Chaloupka K, Malam Y, Seifalian AM (2010) Nanosilver as a new generation of nanoproduct in biomedical applications. *Trends in Biotechnology* **28:** 580-588

Chang CY, Witschi E (1956) Genic control and hormonal reversal of sex differentiation in *Xenopus*. *Proc Soc Exp Biol Med* **93:** 140-144

Chen S, Chang Y, Wu Y, Lin K (2003) Mitogen-activated protein kinases potentiate thyroid hormone receptro transcriptional activity by stabilizing its protein. *Endocrinology* **144:** 1407-1419

Chen X, Schluesener HJ (2008) Nanosilver: A nanoproduct in medical application. *Toxicology Letters* **176:** 1-12

Chen Y, Atkinson BG (1997) Role for the *Rana catesbeiana* homologue of C/EBP alpha in the reprogramming of gene expression in the liver of metamorphosing tadpoles. *Devel Genet* **20:** 152-162

Chiarugi P, Pani G, Giannoni E, Taddei L, Colavitti R, Raugei G, Symons M, Borrello S, Galeotti T, Ramponi G (2003) Reactive oxygen species as essential mediators of cell adhesion: the oxidative inhibition of a FAK tyrosine phosphatase is required for cell adhesion. *Journal of Cell Biology* **161:** 933-944

Choi JE, Kim S, Ahn JH, Youn P, Kang JS, Park K, Yi J, Ryu D-Y (2010) Induction of oxidative stress and apoptosis by silver nanoparticles in the liver of adult zebrafish. *Aquat Toxicol* **100:** 151-159

Comfort KK, Maurer EI, Braydich-Stolle LK, Hussain SM (2011) Interference of Silver, Gold, and Iron Oxide Nanoparticles on Epidermal Growth Factor Signal Transduction in Epithelial Cells. *ACS Nano* **5:** 10000-10008

Costantini D, Marasco V, Møller AP (2011) A meta-analysis of glucocorticoids as modulators of oxidative stress in vertebrates. *Journal of Comparative Physiology B*

Das B, Matsuda H, Fujimoto K, Sun G, Matsuura K, Shi Y-B (2010) Molecular and genetic studies suggest that thyroid hormone receptor is both necessary and sufficient to mediate the developmental effects of thyroid hormone. *General and Comparative Endocrinology* **168:** 174-180

Davey JC, Becker KB, Schneider MJ, St Germain DL, Galton VA (1995) Cloning of a cDNA for the type II iodothyronine deiodinase. *J Biol Chem* **270:** 26786-26789

Davis PJ, Davis FB, Cody V (2005) Membrane receptors mediating thyroid hormone action. *Trends Endocrinol Metab* **16:** 429-435

Davis PJ, Leonard JL, Davis FB (2008) Mechanisms of nongenomic actions of thyroid hormone. *Front Neuroendocrinol* **29:** 211-218

de Hoon MJ, Imoto S, Nolan J, Miyano S (2004) Open source clustering software. *Bioinformatics* **20:** 1453-1454

Denver RJ (2009) Stress hormones mediate environment-genotype interactions during amphibian development. *General and Comparative Endocrinology* **164:** 20-31

Denver RJ, Hu F, Scanlan TS, Furlow JD (2008) Thyroid hormone receptor subtype specificity for hormone-dependent neurogenesis in *Xenopus laevis*. *Dev Biol*

Di Cosmo C, Liao, X., Dumitrescu, A.M., Nancy, P.L., Weiss, R.E., Refetoff, S. (2010) Mice deficient in MCT8 reveal a mechanism regulating thyroid hormone secretion. *The Journal of Clinical Investigation* **120:** 3377-3388

Drake PL (2005) Exposure-Related Health Effects of Silver and Silver Compounds: A Review. *Annals of Occupational Hygiene* **49:** 575-585

Duarte-Guterman P, Langlois VS, Pauli BD, Trudeau VL (2010) Expression and T3 regulation of thyroid hormone- and sex steroid-related genes during *Silurana (Xenopus) tropicalis* early development. *General and Comparative Endocrinology* **166:** 428-435

Duarte-Guterman P, Trudeau VL (2010) Regulation of Thyroid Hormone-, Oestrogen- and Androgen-Related Genes by Triiodothyronine in the Brain of *Silurana tropicalis*. *Journal of Neuroendocrinology* **22:** 1023-1031

Duarte-Guterman P, Trudeau VL (2011) Transcript profiles and triiodothyronine regulation of sex steroid- and thyroid hormone-related genes in the gonad–mesonephros complex of *Silurana tropicalis*. *Mol Cell Endocrinology* **331:** 143-149

Eckey M, Moehren U, Baniahmad A (2003) Gene silencing by the thyroid hormone receptor. *Mol Cell Endocrinol* **213:** 13-22

El Jamil A, Kanhoush R, Magre S, Boizet-Bonhoure B, Penrad-Mobayed M (2008) Sex-Specific Expression of SOX9 During Gonadogenesis in the Amphibian *Xenopus tropicalis*. *Devel Dyn* **237:** 2996-3005

Eom HJ, Choi J (2010) p38 MAPK Activation, DNA Damage, Cell Cycle Arrest and Apoptosis As Mechanisms of Toxicity of Silver Nanoparticles in Jurkat T Cells. *Environmental Science & Technology* **44:** 8337-8342

Evans RM (1988) The steroid and thyroid hormone receptor superfamily. *Science* **240:** 889-895

Fabrega J, Luoma SN, Tyler CR, Galloway TS, Lead JR (2011) Silver nanoparticles: Behaviour and effects in the aquatic environment. *Environment International* **37:** 517-531

Fabrega J, Renshaw JC, Lead JR (2009) Interactions of Silver Nanoparticles with Pseudomonas putida Biofilms. *Environmental Science & Technology* **43:** 9004-9009

Fairclough L, Tata JR (1997) An immunocytochemical analysis of the expression of thyroid hormone receptor alpha and beta proteins during natural and thyroid hormone-induced metamorphosis in *Xenopus*. *Dev Growth Differ* **39:** 273-283

Farkas J, Christian P, Gallego-Urrea JA, Roos N, Hassellöv M, Tollefsen KE, Thomas KV (2011a) Uptake and effects of manufactured silver nanoparticles in rainbow trout (*Oncorhynchus mykiss*) gill cells. *Aquat Toxicol* **101:** 117-125

Farkas J, Peter H, Christian P, Gallego Urrea JA, Hassellöv M, Tuoriniemi J, Gustafsson S, Olsson E, Hylland K, Thomas KV (2011b) Characterization of the effluent from a nanosilver producing washing machine. *Environment International* **37:** 1057-1062

Farmen E, Mikkelsen HN, Evensen Ø, Einset J, Heier LS, Rosseland BO, Salbu B, Tollefsen KE, Oughton DH (2012) Acute and sub-lethal effects in juvenile Atlantic salmon exposed to low µg/L concentrations of Ag nanoparticles. *Aquat Toxicol* **108:** 78-84

Foldbjerg R, Dang DA, Autrup H (2010) Cytotoxicity and genotoxicity of silver nanoparticles in the human lung cancer cell line, A549. *Archives of Toxicology* **85:** 743-750

Fort DJ, Degitz S, Tietge J, Touart LW (2007) The hypothalamic-pituitary-thyroid (HPT) axis in frogs and its role in frog development and reproduction. *Crit Rev Toxicol* **37:** 117-161

Fristensky B (2007) BIRCH: A user-oriented, locally-customizable, bioinformatics system. *BMC Bioinformatics* **8**

Furlow JD, Kanamori A (2002) The transcription factor basic transcription element-binding protein 1 is a direct thyroid hormone response gene in the frog *Xenopus laevis*. *Endocrinology* **143:** 3295-3305

Furuyama K, Kawaguchi Y, Akiyama H, Horiguchi M, Kodama S, Kuhara T, Hosokawa S, Elbahrawy A, Soeda T, Koizumi M, Masui T, Kawaguchi M, Takaori K, Doi R, Nishi E, Kakinoki R, Deng JM, Behringer RR, Nakamura T, Uemoto S (2011) Continuous cell supply from a Sox9-expressing progenitor zone in adult liver, exocrine pancreas and intestine. *Nature Genetics* **43:** 34-U52

Gagné F, André C, Skirrow R, Gélinas M, Auclair J, van Aggelen G, Turcotte P, Gagnon C (2012) Toxicity of silver nanoparticles to rainbow trout: A toxicogenomic approach. *Chemosphere* **89:** 615-622

Galton VA (2005) The roles of the iodothyronine deiodinases in mammalian development. *Thyroid* **15:** 823-834

Gervasi SS, Foufopoulos J (2007) Costs of plasticity: responses to desiccation decrease post-metamorphic immune function in a pond-breeding amphibian. *Functional Ecology* **0:** 071005010407002-???

Goleman WL, Carr JA, Anderson TA (2002) Environmentally relevant concentrations of ammonium perchlorate inhibit thyroid function and alter sex ratios in developing *Xenopus laevis*. *Environ Toxicol Chem* **21:** 590-597

Gottschalk F, Sonderer T, Scholz RW, Nowack B (2009) Modeled Environmental Concentrations of Engineered Nanomaterials (TiO2, ZnO, Ag, CNT, Fullerenes) for Different Regions. *Environmental Science & Technology* **43:** 9216-9222

Gou N, Onnis-Hayden A, Gu AZ (2010) Mechanistic toxicity assessment of nanomaterials by whole-cell-array stress genes expression analysis. *Environ Sci Technol* **44:** 5964-5970

Gray KM, Janssens PA (1990) Gonadal hormones inhibit the induction of metamorphosis by thyroid hormones in *Xenopus laevis* tadpoles in vivo, but not in vitro. *General and Comparative Endocrinology* **77:** 202-211

Griffitt RJ, Brown-Peterson NJ, Savin DA, Manning CS, Boube I, Ryan RA, Brouwer M (2012) Effects of chronic nanoparticulate silver exposure to adult and juvenile sheepshead minnows (*Cyprinodon variegatus*). *Env Tox Chemistry* **31:** 160-167

Griffitt RJ, Hyndman K, Denslow ND, Barber DS (2009) Comparison of Molecular and Histological Changes in Zebrafish Gills Exposed to Metallic Nanoparticles. *Tox Sci* **107:** 404-415

Griffitt RJ, Luo J, Gao J, Bonzongo JC, Barber DS (2008) Effects of particle composition and species on toxicity of metallic nanomaterials in aquatic organisms. *Env Tox Chemistry* **27:** 1972-1978

Gupta A, Maynes M, Silver S (1998) Effects of halides on plasmid-mediated silver resistance in *Escherichia coli*. *Applied and Environmental Microbiology* **64:** 5042-5045

Haddad JJ, Saade NE, Safieh-Garabedian B (2002) Cytokines and neuro-immune-endocrine interactions: a role for the hypothalamic-pituitary-adrenal revolving axis. *J Neuroimmunol* **133:** 1-19

Handy RD, Cornelis G, Fernandes T, Tsyusko O, Decho A, Sabo-Attwood T, Metcalfe C, Steevens JA, Klaine SJ, Koelmans AA, Horne N (2012) Ecotoxicity test methods for engineered nanomaterials: Practical experiences and recommendations from the bench. *Env Tox Chemistry* **31:** 15-31

Hayata T, Blitz IL, Iwata N, Cho KWY (2009) Identification of embryonic pancreatic genes using *Xenopus* DNA microarrays. *Devel Dyn* **238:** 1455-1466

Hayes T, Chan R, Licht P (1993) Interactions of temperature and steroids on larval growth, development and metamorphosis in a toad (*Bufo boreas*). *Journal of Experimental Zoology* **266:** 206-215

Hayes TB (1997) Steroids as potential modulators of thyroid hormone activity in anuran metamorphosis. *American Zoologist* **37:** 185-194

Hayes TB (1998) Sex determination and primary sex differentiation in amphibians: Genetic and developmental mechanisms. *Journal of Experimental Zoology* **281:** 373-399

Helbing CC, Bailey CM, Ji L, Gunderson MP, Zhang F, Veldhoen N, Skirrow RC, Mu R, Lesperance M, Holcombe GW, Kosian PA, Tietge J, Korte JJ, Degitz SJ (2007a) Identification of gene expression indicators for thyroid axis disruption in a *Xenopus laevis* metamorphosis screening assay: Part 1: Effects on the brain. *Aquat Toxicol* **82:** 227-241

Helbing CC, Gergely G, Atkinson BG (1992) Sequential up-regulation of thyroid hormone β receptor, ornithine transcarbamylase and carbamyl phosphate synthetase mRNAs in the liver of *Rana catesbeiana* tadpoles during spontaneous and thyroid hormone-induced metamorphosis. *Devel Genet* **13:** 289-301

Helbing CC, Ji L, Bailey CM, Veldhoen N, Zhang F, Holcombe GW, Kosian PA, Tietge J, Korte JJ, Degitz SJ (2007b) Identification of gene expression indicators for thyroid axis disruption in a *Xenopus laevis* metamorphosis screening assay Part 2. Effects on the tail and hindlimb. *Aquat Toxicol* **82:** 215-226

Helbing CC, Wagner MJ, Pettem K, Johnston J, Heimeier RA, Veldhoen N, Jirik FR, Shi YB, Browder LW (2011) Modulation of Thyroid Hormone-Dependent Gene Expression in *Xenopus laevis* by INhibitor of Growth (ING) Proteins. *PLoS One* **6**

Helmreich DL, Parfitt DB, Lu XY, Akil LH, Watson SJ (2005) Relation between the Hypothalamic-Pituitary-Thyroid (HPT) Axis and the Hypothalamic-Pituitary-Adrenal (HPA) Axis during Repeated Stress. *Neuroendocrinology* **81:** 183-192

Hetzel BS, Mano MT (1989) A review of experimental studies of iodine deficiency during fetal development. *J Nutr* **119:** 145-151

Heyland A (2005) Cross-kingdom hormonal signaling: an insight from thyroid hormone functions in marine larvae. *Journal of Experimental Biology* **208:** 4355-4361

Hinther A, Bromba CM, Wulff JE, Helbing CC (2011) Effects of triclocarban, triclosan, and methyl triclosan on thyroid hormone action and stress in frog and mammalian culture systems. *Environ Sci Technol* **45:** 5395-5402

Hinther A, Domanski D, Vawda S, Helbing CC (2010a) C-fin: a cultured frog tadpole tail fin biopsy approach for detection of thyroid hormone-disrupting chemicals. *Environ Toxicol Chem* **29:** 380-388

Hinther A, Vawda S, Skirrow RC, Veldhoen N, Collins P, Cullen JT, van Aggelen G, Helbing CC (2010b) Nanometals induce stress and alter thyroid hormone action in amphibia at or below North American water quality guidelines. *Environ Sci Technol* **44:** 8314-8321

Hogan NS, Duarte P, Wade MG, Lean DRS, Trudeau VL (2008) Estrogenic exposure affects metamorphosis and alters sex ratios in the northern leopard frog (*Rana pipiens*): Identifying critically vulnerable periods of development. *General and Comparative Endocrinology* **156:** 515-523

Hoque ME, Khosravi K, Newman K, Metcalfe CD (2012) Detection and characterization of silver nanoparticles in aqueous matrices using asymmetric-flow field flow fractionation with inductively coupled plasma mass spectrometry. *Journal of Chromatography A* **1233:** 109-115

Hossain Z, Huq F (2002) Studies on the interaction between Ag+ and DNA. *J Inorg Biochem* **91:** 398-404

Hourdry J, Lhermite A, Ferrand R (1996) Changes in the digestive tract and feeding behavior of anuran amphibians during metamorphosis. *Physiol Zool* **69:** 219-251

Hsin Y-H, Chen C-F, Huang S, Shih T-S, Lai P-S, Chueh PJ (2008) The apoptotic effect of nanosilver is mediated by a ROS- and JNK-dependent mechanism involving the mitochondrial pathway in NIH3T3 cells. *Toxicology Letters* **179:** 130-139

Hussain SM, Hess KL, Gearhart JM, Geiss KT, Schlager JJ (2005) In vitro toxicity of nanoparticles in BRL 3A rat liver cells. *Toxicology in Vitro* **19:** 975-983

Iavicoli I, Nascarella MA, Calabrese EJ (2010) Exposure to Nanoparticles and Hormesis. *Dose-Response* **8:** 501-517

Inoue M, Sato EF, Nishikawa M, Hiramoto K, Kashiwagi A, Utsumi K (2004) Free radical theory of apoptosis and metamorphosis. *Redox Report* **9:** 238-248

Ji L, Domanski D, Skirrow RC, Helbing CC (2007) Genistein prevents thyroid hormone-dependent tail regression of *Rana catesbeiana* tadpoles by targetting protein kinase C and thyroid hormone receptor α. *Devel Dyn* **236:** 777-790

Johnston HJ, Hutchison G, Christensen FM, Peters S, Hankin S, Stone V (2010) A review of the in vivo and in vitro toxicity of silver and gold particulates: Particle attributes and biological mechanisms responsible for the observed toxicity. *Critical Reviews in Toxicology* **40:** 328-346

Kahru A, Dubourguier H-C (2010) From ecotoxicology to nanoecotoxicology. *Toxicology* **269:** 105-119

Kang SJ, Ryoo IG, Lee YJ, Kwak MK (2012) Role of the Nrf2-heme oxygenase-1 pathway in silver nanoparticle-mediated cytotoxicity. *Toxicology and Applied Pharmacology* **258:** 89-98

Kashiwagi A, Hanada H, Yabuki M, Kanno T, Ishisaka R, Sasaki J, Inoue M, Utsumi K (1999) Thyroxine enhancement and the role of reactive oxygen species in tadpole tail apoptosis. *Free Radic Biol Med* **26:** 1001-1009

Kavlock RJ, Daston GP, DeRosa C, FennerCrisp P, Gray LE, Kaattari S, Lucier G, Luster M, Mac MJ, Maczka C, Miller R, Moore J, Rolland R, Scott G, Sheehan DM, Sinks T, Tilson HA (1996) Research needs for the risk assessment of health and environmental effects of endocrine disruptors: A report of the US EPA-sponsored workshop. *Environ Health Persp* **104:** 715-740

Kawata K, Osawa M, Okabe S (2009) In vitro toxicity of silver nanoparticles at noncytotoxic doses to HepG2 human hepatoma cells. *Environ Sci Technol* **43:** 6046-6051

Kelley DB (1996) Sexual differentiation in *Xenopus laevis*. In *The Biology of Xenopus*, Tinsely R, Kobel H (eds), 143-176. Oxford University Press

Kendig EL, Le HH, Belcher SM (2010) Defining Hormesis: Evaluation of a Complex Concentration Response Phenomenon. *International Journal of Toxicology* **29:** 235-246

Kettlewell JR, Raymond CS, Zarkower D (2000) Temperature-dependent expression of turtle Dmrt1 prior to sexual differentiation. *Genesis* **26:** 174-178

Kikuyama S, Kawamura K, Tanaka S, Yamamoto K (1993) Aspects of amphibian metamorphosis: hormonal control. *Int Rev Cytol* **145:** 105-148

Kim S, Choi JE, Choi J, Chung K-H, Park K, Yi J, Ryu D-Y (2009a) Oxidative stress-dependent toxicity of silver nanoparticles in human hepatoma cells. *Toxicology in Vitro* **23:** 1076-1084

Kim W-Y, Kim J, Park JD, Ryu HY, Yu IJ (2009b) Histological Study of Gender Differences in Accumulation of Silver Nanoparticles in Kidneys of Fischer 344 Rats. *Journal of Toxicology and Environmental Health, Part A* **72:** 1279-1284

Kobayashi N, Machida T, Takahashi T, Takatsu H, Shinkai T, Abe K, Urano S (2009) Elevation by Oxidative Stress and Aging of Hypothalamic-Pituitary-Adrenal Activity in Rats and Its Prevention by Vitamin E. *Journal of Clinical Biochemistry and Nutrition* **45:** 207-213

Kovacic P, Edwards C (2010) Integrated approach to the mechanisms of thyroid toxins: electron transfer, reactive oxygen species, oxidative stress, cell signaling, receptors, and antioxidants. *Journal of Receptors and Signal Transduction* **30:** 133-142

Krain LP, Denver RJ (2004) Developmental expression and hormonal regulation of glucocorticoid and thyroid hormone receptors during metamorphosis in *Xenopus laevis*. *J Endocrinol* **181:** 91-104

Kress E, Samarut J, Plateroti M (2009) Thyroid hormones and the control of cell proliferation or cell differentiation: paradox or duality? *Mol Cell Endocrinol* **313:** 36-49

Kuan SH, Lin YK (2011) Bigger or faster? Spring and summer tadpole cohorts use different life-history strategies. *Journal of Zoology* **285:** 165-171

Kumari M, Mukherjee A, Chandrasekaran N (2009) Genotoxicity of silver nanoparticles in *Allium cepa*. *Science of the Total Environment* **407:** 5243-5246

Kurzawa R, Glabowski W, Baczkowski T, Wiszniewska B, Marchlewicz M (2004) Growth factors protect in vitro cultured embryos from the consequences of oxidative stress. *Zygote* **12:** 231-240

Kutschera U (2009) Symbiogenesis, natural selection, and the dynamic Earth. *Theory Biosci* **128:** 191-203

Lankoff A, Sandberg WJ, Wegierek-Ciuk A, Lisowska H, Refsnes M, Sartowska B, Schwarze PE, Meczynska-Wielgosz S, Wojewodzka M, Kruszewski M (2012) The effect of agglomeration state of silver and titanium dioxide nanoparticles on cellular response of HepG2, A549 and THP-1 cells. *Toxicology Letters* **208:** 197-213

Lee H-Y, Choi Y-J, Jung E-J, Yin H-Q, Kwon J-T, Kim J-E, Im H-T, Cho M-H, Kim J-H, Kim H-Y, Lee B-H (2009) Genomics-based screening of differentially expressed genes in the brains of mice exposed to silver nanoparticles via inhalation. *Journal of Nanoparticle Research* **12:** 1567-1578

Lei J, Nowbar S, Mariash CN, Ingbar DH (2003) Thyroid hormone stimulates Na-K-ATPase activity and its plasma membrane insertion in rat alveolar epithelial cells. *Am J Physiol Lung Cell Mol Physiol* **285:** L762-772

Leloup J, Buscaglia M (1977) La triiodothyronine, hormone de la metamorphose des amphibiens. *Comptes Rendues de l'Academie de les Sciences Paris Serie D* **284:** 2261-2263

Li J, Chen M, Wang ZJ, Ma M, Peng XZ (2011) Analysis of Environmental Endocrine Disrupting Activities in Wastewater Treatment Plant Effluents Using Recombinant Yeast Assays Incorporated with Exogenous Metabolic Activation System. *Biomed Environ Sci* **24:** 132-139

Lim D, Roh J-y, Eom H-j, Choi J-Y, Hyun J, Choi J (2012) Oxidative stress-related PMK-1 P38 MAPK activation as a mechanism for toxicity of silver nanoparticles to reproduction in the nematode *Caenorhabditis elegans*. *Env Tox Chemistry* **31:** 585-592

Limbach LK, Wick P, Manser P, Grass RN, Bruinink A, Stark WJ (2007) Exposure of engineered nanoparticles to human lung epithelial cells: Influence of chemical composition and catalytic activity on oxidative stress. *Environmental Science & Technology* **41:** 4158-4163

Liu C, Zhang X, Deng J, Hecker M, Al-Khedhairy A, Giesy JP, Zhou B (2011) Effects of prochloraz or propylthiouracil on the cross-talk between the HPG, HPA, and HPT axes in zebrafish. *Environ Sci Technol* **45:** 769-775

Liu JY, Hurt RH (2010) Ion Release Kinetics and Particle Persistence in Aqueous Nano-Silver Colloids. *Environmental Science & Technology* **44:** 2169-2175

Liu SL, Lin X, Shi DY, Cheng J, Wu CQ, Zhang YD (2002) Reactive oxygen species stimulated human hepatoma cell proliferation via cross-talk between PI3-K/PKB and JNK signaling pathways. *Archives of Biochemistry and Biophysics* **406:** 173-182

Liu W, Wu Y, Wang C, Li HC, Wang T, Liao CY, Cui L, Zhou QF, Yan B, Jiang GB (2010) Impact of silver nanoparticles on human cells: Effect of particle size. *Nanotoxicology* **4:** 319-330

Livak KJ, Schmittgen TD (2001) Analysis of relative gene expression data using real-time quantitative PCR and the $2^{-\Delta\Delta Ct}$ Method. *Methods* **25:** 402-408

Lu W, Senapati D, Wang S, Tovmachenko O, Singh AK, Yu H, Ray PC (2010) Effect of surface coating on the toxicity of silver nanomaterials on human skin keratinocytes. *Chem Phys Lett* **487:** 92-96

MacCuspie RI (2010) Colloidal stability of silver nanoparticles in biologically relevant conditions. *Journal of Nanoparticle Research* **13:** 2893-2908

Marambio-Jones C, Hoek EMV (2010) A review of the antibacterial effects of silver nanomaterials and potential implications for human health and the environment. *Journal of Nanoparticle Research* **12:** 1531-1551

McDiarmid R, Altig R (1999) *Tadpoles: the biology of anuran larvae*, Chicago: The University of Chicago Press.

McLachlan JA (2001) Environmental signaling: What embryos and evolution teach us about endocrine disrupting chemicals. *Endocrine Reviews* **22:** 319-341

Menon J, Roman R (2007) Oxidative stress, tissue remodeling and regression during amphibian metamorphosis. *Comp Biochem Phys C* **145:** 625-631

Monteiro-Riviere NA, Inman AO, Zhang LW (2009) Limitations and relative utility of screening assays to assess engineered nanoparticle toxicity in a human cell line. *Toxicology and Applied Pharmacology* **234:** 222-235

Mueller NC, Nowack B (2008) Exposure modeling of engineered nanoparticles in the environment. *Environmental Science & Technology* **42:** 4447-4453

Mukhi S, Cai L, Brown DD (2010) Gene switching at *Xenopus laevis* metamorphosis. *Devel Biol* **338:** 117-126

Musee N (2011) Simulated environmental risk estimation of engineered nanomaterials: A case of cosmetics in Johannesburg City. *Hum Exp Toxicol* **30:** 1181-1195

Nair PMG, Choi J (2012) Modulation in the mRNA expression of ecdysone receptor gene in aquatic midge, *Chironomus riparius* upon exposure to nonylphenol and silver nanoparticles. *Environmental Toxicology and Pharmacology* **33:** 98-106

Nair PMG, Park SY, Lee S-W, Choi J (2011) Differential expression of ribosomal protein gene, gonadotrophin releasing hormone gene and Balbiani ring protein gene in silver nanoparticles exposed *Chironomus riparius*. *Aquat Toxicol* **101:** 31-37

Nakamura Y, Hornsby PJ, Casson P, Morimoto R, Satoh F, Xing YW, Kennedy MR, Sasano H, Rainey WE (2009) Type 5 17 beta-Hydroxysteroid Dehydrogenase (AKR1C3) Contributes to Testosterone Production in the Adrenal Reticularis. *J Clin Endocrinol Metab* **94:** 2192-2198

Nanda I, Kondo M, Hornung U, Asakawa S, Winkler C, Shimizu A, Shan ZH, Haaf T, Shimizu N, Shima A, Schmid M, Schartl M (2002) A duplicated copy of DMRT1 in the sex-determining region of the Y chromosome of the medaka, *Oryzias latipes*. *Proc Nat Acad Sci (USA)* **99:** 11778-11783

Navarro E, Piccapietra F, Wagner B, Marconi F, Kaegi R, Odzak N, Sigg L, Behra R (2008) Toxicity of Silver Nanoparticles to *Chlamydomonas reinhardtii*. *Environmental Science & Technology* **42:** 8959-8964

Nicoll JB, Gwinn BL, Iwig JS, Garcia PP, Bunn CF, Allison LA (2003) Compartment-specific phosphorylation of rat thyroid hormone receptor alpha 1 regulates nuclear localization and retention. *Mol Cell Endocrinology* **205:** 65-77

Nieuwkoop PD, Faber F (1994) *Normal table of Xenopus laevis*, New York, NY.: Garland Publishing,.

Nishanth RP, Jyotsna RG, Schlager JJ, Hussain SM, Reddanna P (2011) Inflammatory responses of RAW 264.7 macrophages upon exposure to nanoparticles: Role of ROS-NFκB signaling pathway. *Nanotoxicology* **5:** 502-516

Nowack B, Ranville JF, Diamond S, Gallego-Urrea JA, Metcalfe C, Rose J, Horne N, Koelmans AA, Klaine SJ (2012) Potential scenarios for nanomaterial release and subsequent alteration in the environment. *Env Tox Chemistry* **31:** 50-59

OECD. (2009) 231: OECD Guideline for the Testing of Chemicals, The Amphibian Metamorphosis Assay.

Park E-J, Bae E, Yi J, Kim Y, Choi K, Lee SH, Yoon J, Lee BC, Park K (2010) Repeated-dose toxicity and inflammatory responses in mice by oral administration of silver nanoparticles. *Environmental Toxicology and Pharmacology* **30:** 162-168

Penning TM, Burczynski ME, Jez JM, Hung CF, Lin HK, Ma HC, Moore M, Palackal N, Ratnam K (2000) Human 3 alpha-hydroxysteroid dehydrogenase isoforms (AKR1C1-AKR1C4) of the aldo-keto reductase superfamily: functional

plasticity and tissue distribution reveals roles in the inactivation and formation of male and female sex hormones. *Biochemical Journal* **351:** 67-77

Perissi V, Staszewski LM, McInerney EM, Kurokawa R, Krones A, Rose DW, Lambert MH, Milburn MV, Glass CK, Rosenfeld MG (1999) Molecular determinants of nuclear receptor-corepressor interaction. *Genes & Development* **13:** 3198-3208

Pettersson I, Arukwe A, Lundstedt-Enkel K, Mortensen AS, Berg C (2006) Persistent sex-reversal and oviducal agenesis in adult *Xenopus (Silurana) tropicalis* frogs following larval exposure to the environmental pollutant ethynylestradiol. *Aquat Toxicol* **79:** 356-365

Pham CH, Yi J, Gu MB (2012) Biomarker gene response in male Medaka (*Oryzias latipes*) chronically exposed to silver nanoparticle. *Ecotoxicology and Environmental Safety* **78:** 239-245

Pokhrel LR, Dubey B (2012) Potential Impact of Low-Concentration Silver Nanoparticles on Predator–Prey Interactions between Predatory Dragonfly Nymphs and Daphnia magna as a Prey. *Environmental Science & Technology* **46:** 7755-7762

Posgai R, Cipolla-McCulloch CB, Murphy KR, Hussain SM, Rowe JJ, Nielsen MG (2011) Differential toxicity of silver and titanium dioxide nanoparticles on *Drosophila melanogaster* development, reproductive effort, and viability: Size, coatings and antioxidants matter. *Chemosphere* **85:** 34-42

Pudney M, Varma MG, Leake CJ (1973) Establishment of a cell line (XTC-2) from the South African clawed toad, *Xenopus laevis*. *Experientia* **29:** 466-467

Rabelo EM, Baker BS, Tata JR (1994) Interplay between thyroid hormone and estrogen in modulating expression of their receptor and vitellogenin genes during *Xenopus* metamorphosis. *Mech Dev* **45:** 49-57

Rahman MF, Wang J, Patterson TA, Saini UT, Robinson BL, Newport GD, Murdock RC, Schlager JJ, Hussain SM, Ali SF (2009) Expression of genes related to oxidative stress in the mouse brain after exposure to silver-25 nanoparticles. *Toxicology Letters* **187:** 15-21

Raymond CS, Kettlewell JR, Hirsch B, Bardwell VJ, Zarkower D (1999) Expression of Dmrt1 in the genital ridge of mouse and chicken embryos suggests a role in vertebrate sexual development. *Devel Biol* **215:** 208-220

Raymond CS, Murphy MW, O'Sullivan MG, Bardwell VJ, Zarkower D (2000) Dmrt1, a gene related to worm and fly sexual regulators, is required for mammalian testis differentiation. *Genes & Development* **14:** 2587-2595

Richards CM, Nace GW (1978) Gynogenic and Hormonal Sex Reversal used in tests of XX-XY Hypothesis of Sex Determination in *Rana pipiens*. *Growth* **42:** 319-331

Ringwood AH, McCarthy M, Bates TC, Carroll DL (2010) The effects of silver nanoparticles on oyster embryos. *Marine Environmental Research* **69:** S49-S51

Ritchie JW, Shi YB, Hayashi Y, Baird FE, Muchekehu RW, Christie GR, Taylor PM (2003) A role for thyroid hormone transporters in transcriptional regulation by thyroid hormone receptors. *Mol Endocrinol* **17:** 653-661

Roh JY, Sim SJ, Yi J, Park K, Chung KH, Ryu DY, Choi J (2009) Ecotoxicity of Silver Nanoparticles on the Soil Nematode *Caenorhabditis elegans* Using Functional Ecotoxicogenomics. *Environmental Science & Technology* **43:** 3933-3940

Ruijter JM, Ramakers C, Hoogaars WMH, Karlen Y, Bakker O, van den Hoff MJB, Moorman AFM (2009) Amplification efficiency: linking baseline and bias in the analysis of quantitative PCR data. *Nucleic Acids Research* **37:** e45-e45

Schaffer WM, Bronnikova TV (2012) Peroxidase-ROS interactions. *Nonlinear Dyn* **68:** 413-430

Scown TM, Santos EM, Johnston BD, Gaiser B, Baalousha M, Mitov S, Lead JR, Stone V, Fernandes TF, Jepson M, van Aerle R, Tyler CR (2010) Effects of Aqueous Exposure to Silver Nanoparticles of Different Sizes in Rainbow Trout. *Tox Sci* **115:** 521-534

Shi Y-B (2000) *Amphibian Metamorphosis: From morphology to molecular biology*, New York: Wiley-Liss.

Shi YB, Brown DD (1993) The earliest changes in gene expression in tadpole intestine induced by thyroid hormone. *J Biol Chem* **268:** 20312-20317

Shibusawa N, Hollenberg AN, Wondisford FE (2003) Thyroid hormone receptor DNA binding is required for both positive and negative gene regulation. *J Biol Chem* **278:** 732-738

Shoults-Wilson WA, Reinsch BC, Tsyusko OV, Bertsch PM, Lowry GV, Unrine JM (2011) Effect of silver nanoparticle surface coating on bioaccumulation and reproductive toxicity in earthworms (*Eisenia fetida*). *Nanotoxicology* **5:** 432-444

Singh RP, Ramarao P (2012) Cellular uptake, intracellular trafficking and cytotoxicity of silver nanoparticles. *Toxicology Letters* **213:** 249-259

Skirrow RC, Veldhoen N, Domanski D, Helbing CC (2008) Roscovitine inhibits thyroid hormone-induced tail regression of the frog tadpole and reveals a role for cyclin C/Cdk8 in the establishment of the metamorphic gene expression program. *Dev Dyn* **237:** 3787-3797

Snoek GT, Koster CH, Delaat SW, Heideveld M, Durston AJ, Vanzoelen EJJ (1990) Effects of cell heterogeneity on production of polypeptide growth-factors and mesoderm-inducing activity by *Xenopus laevis* XTC cells. *Experimental Cell Research* **187:** 203-210

St Germain DL, Galton VA (1997) The deiodinase family of selenoproteins. *Thyroid* **7:** 655-668

St Germain DL, Schwartzman RA, Croteau W, Kanamori A, Wang Z, Brown DD, Galton VA (1994) A thyroid hormone-regulated gene in *Xenopus laevis* encodes a type III iodothyronine 5-deiodinase. *Proc Natl Acad Sci U S A* **91:** 7767-7771

Tata JR (1993) Gene expression during metamorphosis: an ideal model for post-embryonic development. *Bioessays* **15:** 239-248

Tata JR (2006) Amphibian metamorphosis as a model for the developmental actions of thyroid hormone. *Mol Cell Endocrinology* **246:** 10-20

Taylor AC, Kollros JJ (1946) Stages in the normal development of *Rana pipiens* larvae. *Anatomical Record* **94:** 7-24

Teow Y, Asharani PV, Hande MP, Valiyaveettil S (2011) Health impact and safety of engineered nanomaterials. *Chem Commun* **47:** 7025

Tzagarakis-Foster C, Privalsky ML (1998) Phosphorylation of thyroid hormone receptors by protein kinase A regulates DNA recognition by specific inhibition of receptor monomer binding. *J Biol Chem* **273:** 10926-10932

Utiger RD (1995) Altered thyroid function in nonthyroidal illness and surgery. To treat or not to treat? *N Engl J Med* **333:** 1562-1563

Vandenberg LN, Colborn T, Hayes TB, Heindel JJ, Jacobs DR, Lee DH, Shioda T, Soto AM, vom Saal FS, Welshons WV, Zoeller RT, Myers JP (2012) Hormones and Endocrine-Disrupting Chemicals: Low-Dose Effects and Nonmonotonic Dose Responses. *Endocrine Reviews* **33:** 378-455

Veldhoen N, Skirrow RC, Ji L, Domanski D, Bonfield ER, Bailey CM, Helbing CC (2006) Use of heterologous cDNA arrays and organ culture in the detection of thyroid hormone-dependent responses in a sentinel frog, *Rana catesbeiana*. *Comp Biochem Physiol D* **1:** 187-199

vom Saal F, Welshons W (2006) Large effects from small exposures. II. The importance of positive controls in low-dose research on bisphenol A. *Environmental Research* **100:** 50-76

von der Kammer F, Ferguson PL, Holden PA, Masion A, Rogers KR, Klaine SJ, Koelmans AA, Horne N, Unrine JM (2012) Analysis of engineered nanomaterials in complex matrices (environment and biota): General considerations and conceptual case studies. *Env Tox Chemistry* **31:** 32-49

Wan R, Mo Y, Zhang X, Chien S, Tollerud DJ, Zhang Q (2008) Matrix metalloproteinase-2 and -9 are induced differently by metal nanoparticles in human monocytes: The role of oxidative stress and protein tyrosine kinase activation. *Toxicology and Applied Pharmacology* **233:** 276-285

Wang D, Xia X, Liu Y, Oetting A, Walker RL, Zhu Y, Meltzer P, Cole PA, Shi YB, Yen PM (2009) Negative Regulation of TSHalpha Target Gene by Thyroid Hormone Involves Histone Acetylation and Corepressor Complex Dissociation. *Mol Endocrinology* **23:** 600-609

White BA, Nicoll CS (1981) Hormonal control of amphibian metamorphosis. In *Metamorphosis: a problem in developmental biology*, Gilbert LI, Frieden E (eds). New York: Plenum Publishing

Wise JP, Goodale BC, Wise SS, Craig GA, Pongan AF, Walter RB, Thompson WD, Ng AK, Aboueissa AM, Mitani H, Spalding MJ, Mason MD (2010) Silver nanospheres are cytotoxic and genotoxic to fish cells. *Aquat Toxicol* **97:** 34-41

Wong J, Shi YB (1995) Coordinated regulation of and transcriptional activation by *Xenopus* thyroid hormone and retinoid X receptors. *J Biol Chem* **270:** 18479-18483

Xiu Z-M, Ma J, Alvarez PJJ (2011) Differential Effect of Common Ligands and Molecular Oxygen on Antimicrobial Activity of Silver Nanoparticles versus Silver Ions. *Environmental Science & Technology* **45:** 9003-9008

Yamauchi K, Nakajima J (2002) Effect of coenzymes and thyroid hormones on the dual activities of Xenopus cytosolic thyroid-hormone-binding protein (xCTBP) with aldehyde dehydrogenase activity. *European Journal of Biochemistry* **269:** 2257-2264

Yang X, Gondikas AP, Marinakos SM, Auffan M, Liu J, Hsu-Kim H, Meyer JN (2012) Mechanism of Silver Nanoparticle Toxicity Is Dependent on Dissolved Silver and Surface Coating in *Caenorhabditis elegans*. *Environmental Science & Technology* **46:** 1119-1127

Yen PM (2001) Physiological and molecular basis of thyroid hormone action. *Physiological Reviews* **81:** 1097-1142

Yen PM, Ando S, Feng X, Liu Y, Maruvada P, Xia X (2006) Thyroid hormone action at the cellular, genomic and target gene levels. *Mol Cell Endocrinology* **246:** 121-127

Yildirimer L, Thanh NTK, Loizidou M, Seifalian AM (2011) Toxicological considerations of clinically applicable nanoparticles. *Nano Today* **6:** 585-607

Yoo HG, Shin BA, Park JS, Lee KH, Chay KO, Yang SY, Ahn BW, Jung YD (2002) IL-1 beta induces MMP-9 via reactive oxygen species and NF-kappa B in murine macrophage RAW 264.7 cells. *Biochemical and biophysical research communications* **298:** 251-256

Yoshimoto S, Okada E, Umemoto H, Tamura K, Uno Y, Nishida-Umehara C, Matsuda Y, Takamatsu N, Shiba T, Ito M (2008) A W-linked DM-domain gene, DM-W, participates in primary ovary development in *Xenopus laevis*. *Proc Nat Acad Sci (USA)* **105:** 2469-2474

Zanette C, Pelin M, Crosera M, Adami G, Bovenzi M, Larese FF, Florio C (2011) Silver nanoparticles exert a long-lasting antiproliferative effect on human keratinocyte HaCaT cell line. *Toxicology in Vitro* **25:** 1053-1060

Zhang J, Lazar MA (2000) The mechanism of action of thyroid hormones. *Annu Rev Physiol* **62:** 439-466

Zhang R, Piao MJ, Kim KC, Kim AD, Choi JY, Choi J, Hyun JW (2012) Endoplasmic reticulum stress signaling is involved in silver nanoparticles-induced apoptosis. *International Journal of Biochemistry & Cell Biology* **44:** 224-232

Zhang YJ, Klein K, Sugathan A, Nassery N, Dombkowski A, Zanger UM, Waxman DJ (2011) Transcriptional Profiling of Human Liver Identifies Sex-Biased Genes Associated with Polygenic Dyslipidemia and Coronary Artery Disease. *PLoS One* **6**

Zhao J, Castranova V (2011) Toxicology of Nanomaterials Used in Nanomedicine. *Journal of Toxicology and Environmental Health, Part B* **14:** 593-632

Zook JM, MacCuspie RI, Locascio LE, Halter MD, Elliott JT (2011) Stable nanoparticle aggregates/agglomerates of different sizes and the effect of their size on hemolytic cytotoxicity. *Nanotoxicology* **5:** 517-530

Appendix

Table A.1 – QPCR normalizer gene transcripts and variation across datasets

Species	Tissue	Exposure	Time pt	Normalizer(s)[a]	p-value[b]	Cronbach's α
R. catesbeiana	brain	HiAg	Day 6	*eef1a, rps10, rpl8*	0.243	0.929
R. catesbeiana	liver	HiAg	Day 6	*eef1a, rps10, rpl8*	0.161	0.882
R. catesbeiana	tailfin	HiAg	Day 6	*eef1a, rps10, rpl8*	0.169	0.928
R. catesbeiana	tailfin	HiAg	Day 28	*eef1a, rps10, rpl8*	0.394	0.973
R. catesbeiana	brain	LoAg	Day 6	*eef1a, rps10, rpl8*	0.170	0.814
R. catesbeiana	liver	LoAg	Day 6	*eef1a, rps10, rpl8*	0.118	0.883
R. catesbeiana	tailfin	LoAg	Day 6	*eef1a, rps10, rpl8*	0.448	0.742
R. catesbeiana	tailfin	LoAg	Day 28	*eef1a, rps10, rpl8*	0.277	0.961
X. laevis	liver	Premet	Day 2	*eef1a, rps10*	0.624	0.896
X. laevis	liver	Promet	Day 2	*eef1a, rps10*	0.424	0.870
X. laevis	XTC-2	stock, monocultures	24hrs	*rpl8*	0.421	-
X. laevis	XTC-2	Ctrl, nAg ± T3	24hrs	*eef1a, rps10, rpl8*	0.372	0.661

a = QPCR normalization used geometric mean of listed genes

b = Kruskal-Wallis test across all treatments in dataset

Table A.2 – QPCR primer sequences and quality control information

Gene Target	Species[a]	Tissue(s)[b]	Primer Name	Up Primer Sequence	Dn Primer Sequence	Probe Sequence	Product size (bp)	Fluorophore	Annealing Temp (°C)	Thermocycle program[c]	Amplicon sequence confirmed[d]	dCt slope < 0.1[e]
eef1a	Rcat	liver, brain, tailfin										
eef1a	Xlae	liver, XTC-2	EF1aF1/R4/P1	GCTGCTGGTGTTGGTGAAT	AGCATGTTGTCACCGTTCC	ATGCCCTCCTTGCCTACACTCT	239	HEX	64	15s, 30s, 30s	multiplex	-
rps10	Rcat	liver, brain, tailfin										
rps10	Xlae	liver, XTC-2	rpS10F2/R1/P1	GCYTGGCGTCACTTTTACTG	CACGTCCAAAYCCTCCTCTAA	AAGGCTGAGGCTGGWGCTGGAG	289	FAM	64	15s, 30s, 30s	multiplex	-
rpl8	Rcat	liver, brain, tailfin	UL8A	CAGGGGACAGAGAAAAGGTG	TGAGCTTTCTTGCCACAG	-	270	SYBR green	55	15s, 30s, 45s	Operon	-
rpl8	Xlae	liver, XTC-2	AMM1/2/3	AGGCAGGTCGTGCNTACCA	GGGATGTTCTACAGGATTCATAGC	AAACTGCTGGCCACGTGTCCGT	89	Cy5	64	15s, 30s, 30s	multiplex	-
Thra	Rcat	liver, brain, tailfin	rTRa 2 up/FE021dn	GGACCAGAATCTTAGCGG	CATTGGTGCTTCGGTGAG	-	560	SYBR green	60	15s, 30s, 45s	Operon	Yes
Thra	Xlae	liver, XTC-2	AMM4/5/6	TGATAAGGCCACAGGRTACCACTA	CGGGTGATCTTGTCGATRA	ACTATCCAGAAGAACCTGCACCCCTC	141	FAM	64	15s, 30s, 30s	multiplex	Yes
Thrb	Rcat	liver, tailfin	pacTRb up/dn	AAAGTGCATCGCTGTTGG	TTCCCTGTGCATTGGTGG	-	209	SYBR green	55	15s, 30s, 45s	Operon	Yes
Thrb	Xlae	liver, XTC-2	AMM7/8/9	CTCATAGAAGAAAACAGAGAAAARAGA	GAAGGCTTCTAAGTCCACTTTTCC	CATGTGGCCACCAATGCACAGG	237	HEX	64	15s, 30s, 30s	multiplex	Yes
rlk1	Rcat	brain	DDKerF3/RQ	GTTGGCGTTGGTGTTAGCGG	GGCACTGCTTCTTGCAACTTG	-	342	SYBR green	60	15s, 30s, 30s	-	Yes
rlk1	Rcat	tailfin	DDKerF3/RQ	GTTGGCGTTGGTGTTAGCGG	GGCACTGCTTCTTGCAACTTG	-	342	SYBR green	55	15s, 30s, 45s	Operon	Yes
hsp30	Rcat	liver, brain, tailfin	FN028up/RCHSP30dn	GCCTCCACCAGACTTACCA	GTCTCCTTCCTTCCGTCCTC	-	198	SYBR green	61	15s, 30s, 45s	Operon	Yes
cps	Rcat	liver	FM013up/dn	CCATAGTTGTCGCTCCTT	ACATCCTCAGGGCTTTCT	-	459	SYBR green	55	15s, 30s, 45s	Operon	Yes
cat	Rcat	tailfin	Q556a/b	GAATGGTTACGGCTCACA	GCAATGGCTTCATACAGAT	-	174	SYBR green	60	15s, 30s, 45s	RD	Yes
mpo	Xlae	liver, XTC-2	359Qa	TCCGTAACAATACAAACCA	CAAGGGATACCAGACGATCT	-	136	SYBR green	60	15s, 30s, 45s	Operon	Yes
pox2	Xlae	liver, XTC-2	494Qc	GTGCTTCCACGCTACACT	CGATGCTGAGGTCCTGT	-	141	SYBR green	60	15s, 30s, 45s	Operon	Yes
cdknx	Xlae	liver, XTC-2	MAGEX 255	GCCCTGCAAGAAGAAATG	ATCGGTGATAGGAGTGGTGA	-	507	SYBR green	60	15s, 30s, 45s	Operon	Yes
igf2	Xlae	liver, XTC-2	481Q	CACAGCAATACCACCACT	TTCTTCAGCCTTCTCCAT	-	169	SYBR green	60	15s, 30s, 45s	RD	Yes
nr5a2	Xlae	liver, XTC-2	275Qa	ATGAAGCTGGAAGCTGTG	AGTCCCTTGGATGCTGA	-	218	SYBR green	55	15s, 30s, 45s	RD	Yes
actb	Xlae	liver, XTC-2	MAGEX 129	TCACCACCACAGCCGAAAG	GGGCCAGACTCATCATACTCCT	-	502	SYBR green	55	15s, 30s, 45s	Operon	Yes
actb	Xlae	heart gDNA	MAGEX 129	TCACCACCACAGCCGAAAG	GGGCCAGACTCATCATACTCCT	-	675	SYBR green	60	15s, 30s, 45s	-	-
xdm-w	Xlae	heart gDNA	DMWe1/e4	GCACCTCCACCATCATCT	GACTACTAGACGAGGAGTGTTA	-	203	SYBR green	68	15s, 30s, 45s	-	-

a = Rcat: *R. catesbeiana*, Xlae=*X. laevis*

b = unless otherwise stated, all template is cDNA

c = denaturation phase at 95°C, annealing phase at specified temperature, elongation phase at 72°C

d = sequence confirmed via Operon: Eurofins MWG Operon; RD = restriction digestion of purified amplicon; multiplex: multiplex primer/probe combination specificity

e = difference in Ct's from geometric mean of respective normalizer transcripts along a 2x dilution series. Refer to Table A.1 for normalizers

■ = patent pending

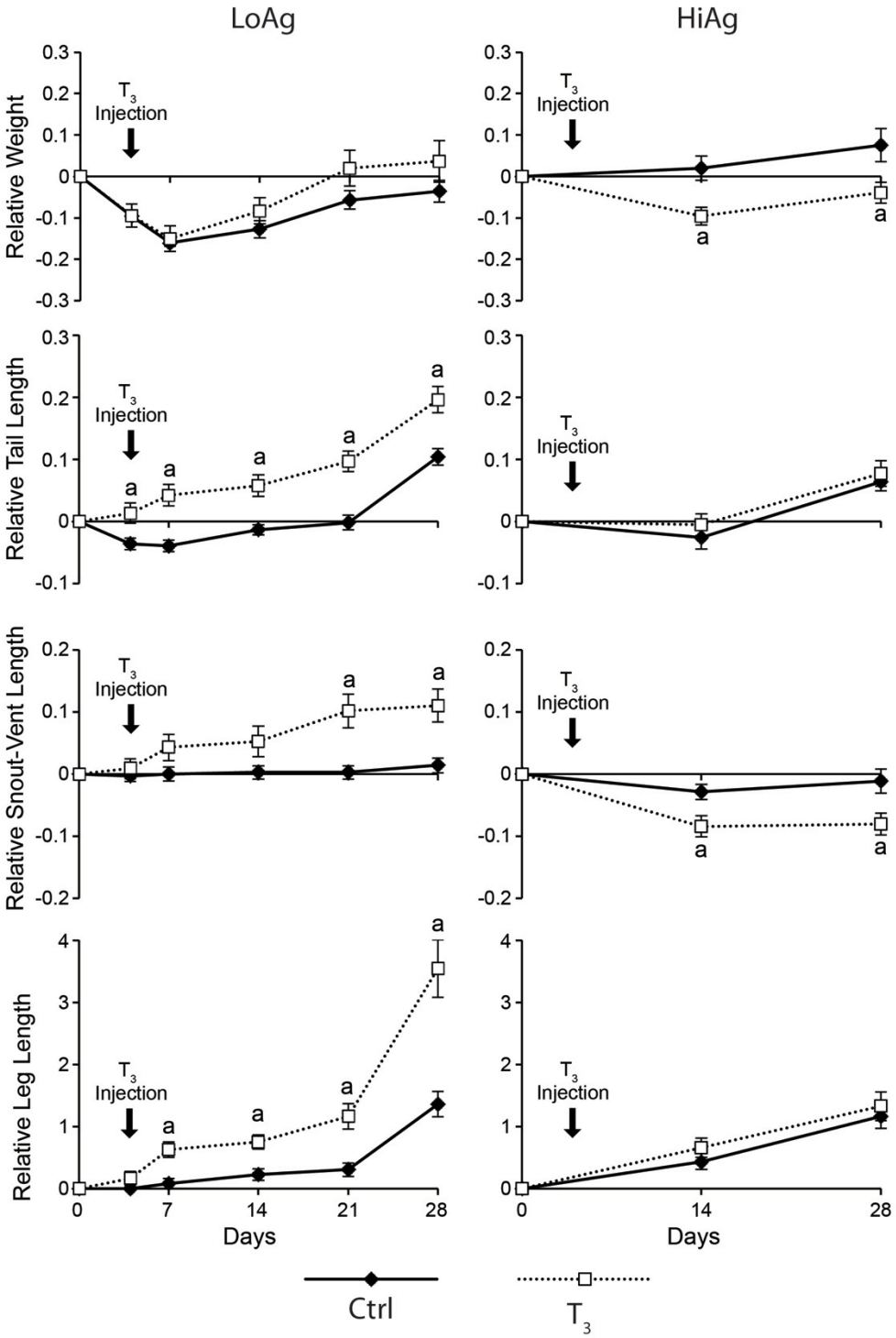

Figure A.1 – Morphometric response of control premet *R. catesbeiana* tadpoles to exogenous T_3-injection in the LoAg and HiAg exposures. Significance at each time point denoted when p-value <0.05 (a).

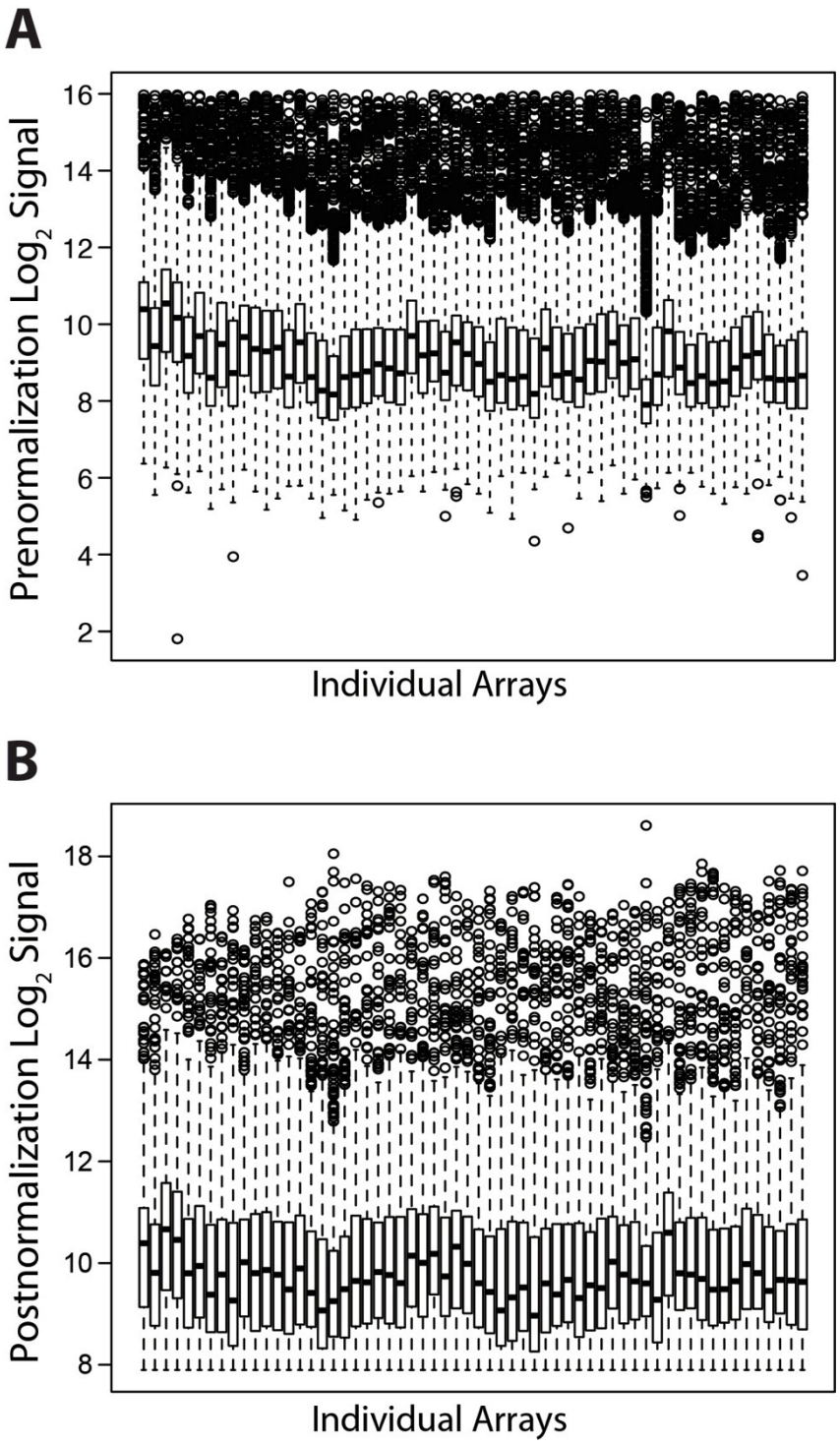

Figure A.2 – Microarray Normalization. The effect of normalization on the distribution of spot intensities pre- (A) and post- (B) normalization. Refer to Figure 2.6 for boxplot details.

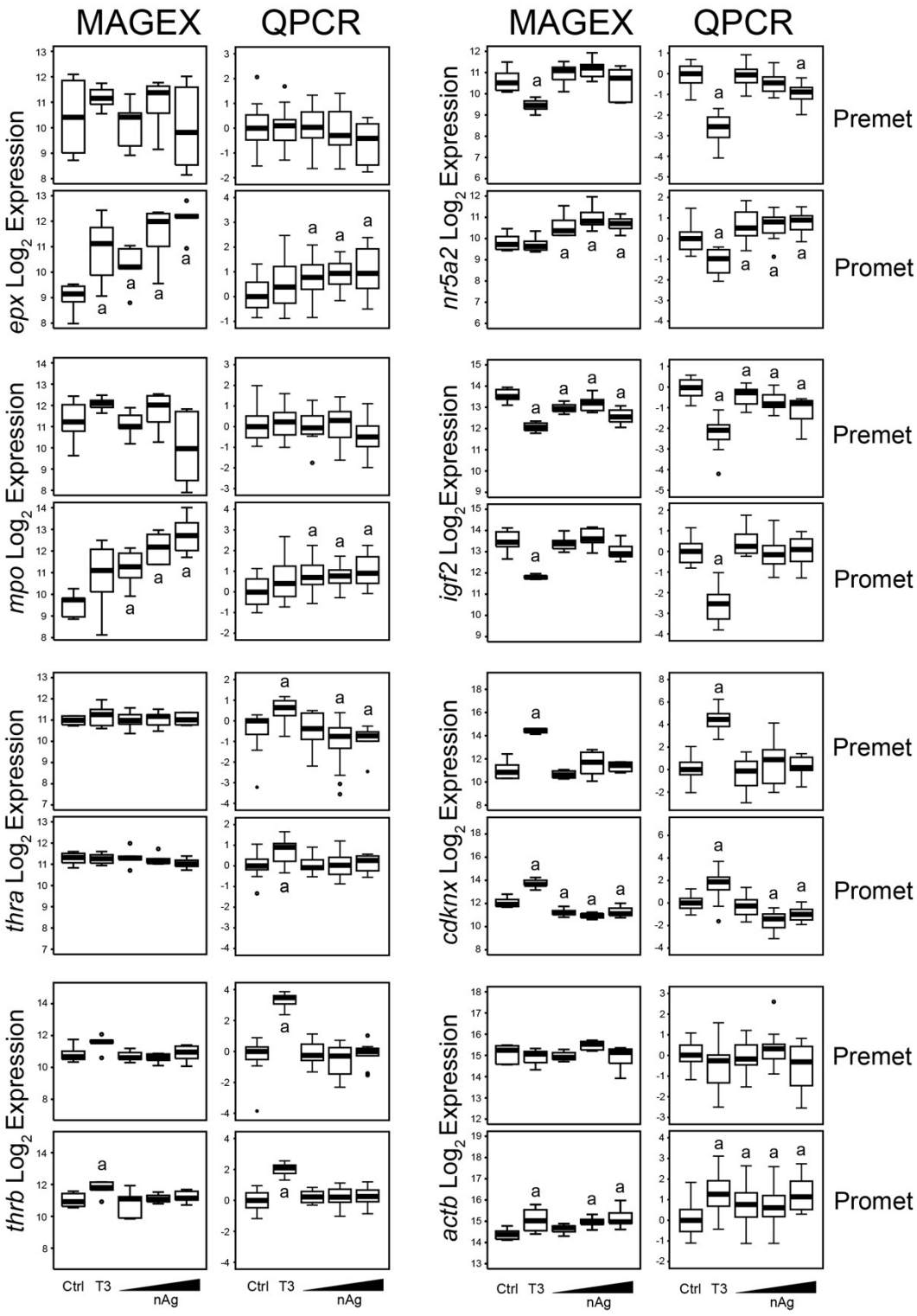

Figure A.3 – MAGEX microarray validation. QPCR response of selected targets within the sample subset used for microarray analysis. MAGEX data represents the Log_2 median spot signal, while QPCR data is Median fold change from the negative control. Significance from respective controls denoted (a) when $p<0.05$. Refer to Figure 2.6 for boxplot details.